



**US Army Corps
of Engineers®**
Engineer Research and
Development Center



New Hampshire Department of Transportation (NHDOT)

Structural Condition Assessment of Reinforced Base-Course Pavement

Rosa T. Affleck, Charles Smith, Andrew Bernier, Jude
Arbogast, Aaron Smart, and Ann Scholz

November 2015



The U.S. Army Engineer Research and Development Center (ERDC) solves the nation's toughest engineering and environmental challenges. ERDC develops innovative solutions in civil and military engineering, geospatial sciences, water resources, and environmental sciences for the Army, the Department of Defense, civilian agencies, and our nation's public good. Find out more at www.erdcenter.usace.army.mil.

To search for other technical reports published by ERDC, visit the ERDC online library at <http://acwc.sdp.sirsi.net/client/default>.

Structural Condition Assessment of Reinforced Base-Course Pavement

Rosa T. Affleck, Charles Smith, and Andrew Bernier

*US Army Engineer Research and Development Center (ERDC)
Cold Regions Research and Engineering Laboratory (CRREL)
72 Lyme Road
Hanover, NH 03755-1290*

Jude Arbogast

*Northeastern University
360 Huntington Avenue
Boston, MA 02115*

Aaron Smart and Ann Scholz

*New Hampshire Department of Transportation (NHDOT)
PO Box 483, 5 Hazen Drive
Concord, NH 03302-0483*

Final Report

Approved for public release; distribution is unlimited.

Prepared for New Hampshire Department of Transportation (NHDOT) in cooperation with
the U.S. Department of Transportation, Federal Highway Administration

Under Cooperative Research and Development Agreement (CRADA)
between ERDC-CRREL and NHDOT
CRADA-13-CRL-01, Appendix B, "Assessment of Reinforced Base Course"

Abstract

In 2011, the New Hampshire Department of Transportation (NHDOT) re-constructed 2 miles of Pickering Road in Rochester. This included building three distinct reinforcement conditions: a geogrid reinforcement within the granular base-course layer and no geotextile separator, a geotextile separator between the subgrade soil and the subbase course, and a geogrid reinforcement within the granular base-course layer with a geotextile separator between the subgrade and the subbase layer.

The Cold Regions Research and Engineering Laboratory (CRREL) conducted a series of falling weight deflectometer (FWD) tests to monitor changes in layer moduli as the seasons changed. FWD tests occurred several times throughout the year on selected locations along the reinforced and non-reinforced (southern portion) pavement. Based on the seasonal back-calculated moduli for 2014 and 2015 values, the reinforced geogrid granular base-course layer provided higher moduli than the non-reinforced sections, and it appears that the aggregate layer thickness can be reduced to 33%–42% if the base course is reinforced with a geogrid mesh. This higher stiffness should allow the pavement to withstand many more traffic repetitions before fatigue cracking develops; and the geogrid should minimize the influence on thermal cracking.

DISCLAIMER: The contents of this report are not to be used for advertising, publication, or promotional purposes. Citation of trade names does not constitute an official endorsement or approval of the use of such commercial products. All product names and trademarks cited are the property of their respective owners. The findings of this report are not to be construed as an official Department of the Army position unless so designated by other authorized documents.

This document is disseminated under the sponsorship of the New Hampshire Department of Transportation (NHDOT) and the Federal Highway Administration (FHWA) in the interest of information exchange. It does not constitute a standard, specification, or regulation. The NHDOT and FHWA assume no liability for the use of information contained in this document.

The State of New Hampshire and the Federal Highway Administration do not endorse products, manufacturers, engineering firms, or software. Products, manufacturers, engineering firms, software, or proprietary trade names appearing in this report are included only because they are considered essential to the objectives of the document.

DESTROY THIS REPORT WHEN NO LONGER NEEDED. DO NOT RETURN IT TO THE ORIGINATOR.

Contents

Abstract	ii
Illustrations	iv
Preface	vii
Acronyms and Abbreviations	viii
Unit Conversion Factors	ix
1 Introduction	1
1.1 Purpose and scope of project	1
1.2 Project collaboration	4
3 Road Section Description	7
4 Approach	9
4.1 Explorations—pavement cores and test borings	9
4.2 Surface slope and banks	16
4.3 Manual instrumentation—frost penetration	17
4.4 Digital instrumentation—soil temperature and moisture	21
4.5 Climate	24
4.6 Falling weight deflectometer test	28
4.6.1 Test Sections	29
4.6.2 Falling weight deflectometer test schedule and conditions	31
4.6.3 Modulus estimation (back-calculation)	34
5 Results	37
5.1 Loads and deflection	37
5.2 Moduli comparison between loads	39
5.3 Seasonal moduli comparison	40
5.4 Base-course equivalent thickness	44
6 Summary and Conclusions	46
7 Recommendations	48
References	49
Appendix A: Pickering Road Construction Background, Geogrid Specification, and Cross Sections	52
Appendix B: Pickering Road Test-Boring Report and AASHTO Soil Classifications	68
Appendix C: Climate	82
Appendix D: Moduli Comparison Between Loads, and PCASE vs. ELMOD FWD Analysis	94
Report Documentation Page	

Illustrations

Figures

1	Pickering Road, Rochester, NH, test-section descriptions. Geogrid-reinforced base course along the <i>yellow</i> section. Geogrid-reinforced base course and geotextile between the subbase and subgrade along the <i>green</i> section. Geotextile between the subbase and subgrade along the <i>blue</i> section	3
2	Test boring locations along the test sections	10
3	Coring operation and sample collection.....	11
4	Cored asphalt concrete at location FT5	11
5	A core of base materials through the geotextile and down to the subgrade at location FT1. The light brown sand subbase material is above the geotextile and natural gray sandy silt subgrade material.....	12
6	Geogrid and geotextile from the core sampling at FT4	12
7	Test-section pavement profiles based on the location labels in Fig. 2	13
8	Grain size distribution from core samples along the test sections	15
9	Selected as-built cross-section profiles. Horizontal scale is equal to vertical scale.....	16
10	Frost-tube installation, backfilling with the PVC pipe covered to prevent clogging the pipe.....	18
11	The method of measuring the frost and thaw depth with the frost tube at FT2 on 2 March 2015. The depth from the pavement surface to the top of the tube at this location ranged from 2 to 3 in. Frost-depth measurements provided in Fig. 12 and 13 reflected this dimension	19
12	Frost depths from frost tubes from February to March 2014	20
13	Frost depths from frost tubes from February to early April 2015	21
14	Pavement moisture from the five 5TM combination soil temperature and moisture probes.....	25
15	Pavement temperature from the five 5TM combination soil temperature and moisture probes.....	26
16	Daily precipitation data during the test period	27
17	Test-location plan using the FWD along the test sections	29
18	Close-up map of the transition area	30
19	FWD along the test sections. <i>Top left</i> , 3 April 2014 at FWD4-4 southbound wheel path, 10:41 a.m.; <i>top right</i> , 17 March 2015 at FWD4-4 southbound wheel path, 10:32 a.m.; <i>bottom left</i> , 1 April 2015 at FWD4-3 southbound center lane, 12:23 p.m.; <i>bottom right</i> , 27 October 2014 at FWD4-1, southbound wheel path, 9:12 a.m.....	34
20	Deflection responses from the 3 April 2014 FWD test for selected test locations	38
21	Average values of back-calculated moduli for four loads	39
22	Seasonal moduli values of reinforced and non-reinforced base-course layers for the test locations. NW means northbound wheel path; NC means northbound center lane; SW means southbound wheel path; SC means southbound center lane.....	41
23	Seasonal moduli values of the base-course layer for the test locations	44

A-1	The as-built cross section of the test section FWD1.....	65
A-2	The as-built cross section of the test section FWD2.....	65
A-3	The as-built cross section of the test section FWD3.....	65
A-4	The as-built cross section of the test section FWD4-1.....	65
A-5	The as-built cross section of the test section FWD4-2.....	65
A-6	The as-built cross section of the test section FWD4-3.....	65
A-7	The as-built cross section of the test section FWD4-4.....	66
A-8	The as-built cross section of the test section FWD4-5.....	66
A-9	The as-built cross section of the test section FWD4-6.....	66
A-10	The as-built cross section of the test section FWD4-7.....	66
A-11	The as-built cross section of the test section FWD4-8.....	66
A-12	The as-built cross section of the test section FWD4-9.....	66
A-13	The as-built cross section of the test section FWD5-1.....	67
A-14	The as-built cross section of the test section FWD5-2.....	67
A-15	The as-built cross section of the test section FWD6-1.....	67
A-16	The as-built cross section of the test section FWD6-2.....	67
C-1	Precipitation data from Skyhaven Airport in Rochester, NH, for 2000 to 2003.....	82
C-2	Precipitation data from Skyhaven Airport in Rochester, NH, for 2004 to 2007.....	83
C-3	Precipitation data from Skyhaven Airport in Rochester, NH, for 2008 to 2011.....	83
C-4	Precipitation data from Skyhaven Airport in Rochester, NH, for 2012 to 2015.....	84
C-5	Maximum daily temperatures for 2000 to 2002.....	86
C-6	Maximum daily temperatures for 2003 to 2005.....	86
C-7	Maximum daily temperatures for 2006 to 2008.....	86
C-8	Maximum daily temperatures for 2009 to 2011.....	87
C-9	Maximum daily temperatures for 2012 to 2015.....	87
C-10	Minimum daily temperatures for 2000 to 2002.....	88
C-11	Minimum daily temperatures for 2003 to 2005.....	88
C-12	Minimum daily temperatures for 2006 to 2008.....	88
C-13	Minimum daily temperatures for 2009 to 2011.....	89
C-14	Minimum daily temperatures for 2012 to 2015.....	89
C-15	Cumulative freezing degree-days (FDD) for winter 2000-01 to winter 2007-08.....	91
C-16	Cumulative freezing degree-days (FDD) for winter 2008-09 to winter 2014-15.....	92
D-1	Load comparisons for asphalt concrete for 3 April 2014.....	94
D-2	Load comparisons for asphalt concrete for 17 March 2015.....	94
D-3	Load comparisons for asphalt concrete for 1 April 2015.....	95
D-4	Load comparisons for asphalt concrete for 23 July 2014.....	95
D-5	Load comparisons for asphalt concrete for 27 October 2014.....	95
D-6	Load comparisons for the base course for 3 April 2014.....	96
D-7	Load comparisons for the base course for 17 March 2015.....	96
D-8	Load comparisons for the base course for 1 April 2015.....	96

D-9	Load comparisons for the base course for 23 July 2014	97
D-10	Load comparisons for the base course for 27 October 2014	97
D-11	Moduli for the base layers from the 27 October 2014 tests from ELMOD6	98
D-12	Averages of the moduli for the base layers from the 27 October 2014 tests from ELMOD6.....	98
D-13	Moduli for the base layers from the 23 July 2014 tests from ELMOD6	98
D-14	Averages of the moduli for the base layers from the 23 July 2014 tests from ELMOD6.....	99
D-15	Moduli for the base layers from the 1 April 2015 tests from ELMOD6.....	99
D-16	Averages of the moduli for the base layers from the 1 April 2015 tests from ELMOD6.....	99
D-17	A comparison of the PCASE and ELMOD6 FWD analyses.....	100
D-18	Averages of the moduli for the base layers from PCASE.....	101
D-19	Averages of the moduli for the base layers from ELMOD6.....	101

Tables

1	Summary of pavement profile and thickness based on the location labels in Fig. 1.....	14
2	Summary of soil gradation in both USCS and AASHTO (brackets) at various locations	14
3	Falling weight deflectometer (FWD) test locations.....	31
4	FWD test dates and conditions	32
5	Seed modulus used for back-calculation in the ELMOD6 program	36
6	Summary of the actual test loading distribution for four load settings and for all locations	37
7	Back-calculated layer moduli for spring, summer, and fall 2014 and spring 2015 tests.....	43
8	Back-calculated ratio comparison for spring, summer, and fall 2014 and spring 2015 tests	43
9	Non-reinforced and reinforced base-course equivalent thickness and moduli values.....	45
C-1	Total yearly precipitation for Skyhaven Airport in Rochester, NH	84
C-2	Total yearly precipitation for Skyhaven Airport (through June 30)	85
C-3	Length of freeze season by year.....	90
C-4	Cumulative freezing degree-days (FDD) from 2000 to 2015.....	93

Preface

Funding for this effort was provided by the New Hampshire Department of Transportation (NHDOT) under a Cooperative Research and Development Agreement (CRADA) between the U.S. Army Engineer Research and Development Center, Cold Regions Research and Engineering Laboratory (ERDC-CRREL), and NHDOT (CRADA-13-CRL-01, Appendix B, “Assessment of Reinforced Base Course”). The technical monitor was Glenn Roberts, NHDOT.

This report was prepared by Rosa Affleck (Force Projection and Sustainment Branch, Dr. Toyooki Nogami, Chief) and Charles Smith and Andrew Bernier (Engineering Resources Branch, Jared Oren, Chief), ERDC-CRREL; Aaron Smart and Ann Scholz, NHDOT Bureau of Materials and Research; and Jude Arbogast, an undergraduate student at Northeastern University working at CRREL during the summer of 2015. At the time of publication, Dr. Loren Wehmeyer was Chief of the Research and Engineering Division, ERDC-CRREL. The Deputy Director of ERDC-CRREL was Dr. Lance Hansen, and the Director was Dr. Robert Davis.

The field investigation would not have been possible without assistance from the NHDOT District 6 staff, who provided the traffic control and safety during the testing, and the NHDOT coring crew, who collected the samples. The materials testing was conducted by the NHDOT Bureau of Materials and Testing. In addition, the authors would like to acknowledge Eric Thibodeau, Glenn Roberts, and Alan Rawson for their technical support on this project.

Emily Moynihan provided our editing support. Robert Eaton, a retired pavement researcher with USACE-CRREL (1970–2002) and the NHDOT Bureau of Maintenance and Operations District 2, Enfield (2002–2010), and Dr. Edel Cortez, a research civil engineer at the ERDC-CRREL, provided technical reviews.

COL Bryan S. Green was Commander of ERDC, and Dr. Jeffery P. Holland was the Director.

Acronyms and Abbreviations

AASHTO	Association of State Highway and Transportation Officials
AADT	Annual Average Daily Traffic
CRREL	Cold Regions Research and Engineering Laboratory
CRADA	Cooperative Research and Development Agreement
ELMOD	Evaluation of Layer Moduli and Overlay Design
ERDC	U.S. Army Engineer Research and Development Center
FDD	Freezing Degree-Days
FT	Frost Tube
FWD	Falling Weight Deflectometer
NCDC	National Climatic Data Center
NHDOT	New Hampshire Department of Transportation
PCASE	Pavement-Transportation Computer Assisted Structural Engineering
USCS	Unified Soil Classification System
WES	Waterways Experiment Station

Unit Conversion Factors

Multiply	By	To Obtain
degrees Fahrenheit	$(F-32)/1.8$	degrees Celsius
feet	0.3048	meters
gallons (U.S. liquid)	3.785412 E-03	cubic meters
inches	0.0254	meters
miles (U.S. statute)	1,609.347	meters
ounces (mass)	0.02834952	kilograms
pounds (force)	4.448222	newtons
pounds (force) per square inch	6.894757	kilopascals
pounds (mass)	0.45359237	kilograms
pounds (mass) per cubic foot	16.01846	kilograms per cubic meter
square yards	0.8361274	square meters

1 Introduction

By definition, all roadways and airfield pavements built in seasonal frost areas undergo annual freeze–thaw cycles. During the spring thaw, the pavement structure becomes weaker due to excess moisture content. Geosynthetics have been used to strengthen pavements with weak subgrade soils; and geosynthetic materials, particularly geogrids, are in widespread use for road applications to reinforce pavements, potentially reducing the rate of distress during the structure’s service life. However, the reinforcement’s performance and optimal benefits depend on the grid constituent material, the mesh shape and size, geogrid material stiffness, and position within the pavement structure. Higher pavement stiffness increases fatigue resistance and reduces rutting.

The cost of the geogrid material is between \$4 and \$6 per sq yd, which is equivalent to 1 in. of asphalt layer. The manufacturer (Tensar International Corporation) claims that the application of this product can reduce asphalt layer thickness 15%–30% and aggregate layer thickness 25%–50% and provides additional strength in comparison to the conventional section. Through both laboratory and in situ investigations, many researchers (Hass et al. 1988; Cancelli and Montanelli 1999; Raymond and Ismail 2003; Kwon et al. 2008; Al-Qadi et al. 2008; Henry et al. 2009; Shu et al. 2014; Zornberg and Gupta 2009, 2010; Zornberg 2015; and many others) have thoroughly studied its performance and optimal benefits as a reinforcement material, and it remains an important subject of debate.

1.1 Purpose and scope of project

In 2011, the New Hampshire Department of Transportation (NHDOT) reconstructed 2 miles of Pickering Road in Rochester, NH (Figure 1). The layer structure and thicknesses were kept constant along the 2 miles of road. This project built three distinct reinforcement conditions. The northernmost portion of the 2-mile road section included a geogrid reinforcement within the base-course layer* and no geotextile separator. The

* A base-course layer applies to the relatively stiff layer below the pavement surfacing layer (i.e., the asphalt concrete) constructed with aggregate materials to provide drainage or for rapid evacuation of infiltrated water in the pavement system. In this report, we use *base*, *base layer*, *base course layer*, and *granular base* interchangeably.

southernmost portion of the road sections included a geotextile* separator between the subgrade soil and the subbase-course layer. The intermediate section of the road included both a geogrid reinforcement within the base-course layer and a geotextile separator between the subgrade and the subbase course. For half of the northernmost portion of the road, the geogrid was placed 3 in. from the top of the granular base-course layer. For the other half of the northernmost portion of the road, the geogrid reinforcement was placed 6 in. below the top of the granular base-course layer.

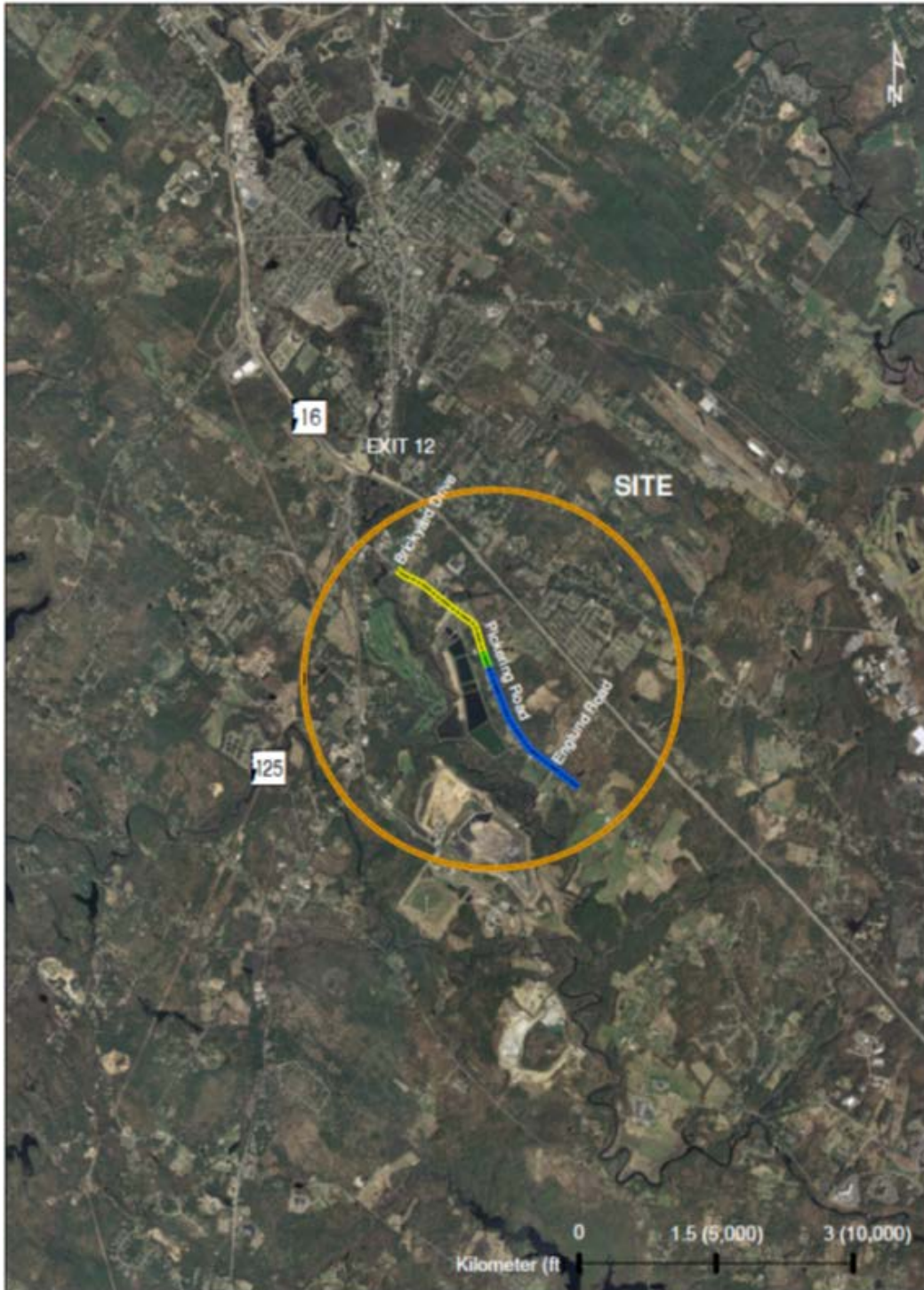
The research study proposed that the U.S. Army Cold Regions Research and Engineering Laboratory (CRREL)

- a. conduct a series of falling weight deflectometer (FWD) tests on the reinforced base-course layer and the adjacent conventional pavement sections once in the summer (representing a normal condition), fall, and spring (under thawing conditions) at selected locations;
- b. calculate and analyze the data to quantify the moduli values of the layers from the FWD data; and
- c. summarize the moduli values to compare the geogrid and the non-geogrid base-course test sections.

The objective of this study was to examine the structural benefit (if any) of the pavement reinforcement application for NHDOT by providing a comparative assessment quantifying the properties of the pavement reinforcement application and how significantly stronger it was compared to the conventional pavement that contained only a geotextile separator fabric between the subgrade soil and the subbase course. The scope of this study included the seasonal assessment using FWD tests on both the geogrid-reinforced and the non-reinforced (control) portions of a reconstructed 2-mile road segment. CRREL conducted FWD tests at various dates throughout the seasons to establish the seasonal variations of layer moduli and pavement stiffness.

* The geotextile used in the study was high-strength woven.

Figure 1. Pickering Road, Rochester, NH, test-section descriptions. Geogrid-reinforced base course along the *yellow* section. Geogrid-reinforced base course and geotextile between the subbase and subgrade along the *green* section. Geotextile between the subbase and subgrade along the *blue* section.



1.2 Project collaboration

In partnership with NHDOT staff, a CRREL team coordinated with NHDOT on the testing dates and traffic safety controls. NHDOT conducted core sampling to quantify and verify the structural layers of the pavements. In addition, NHDOT provided background information of the site, including traffic data, as-built drawings, photographs during construction, surface profile data, and soils information. This report includes and describes all of the data.

It is important to note that CRREL was not involved in the design, construction, or quality control during the reconstruction of the 2-mile test section.

2 Background

Geogrids increase fatigue resistance, reduce degradation over time, reduce crack propagation, and increase structural performance in pavements. For flexible pavements, the maximum reinforcement benefit derived from geogrids is obtained when there is a good interlock between the granular base course and the geogrid (Henry et al. 2009). However, lack of consensus remains with regard to geogrid reinforcement value for a variety of base-course soils used at different geographical locations and with regards to the depth of the geogrid within the base course.

Studies have claimed that the use of geogrid at the unbound aggregate base–subgrade interface have helped to improve pavement performance and to extend service life (Hass et al. 1988; Cancelli and Montanelli 1999; Raymond and Ismail 2003; Kwon et al. 2008; Al-Qadi et al. 2008; Shu et al. 2014). Additionally, pavement experts have indicated that the optimal benefits and effectiveness of the geogrid in flexible pavement may depend on the installation locations or position of the grid in the pavement structure (Brown et al. 2001; Al-Qadi et al. 2012). Previous studies claimed that the reinforcement should be placed at the bottom of the asphalt concrete layers where tensile strains are the highest and can be absorbed by the grid (Brown et al. 2001; Bocci et al. 2007). Another example of this effort is the study conducted by Henry et al. (2008, 2009) in a controlled environment where the geogrid was placed at the bottom of the base course.

Moreover, Brown et al. (2001) found that reinforced pavements provided a service life 1.2–1.8 times higher than the non-reinforced pavements due to the added stiffness of the grid mesh and to the interlocking effect. According to Al-Qadi et al. (2012), the improvement in pavement responses as a result of reinforcement implied that the base–subgrade interface is an effective location for the geogrid. Likewise, having the geogrid placed at one-third of the base-layer thickness reduced the shear flow of the granular material. Other experts claimed that the stiffness of the pavement system is not influenced by the presence of the reinforcement (e.g., geogrid) and that, under repeated traffic loads, the stiffness contribution of geogrid initiates when the asphalt concrete reaches fracture (Austin and Gilchrist 1996).

The influence of geogrid on the pavement structural performance has been examined through in situ investigations using non-destructive methods (i.e., FWD in full-scale laboratory studies) (Zornberg and Gupta 2009; Henry et al. 2009; Kinney et al. 1998a, 1998b). While these studies were done in a controlled environment, the modulus values of the reinforced base layers were generally greater than those of the unreinforced control (Henry et al. 2009), and the geogrid slowed the development of fatigue cracking on pavements.

These studies showed that geogrid is often beneficial when used to reinforce supporting soil layers in pavement systems. However, field trials have been limited and have provided mixed results. Part of the reason is that construction practices also affect geosynthetic-reinforced pavements performance (Zornberg and Gupta 2009, 2010; Zornberg 2015). There have been reports of construction incidents where the contractor laid rolls of geogrid and left a portion of supposedly geogrid-reinforced pavement without the reinforcement (Zornberg and Gupta 2009). Other occurrences of poor performance were due to inadequate junction efficiency (overlap), highlighting the need for better material characterization and the possible inadequacy of commonly used specifications for geogrid-reinforced pavements (Zornberg and Gupta 2009, 2010; Zornberg 2015).

In addition to construction and material irregularities, field case studies are likely to encounter other factors affecting the performance of geogrid-reinforced pavement. These compounding factors include the environmental and topographical variability, which have spatial and temporal characteristics of influence. The reality in research is that budgetary constraints do not allow studying these factors holistically, and this limits the research scope.

Using an FWD, this project provides a seasonal assessment to quantify the significance in structural change and performance of the geogrid compared to the conventional pavement structure. Given a specific research scope and to add to the body of knowledge, this study also characterizes some attributable factors affecting the performance.

3 Road Section Description

As shown in Figure 1, the NHDOT reconstructed Pickering Road as follows:

- A geotextile was placed at the subgrade–subbase interface in the southern part of the 2-mile road section, a line designated in blue in Figure 1.
- A TriAx TX 160 geogrid was placed within the base-course layer in the northern portion of the road section, a line designated in yellow in Figure 1.
- A geotextile at the subgrade and a TriAx TX 160 geogrid within the base course was placed in the middle transition, a hashed line designated in green in Figure 1.

Because CRREL was not involved in the design, construction, or quality control during the reconstruction of the 2-mile test section, NHDOT conducted test borings along the test section to verify the thicknesses of the pavement structure. Section 4 describes the general profile of the road based on these test borings. The wearing course or asphalt pavement layer varied from 5 to 6 in. thick along the test sections. The base-course (and the subbase-course) layer ranged from 18 to 31 in. thick. From the test borings, the geogrid was placed approximately 3 and 6 in. from the top of base-course layer. NHDOT did not have on record final design plans or profiles generated for the pavement section. Tensar was not involved with the project oversight; however, they donated half of the TriAx TX 160 geogrid used for the entire road reconstruction; NHDOT purchased the remainder. Appendix A shows the product specification for TriAx TX 160 geogrid.

The NHDOT District 6 Engineer supplied as-built information (Sanders 2014). This road was constructed with 5 in. of asphalt concrete (Item 403.11, Hot Bituminous Pavement Machine Method). The typical base course was composed of a 6 in. layer of crushed stone fine (Item 304.4), a 6 in. layer of crushed stone coarse material (Item 304.5), and a 12 in., layer of subbase consisting of (natural) sand (Item 304.1) on top of the subgrade. In wet areas with a high surface water table, a layer of sand greater than 12 in. was placed as part of the subbase course (Sanders 2014). The extra sand of approximately 4 ft in depth was placed in close proximity to

the FWD2 location. The extra sand was 165 × 26 ft. Compaction of the base-course material during construction was at approximately 100% compaction (at 145 lb/ft³ optimum compaction). Appendix A provides a summary of the gradation and compaction information during the road construction and a description of the road construction. The typical subgrade soils in the road are sandy silt or silt, a highly frost susceptible soil; and a Marine clay subgrade was prevalent along the southerly end of the project.

The town of Rochester maintains this road in the winter, and NHDOT District 6 maintains this road in the summer. This road test section receives varying vehicle traffic in terms of annual average daily traffic (AADT). In 2012, NHDOT measured the traffic volume along this road (<http://gis.dot.nh.gov/nh-roads/>) in the northern section from NH 125 to Tebbetts Road and in the southern side from Tebbetts Road to England Road. The northern section along locations FWD 6 and 5 had an AADT of 6500 in 2012. The southern section along location FWD 4, 3, 2, and 1 had an AADT of 2800 in 2012.

4 Approach

The following sections describe the methods used in this study.

4.1 Explorations—pavement cores and test borings

NHDOT drilled a total of nine test borings along the test section to verify the thicknesses of the pavement structure (Figure 2). Five test borings (FT1 through FT5, Figure 2) were drilled along the northbound right wheel path from 30 to 31 January 2014 (Figure 3). Four more borings (PC1, PC2, PC3, and PC6) were conducted on 29 December 2014. The test borings used a combination of coring and case and wash drilling methods to depths from 6 to 6.5 ft below the pavement surface. All of these borings were extracted on the northbound lane near the edge of the road. At each location, the existing pavement was cored using a 6 in. diameter core bit. Base, subbase, and subgrade soils beneath the pavement were sampled using a 3 in. inner diameter split-barrel spoon sampler. Materials were characterized in the field by using NHDOT modified visual-manual descriptions and were compiled in a report (Appendix B). The soil samples were taken to the NHDOT Materials Section for grain size distribution testing and for further classification in accordance with the Unified Soil Classification System (USCS). The soils were also classified into American Association of State Highway and Transportation Officials (AASHTO) soil descriptions (Appendix B).

Based on the test boring, the wearing course or asphalt pavement layer varied from 5 to 6 in. thick (Figure 4). The base-course layer was characterized as granular gravel materials in varying depths. The thickness of the base course varied significantly, ranging from 7 in. (at PC2) to 19 in. (at FT2). Similarly, the subbase varied in thicknesses, ranging from 12 in. (FT2) to 29 in. (PC2). According to the District Engineer (Sanders 2014), during construction, a thick subbase (using sand) was placed in locations with a high water table, for example, near FT1. The scope of our work excluded monitoring the water table.

Figure 5 shows core-sample base materials through the geotextile and down to the subgrade at FT1. The geogrid material was placed between approximately 3 and 6 in. from the top base-course layer in locations FT3, FT4, FT5, and PC6, which are in the northern portion of the test section

(Figure 2). Figure 6 shows pieces of geogrid and geotextile retrieved from coring at FT4. The data summary from the borings provided the actual pavement profiles, the location of the geogrid, and soil conditions (Table 1; Figure 7).

Figure 2. Test boring locations along the test sections.



Figure 3. Coring operation and sample collection.



Figure 4. Cored asphalt concrete at location FT5.



Figure 5. A core of base materials through the geotextile and down to the subgrade at location FT1. The light brown sand subbase material is above the geotextile and natural gray sandy silt subgrade material.



Figure 6. Geogrid and geotextile from the core sampling at FT4.

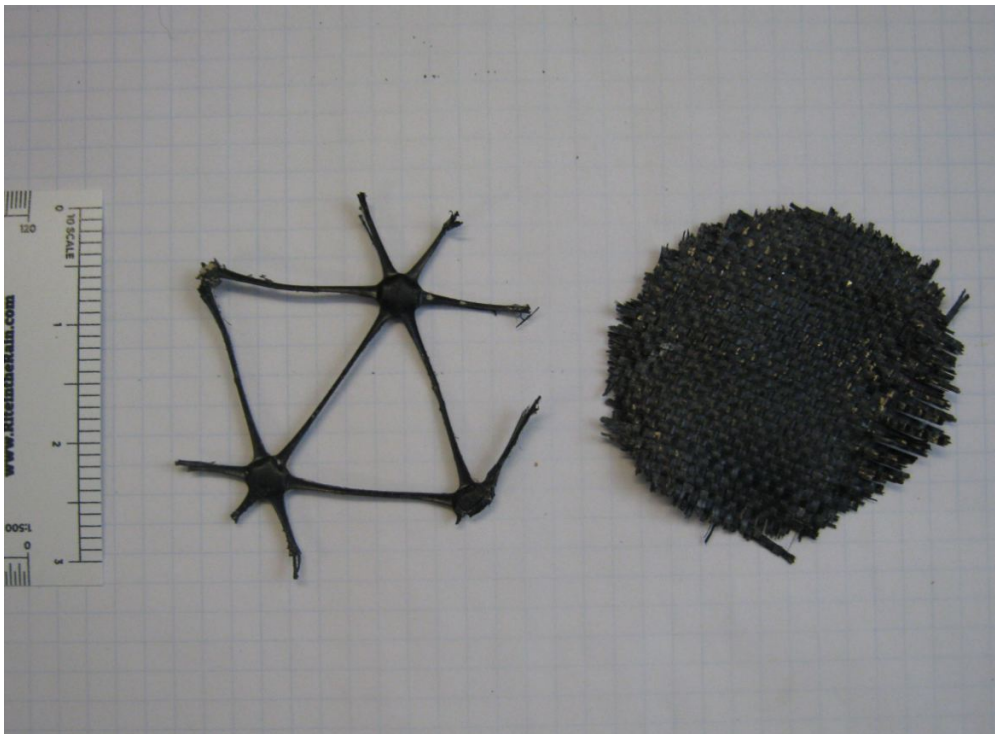


Figure 7. Test-section pavement profiles based on the location labels in Fig. 2.

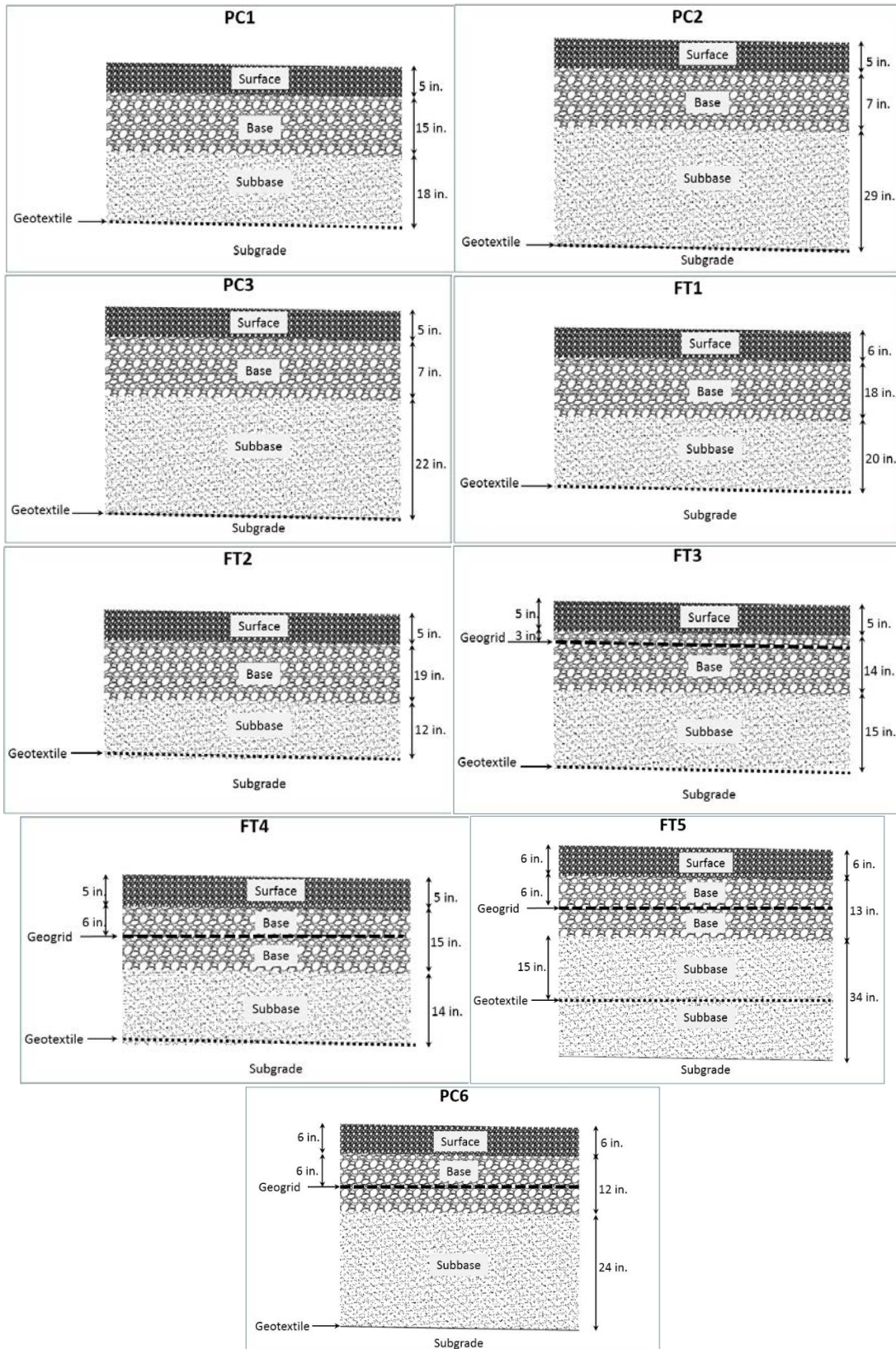


Figure 8 shows gradation results taken from the core samples at the test boring locations (FT1, FT2, FT3, FT4, FT5, PC1, PC2, PC3, and PC6). Appendix D shows the gradation in AASHTO classification. The base course ranged from poorly graded sand with silt and gravel (SP-SM) to poorly graded gravel with silt and sand (GP-GM) or well-graded gravel with silt and sand (GP-GM). The base course in this case was consistently an A-1-a based on AASHTO classification. The representative subbase was classified as poorly graded sand with gravel (SP), with typical AASHTO classifications of A-1-b and A-2-4(0) in other locations (i.e., PC3). The subgrade was characterized as sandy silt or silt (ML) although this was only measured in one location (FT5); discussions with the District Engineer (Sanders 2014) indicated that this is a representative subgrade soil for the area (Table 2).

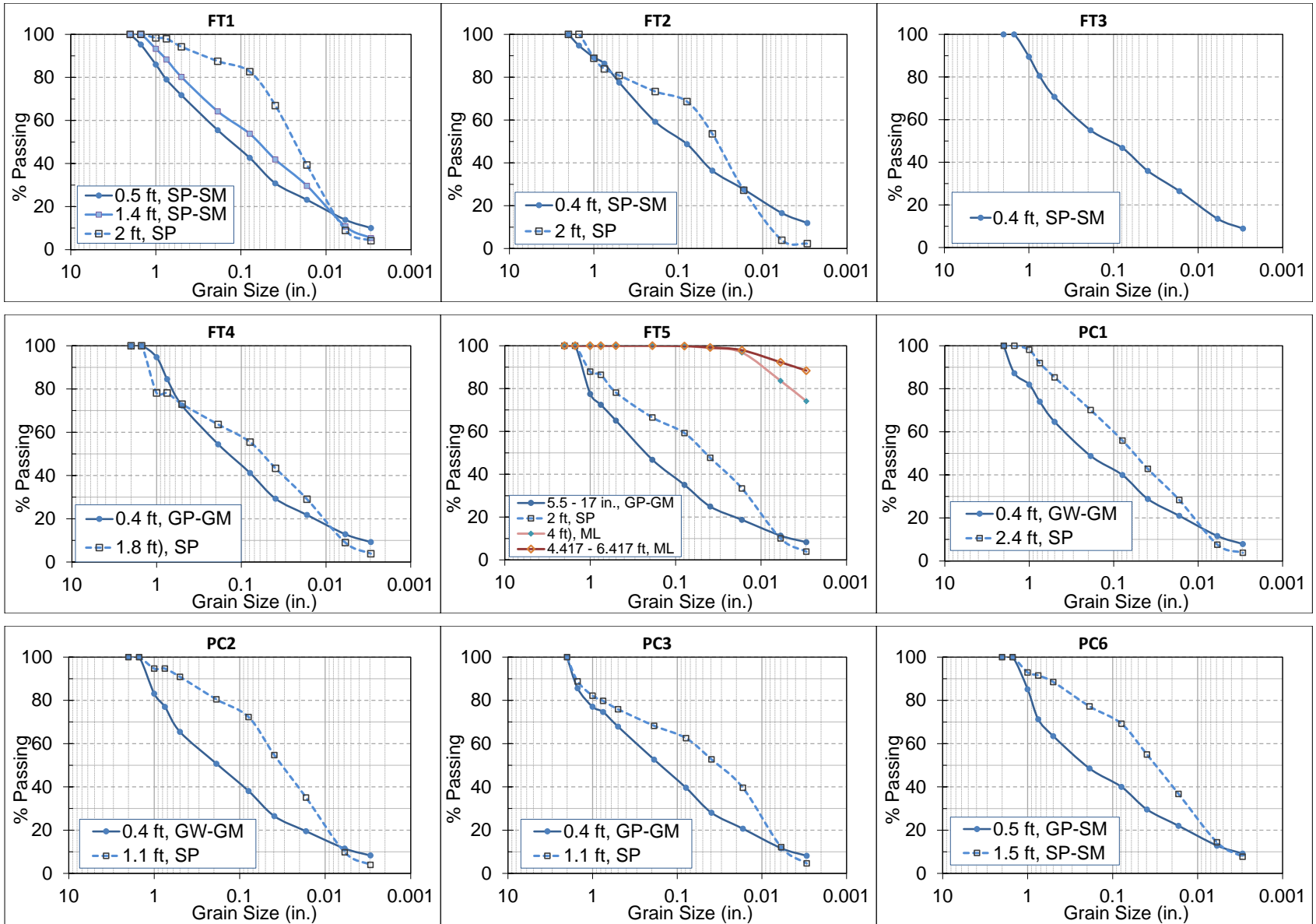
Table 1. Summary of pavement profile and thickness based on the location labels in Fig. 1.

Profiles	Locations from north to south								
	PC6	FT5	FT4	FT3	FT2	FT1	PC3	PC2	PC1
AC (in.)	0-6	0-6	0-5	0-5	0-5	0-6	0-5	0-5	0-5
Base Course (in.)	6-12	6-12	5-11	5-8	5-24	6-24	5-12	5-12	5-20
Geogrid Depth (in.)	12	12	11	8					
Base Course (in.)	12-18	12-19	11-20	8-19					
Subbase (in.)	18-42	19-34	20-34	19-34	24-36	24-44	12-34	12-41	20-38
Geotextile Depth (in.)		34	34	34	36	44	34	41	38
Subbase (in.)		34-53							
Subgrade Depth (in.)	42	53	34	34	36	44	34	41	38

Table 2. Summary of soil gradation in both USCS and AASHTO (brackets) at various locations.

Profiles	Locations from north to south								
	PC6	FT5	FT4	FT3	FT2	FT1	PC3	PC2	PC1
Base Course	GP-SM [A-1-a]	GP-GM [A-1-a]	GW-GP [A-1-a]	SP-SM [A-1-a]	SP-SM [A-1-a]	SP-SM [A-1-a]	GW-GM [A-1-a]	GW-GM [A-1-a]	GW-GM [A-1-a]
Geogrid	yes	yes	yes	yes	none	none	none	none	none
Base Course	SP-SM [A-4(0)]					SP-SM [A-1-b]			
Subbase		SP [A-1-b]	SP [A-1-b]		SP [A-1-b]	SP [A-1-b]	SP [A-2-4(0)]	SP [A-1-b]	SP [A-1-b]
Geotextile	none	yes	yes	yes	yes	yes	yes	yes	yes
Subgrade		ML [A-2-4(0) to A-4(0)]							

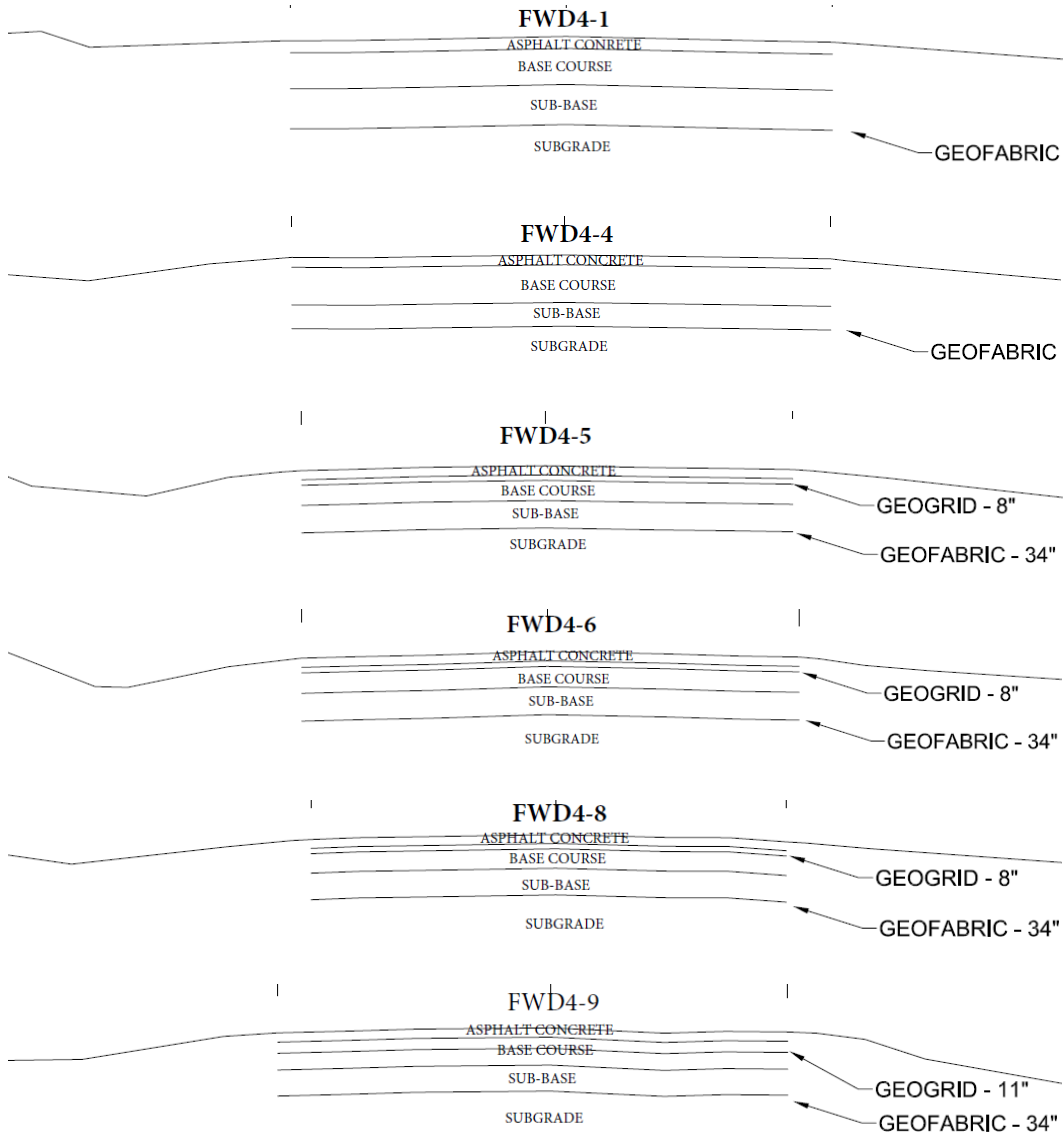
Figure 8. Grain size distribution from core samples along the test sections.



4.2 Surface slope and banks

Pavement cross sections typically include a crown designed to help water drain towards the pavement edges and banks by using appropriate surface-slope criteria (Doré and Zubeck 2009). In addition, roadside drainage ditches should be of sufficient width and depth to handle the design runoff and should be at least 6 in. below the subgrade crown to ensure stability of the base course. The NHDOT team collected a cross-sectional survey along the test locations to assess slope and bank conditions (Figure 9; Appendix A).

Figure 9. Selected as-built cross-section profiles. Horizontal scale is equal to vertical scale.



In this case, the road was built with the design crown sloping away from the road center towards both edges. In certain sections along the west side of the road, the drainage ditch was built too shallow, especially from FWD4-1 to FWD4-9 locations. There are several culverts crossing from east to west for seasonal streams and to drain the surface water from the watershed. We found that these ditches had water ponded, particularly during our spring tests. The low spots of the test section were at FWD1, along FWD3 to FWD4-4, and adjacent to FWD5-1 and FWD5-2.

4.3 Manual instrumentation—frost penetration

Manual instrumentation used for the project consisted of five frost tubes fabricated and installed by NHDOT in general accordance with *The Field Assembled Frost Gage* (Ricard et al. 1976). Frost-tube construction generally consisted of a 3/4 in. inner diameter PVC pipe installed from just below the pavement surface to the bottom of the test boring. Pipe casings were 6 ft (72 in.) long. Boring depths ranged from 6 to 6.4 ft (77 in.). The pipe was sealed at the bottom with a PVC cap. Soil cuttings, minus hand-picked gravel-sized materials, were placed back into the drill hole in the order in which they were removed in 8 to 12 in. thick loose lifts and compacted with a wood dowel around the outside of the casing. A 5 ft long, 5/8 in. outer diameter flexible plastic tube that was filled with water and capped at both ends was inserted into the pipe. The tube was held above the bottom of the pipe by a plastic wire tie fastener. To provide some contrast observing frozen portions of the tube, the water in the tube initially contained a few drops of green food coloring. The green colored water was replaced on 14 January 2014 with fresh water containing a 0.07 oz/gal. (0.5 g/L) concentration of methylene blue indicator dye. After filling with colored water or methylene blue liquid, the stopper was sealed into place with epoxy inside the top of the flexible tube. A wire tie fastener was placed around the top of the tube to act as a stopper to keep the tube from sliding into the pipe casing. The top of the pipe was covered at the surface with a pentagonal-keyed metal roadbox that was sealed slightly below the pavement surface with concrete (Figure 10).

Figure 10. Frost-tube installation, backfilling with the PVC pipe covered to prevent clogging the pipe.



The frost tubes were installed consecutively with test borings FT1 through FT5 (Figure 2) to provide an indication of the frost and thaw depths in the pavement. No frost tubes were installed in PC1, PC2, PC3, and PC6. Locations selected were in close proximity covering the test sections along the geotextile in the subgrade–subbase interface and the geogrid in the base course and the geotextile in the subgrade–subbase interface (Figure 2). The NHDOT team monitored all the frost tubes and measured the actual frost and thaw depths from the frost tubes from which they were able to get readings.

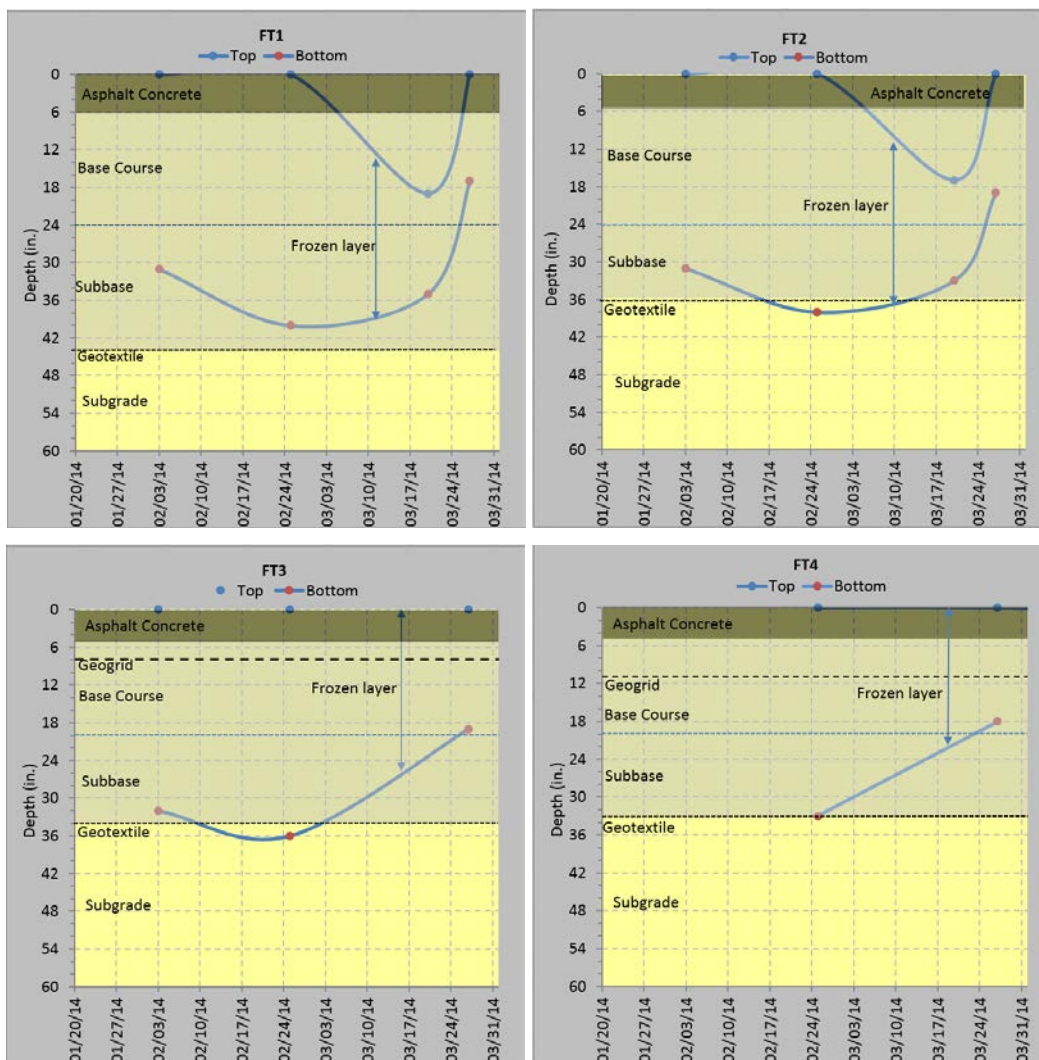
The weather information of the Rochester area was used to determine when it was time to measure the frost and the thaw depths of the frost tubes. (Section 4.5 further discusses site climate.) The frost tubes were monitored based on the forecasted temperature of the Rochester area, particularly when there were cooling and warming patterns. NHDOT took measurements by pulling out the flexible tube and measuring the frozen layer (Figure 11). The frost depths were measured on 3 and 25 February

and on 20 and 27 March 2014. Four of the frost tubes seemed to be working during the first winter as shown in Figure 12 (FT1, FT2, FT3, and FT4). The maximum frost depths measured on 25 February 2014 were 40 in., 38 in., 36 in., and 33 in. at FT1, FT2, FT3, and FT4, respectively. The maximum frost depths were near the bottom of the subbase or in some cases extended into the top of the subgrade layer (Figure 12). Thawing started sometime in mid-March 2014, showing thaw progression in the subbase and surface of the pavement.

Figure 11. The method of measuring the frost and thaw depth with the frost tube at FT2 on 2 March 2015. The depth from the pavement surface to the top of the tube at this location ranged from 2 to 3 in. Frost-depth measurements provided in Fig. 12 and 13 reflected this dimension.

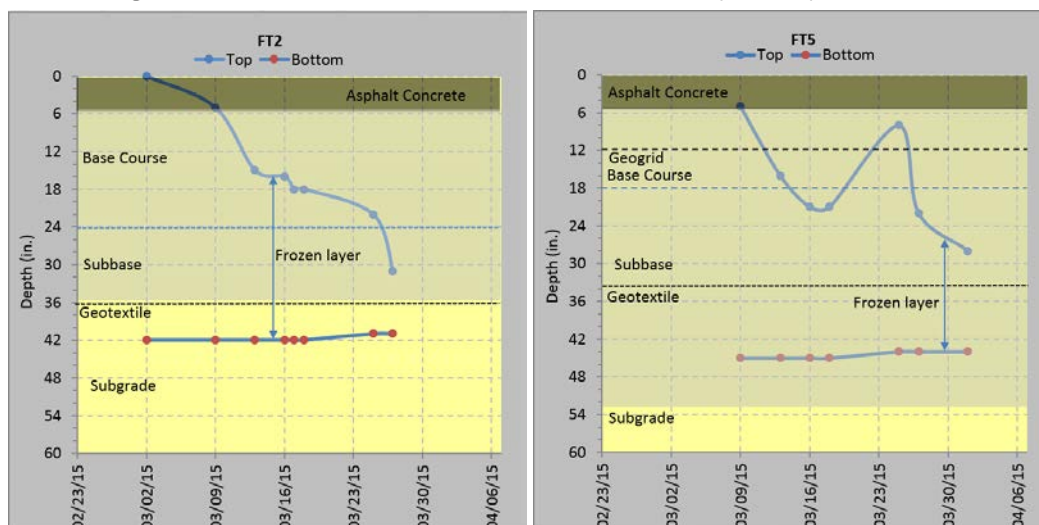


Figure 12. Frost depths from frost tubes from February to March 2014.



In the fall of 2014, only two of the frost tubes (FT2 and FT5) were functioning to monitor the frost depth during winter 2014–15 (Figure 13). (The NHDOT team suspected that the covers on the non-functioning frost tubes were not working properly, leaving them vulnerable to traffic and plowing as the frost pushed the PVC casings upward toward the surface.) The frost tubes were monitored on 2, 9, 13, 16, 18 25, and 27 March and on 1 April 2015. The maximum frost depths measured were 42 in. and 45 in. at FT2 and FT4, respectively (Figure 13). The thawing in the base course started the second week of March and progressed toward the subbase until the end of March 2015. FT2 was completely thawed by 1 April 2015; however, FT5 had 16 in. of frost depth in the subbase.

Figure 13. Frost depths from frost tubes from February to early April 2015.



4.4 Digital instrumentation—soil temperature and moisture

Digital instrumentation used for the project consisted of five Decagon 5TM combination soil temperature and moisture probes connected to an Em50 five-channel digital datalogger manufactured by Decagon Devices, Inc. (<http://www.decagon.com/>). The probes measure temperature and volumetric water content with accuracies of $\pm 1\%$ and $\pm 3\%$, respectively. The datalogger can store up to 1 MB, which is composed of 36,000 scans for up to five instruments per scan, and is powered by five AA alkaline batteries that were reported to provide 8 to 12 months of service for continuous data collection. The NHDOT team programmed the datalogger by using proprietary ECH2O Utility v1.72 software installed on a laptop computer and a proprietary USB/3.5 mm stereo cable.

The NHDOT prepared and installed the instrumentation to measure the generalized freezing and thawing trend at the site to estimate when to perform FWD testing. Their line of thinking was that the temperature precision was of minor importance to that of the temperature trend, and most of the team's effort was applied to understanding the instruments' ability to measure soil moistures at different probe orientation and locations. Prior to field installation, soil temperature and moisture probes were calibrated in the laboratory in three different medium: in the open air; in a sample of silty fine sand (100% passing the #4 sieve); and in a sample of water. In each medium, the probes were scanned at 5 min intervals for 30

min using the Em50 datalogger, which was attached to a laptop and monitored using the ECH20 software. Open air, soil, and water temperatures ranged from 66.7°F to 68.4°F.* Open air and water volumetric water content measurements from the scans were uniformly -2.38% and 101.1%, respectively. For the sand portion of the calibration, the probes were inserted vertically and in a circular array into the sand. After measuring the initial volumetric water content of the soil, the probes were removed; and water was thoroughly mixed into the soil until free water could be seen on the surface of the sample. The probes were reinserted into the soil, and the final volumetric water content was measured. Initial and final soil volumetric moisture content measurements ranged from 1.50% to 2.19% and 25.05% to 29.16%, respectively. These measurements corresponded well with laboratory moisture-content tests and volumetric water content and water content phase relationships.

Soil temperature and moisture probes were installed on 2 April 2014 within the middle third of the test section beneath the narrow gravel shoulder on the east side of the roadway near FT3 (Figure 18). The probes were installed in individual holes drilled parallel with the edge of pavement. They were placed at an approximate horizontal spacing of 2 ft from each other. A 5.25 in. diameter hollow stem auger was used to drill the holes. The probes were installed at approximate 1 ft vertical intervals at depths from 1 to 5 ft below the shoulder surface. After drilling to the proposed depth, the probe was inserted vertically into the soil at the bottom of the drill hole and held into place with a plastic rod during backfilling. Soil cuttings, minus hand-picked gravel-sized materials, were placed back into the drill hole in 8 to 12 in. thick loose lifts and compacted with a wood dowel.

Probe leads were buried in a shallow trench that was hand excavated across the tops of the drill holes. Extensions were attached to the leads by sealing the connections with electrical tape and then passed through a 10 ft long section of PVC electrical conduit oriented perpendicular to the edge of pavement to span or cross the adjacent shallow ditch. Connections were located inside the conduit and were sealed with electrical tape. The

* An ice bath calibration was not conducted to determine the accuracy of these instruments at 0°C. The instrumentation specifications, however, indicated that the volumetric water content had a ± 0.02 m³/m³ (or $\pm 2\%$ volumetric water content) in any porous medium and ± 1 °C for temperature (ICT International, n.d.).

NHDOT team eventually determined that the sensor at a depth of 5 ft had a nick in the cable and yielded intermittent results. The extensions were draped on the ground surface from the end of the conduit to the datalogger, which was mounted on a metal post approximately 25 ft from the edge of the pavement and 4 ft from the ground surface. The logger was always above the snow and away from plowed snow banks. Excess extension wires were looped and fastened to the post with plastic wire tie fasteners and plugged into the datalogger.

The datalogger was programmed to record at 60 min intervals throughout the entire testing period to capture the seasonal variations. The NHDOT team downloaded the data as often as necessary when it was near or during the time of FWD tests. (The data was downloaded on 10 April 2014, 08 July 2014, 23 October 2014, 30 October 2014, 14 January 2015, 02 March 2015, 13 March 2015, 18 March 2015, 25 March 2015, and 01 April 2015.) The data from the moisture sensors were found to be sporadic (

Figure 14), particularly the soil moisture at the 1 ft depth. The moisture content diurnal extremes (high and low) at the 1 ft depth from May to October 2014 could potentially be due to responses from the precipitation events as the base course is designed to drain or pass excess water. However, during this timeframe, the moisture content at the 4 ft and 5 ft depths in subgrade was consistently at approximately 30% (vol.). The moisture sensors continued to provide sporadic data from January to May 2015, which was likely due to moisture intrusion (Figure 13).

Figure 15 shows the pavement temperature downloaded from 2 April 2014 to 1 April 2015. In the summer months, the base course (at a 1 ft depth) reached a temperature of near 80°F while the subgrade reached near 70°F (at a 5 ft depth). As the air temperature decreased in the fall, the pavement temperature followed its trend. Frost depth reached a 1 ft depth between 8 and 10 January 2015. The minimum temperature at a 1 ft depth was approximately 26°F, and the temperature sensor showed that the base course was frozen down to 2 ft in February 2015 (Figure 15). The frost depth measurements from the sensor did not match the frost-tube data showing maximum depth of 24 in. The maximum frost depths measured from frost tubes were 42 in. and 45 in. at FT2 and FT5, respectively

(Figure 13). These variations were likely due to different subsurface conditions (the edge of the pavement where the instruments were installed versus the frost tubes located closer to the middle of the lane).

4.5 Climate

The road is exposed to the typical northeast United States seasonal climate. CRREL and NHDOT compiled air temperature (Figure 15) and daily precipitation data (Figure 16) from the local weather station in Rochester, NH and used them to document the seasonal changes. In 2014, the precipitation events in Rochester, NH, occurred throughout the year with a maximum precipitation of 2.98 in. on 31 August 2014 and a total annual precipitation of 37 in.

In addition, the weather data from 2000 to 2015 were compiled from the National Climatic Data Center (NCDC). Appendix C compiles the data to compare 2014 and 2015 to other annual trends. The average annual precipitation from 2000 to 2014 was 42.5 in. while the total precipitation in 2014 was approximately 37 in., implying that this might have been a relatively dry year. Comparatively otherwise, 2005, 2008, and 2009 were extremely wet years with total annual precipitation of 57, 58.6, and 48.9 in., respectively.

For winters 2013–14 and 2014–15, the length of freezing days was at 164 and 145 days, respectively. When compared to the other years' freeze seasons, it is apparent that the 2013–14 and 2014–15 seasons ended at least two weeks later than all other seasons. Based on this analysis, the 2013–14 and 2014–15 freeze seasons ended unusually late. These seasons also reached lower cumulative temperatures than the average at (absolute) 1857°F-days and (absolute) 2093°F-days, respectively. Based on this data, the 2013–14 and 2014–15 winters were colder and longer than usual with potentially deeper frost depths than in other years.

Figure 14. Pavement moisture from the five 5TM combination soil temperature and moisture probes.

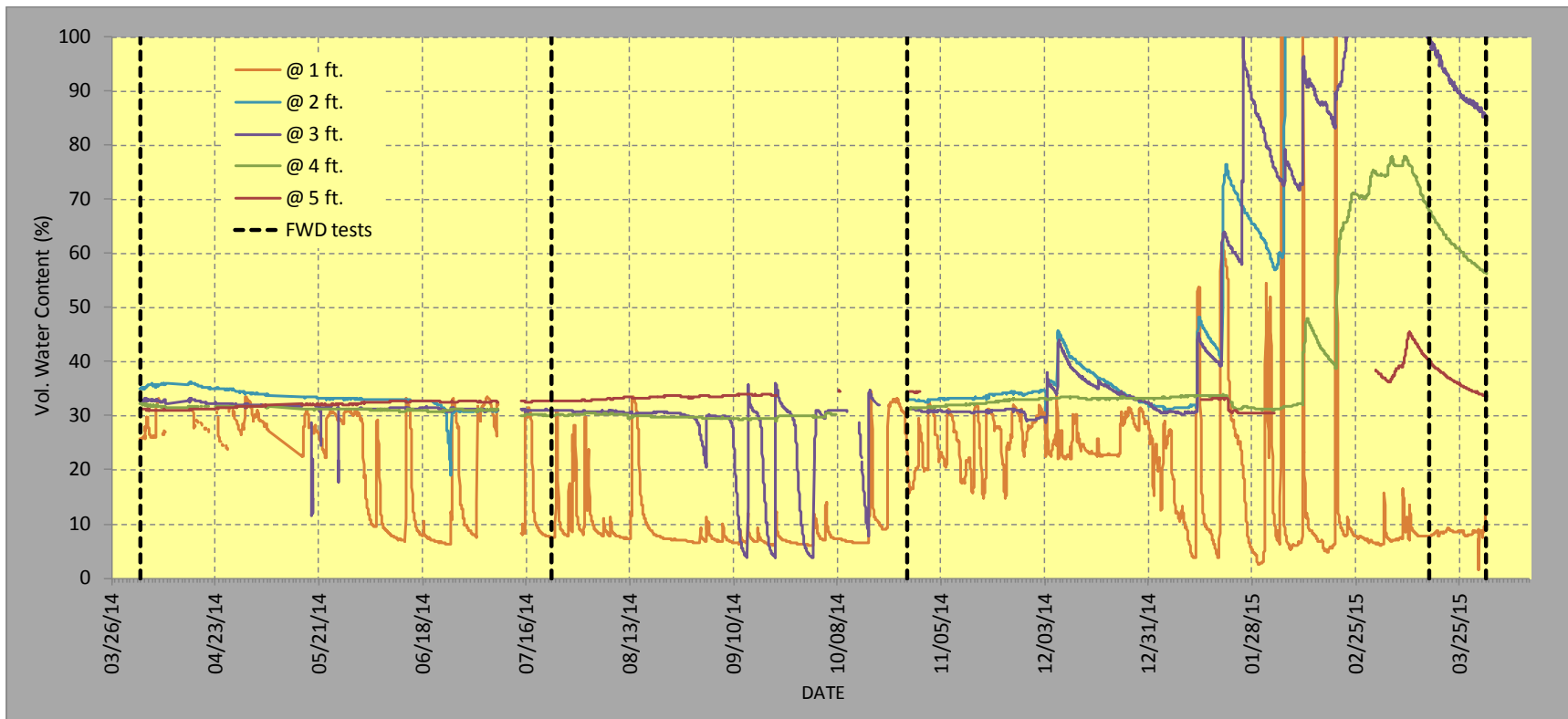


Figure 15. Pavement temperature from the five 5TM combination soil temperature and moisture probes.

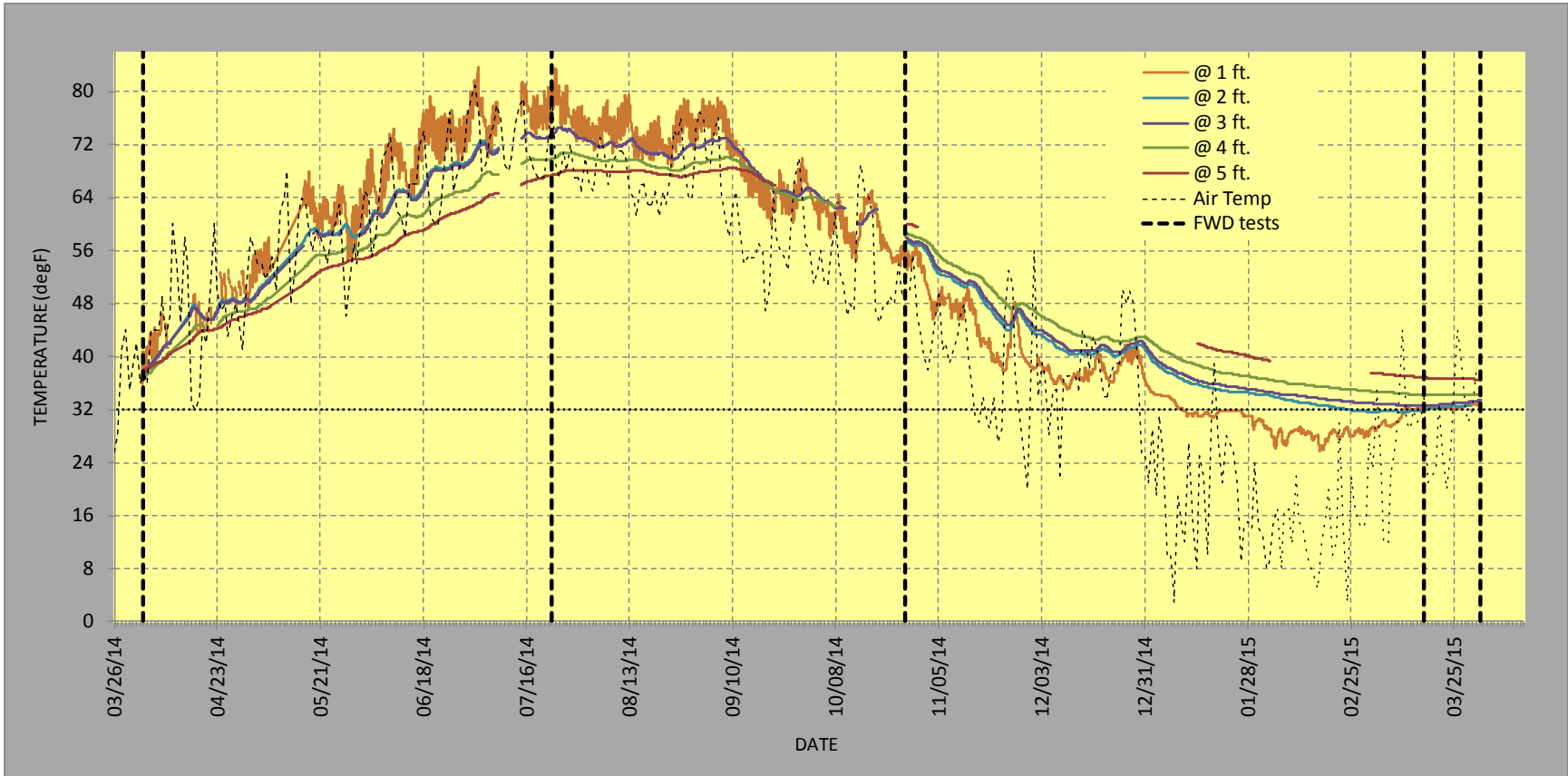
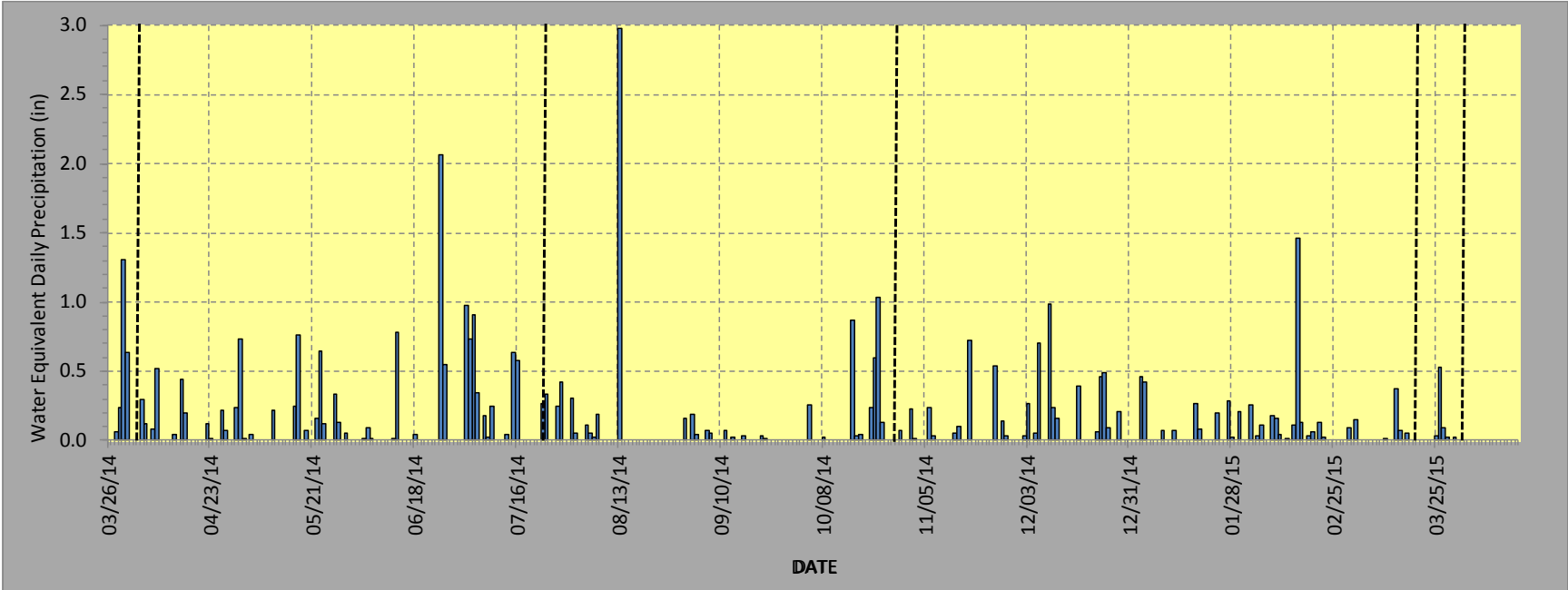


Figure 16. Daily precipitation data during the test period.



4.6 Falling weight deflectometer test

Pavement engineers have used FWD testing extensively for many years to assess structural condition and to determine the in situ moduli of pavement layers (Bush and Alexander 1985; Goel and Das 2008; Mehta and Roque 2003; Henry et al. 2009; Janoo and Berg 1992; Sharma and Stubstad 1980). In an FWD test, an impulsive load is applied on the pavement surface to mimic the vertical loading of a vehicle load at a normal speed on the road. Thus, the magnitude of the load, duration, and area of loading correlate with the standard axle loads on the pavement structure (Sebaaly et al. 1991). The instantaneous deflections of the road surface are measured at a number of points at different distances radially outward from the center of the falling weight, obtaining a bowl shape of deflection. Information on the structural condition of a pavement can be extracted from analysis (by back-calculation) of the FWD data.

The FWD tests are conducted to examine the structural benefit of the pavement reinforcement application. The CRREL team measured the surface deflection at points shown in Figure 17 by using CRREL's Dynatest 8000 FWD (Figure 19). The FWD measurements were collected with seven geophones evenly spaced 12 in. apart to a radial distance of 72 in. from the center of the loading plate. At each load and drop, the deflections (recorded in 1/1000 of an inch) captured by the geophone sensors should be in a decreasing order at increasing distance from the center of loading plate, creating a deflection basin response. In addition, the FWD collected instantaneous asphalt (using an infrared sensor) and air temperatures. Prior to testing for spring 2014, CRREL's FWD was sent in June 2013 to Pennsylvania and was calibrated following AASHTO (2010) or the ASTM equivalent. The vehicle used to tow the FWD was replaced with a new one; Dynatest in Florida connected the vehicle and the FWD and calibrated the connections and sensors before the fall 2014 testing.

CRREL conducted the FWD tests at locations (listed as FWD in Figure 17) along the wheel path and center lane for north and south directions, according to ASTM (2015a, 2015b, 2015c) and AASHTO (1993) procedures. The FWD measurements were conducted at four load settings: at approximately 6000; 10,000; 13,000; and 17,000 lb. There were four drops for each set of loading, with a total of 16 drops at each location.

4.6.1 Test Sections

From three test sections—geotextile in subgrade, geogrid in the base course with geotextile on top of the subgrade, and geogrid in the base course (Figures 17 and 18)—the test locations at each test section were selected based on representative and relatively consistent locations with similar characteristics for roadway geometry, gradient, surrounding topography, drainage, and solar exposure.

Figure 17. Test-location plan using the FWD along the test sections.

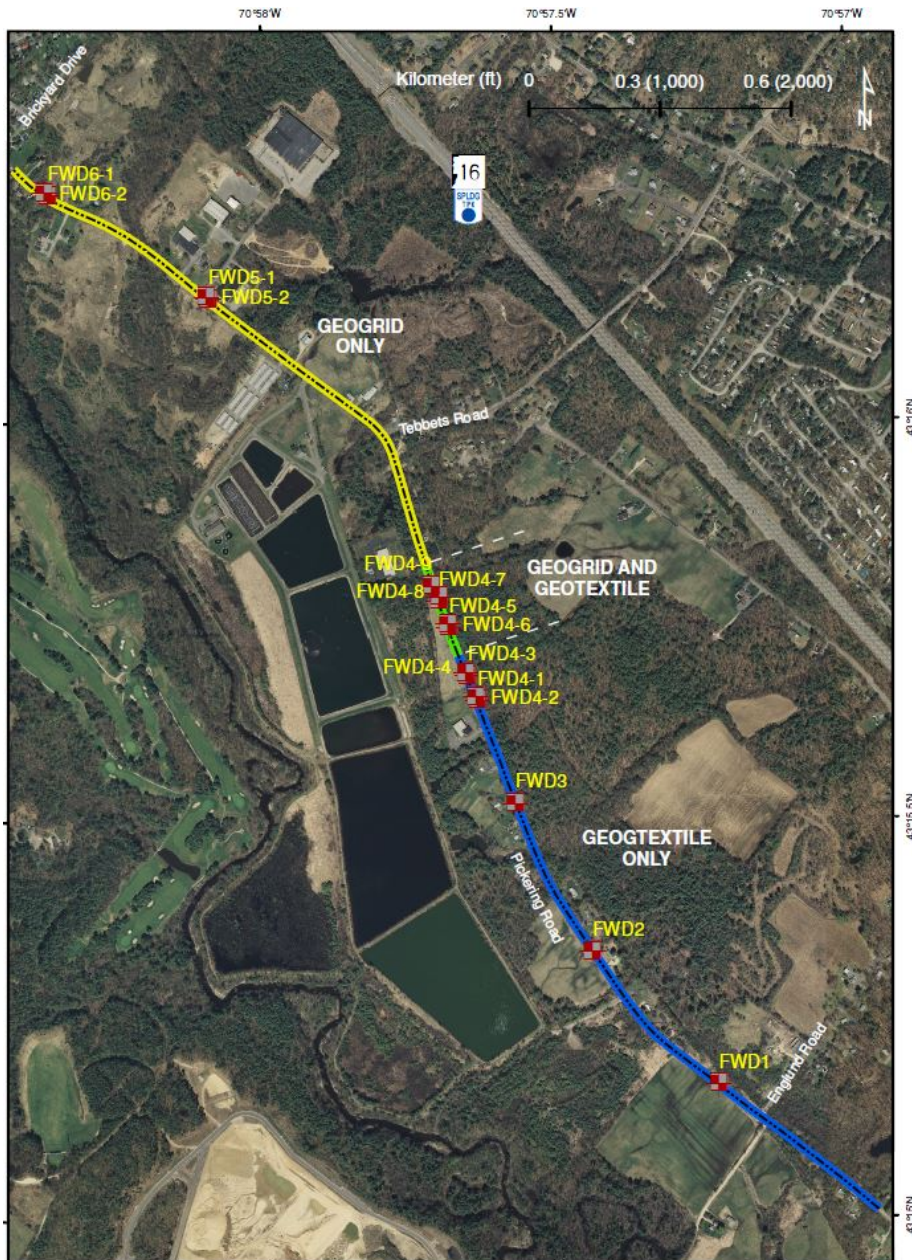
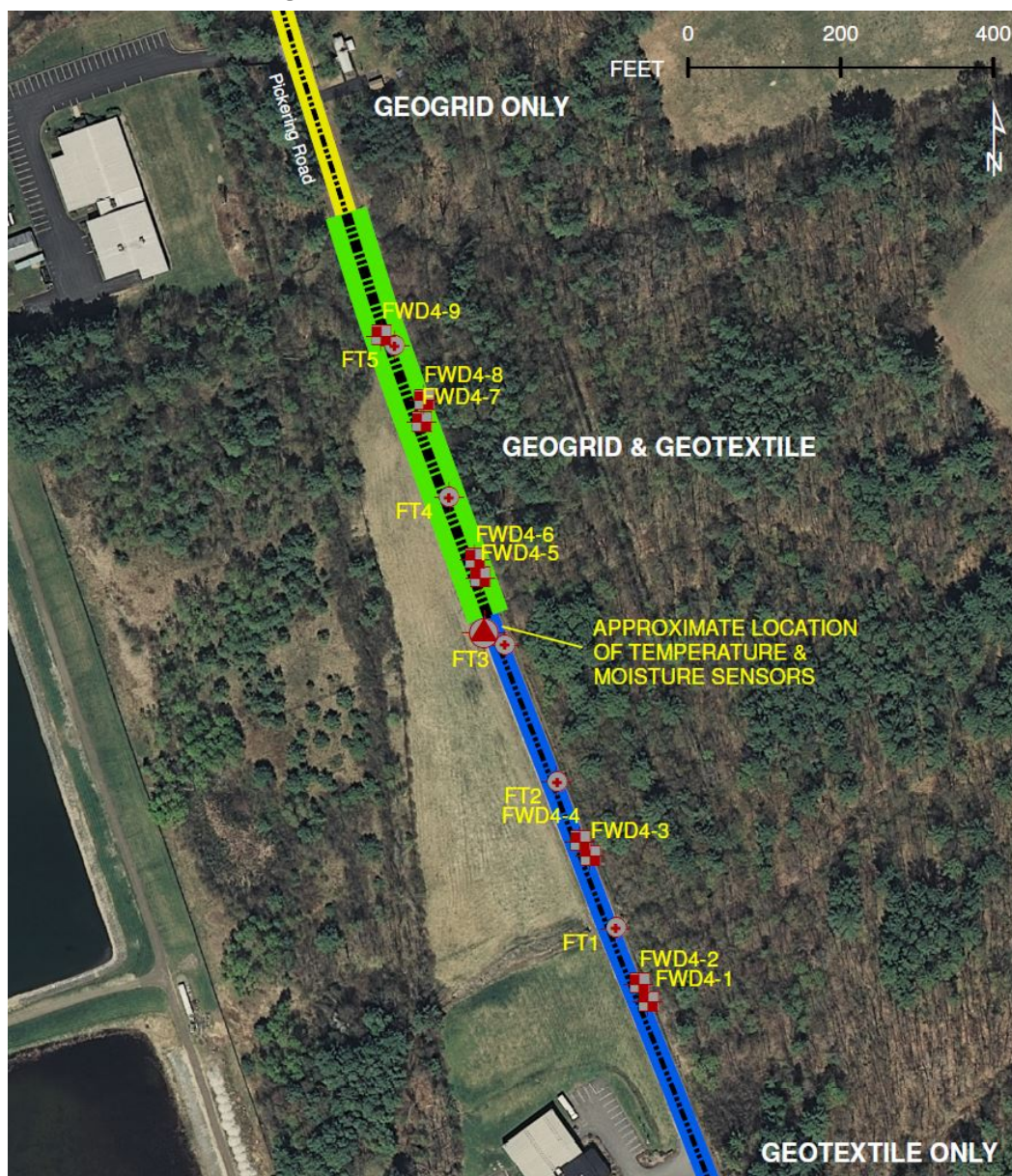


Figure 18. Close-up map of the transition area



NHDOT and CRREL selected fourteen FWD locations. Figure 7 shows the profiles of each of the test location. The test locations were divided into sections corresponding to each unique structural pavement section and thickness (Table 3). Test sections FWD1 through FWD4-4 were located with the geotextile on top of the subgrade and non-reinforced base course. Locations FWD4-5 through FWD4-9 captured geogrid in the base course with geotextile on top of the subgrade while FWD5 and FWD6 were located in test sections with geogrid in the base course. The geogrid was placed between 3 (FWD4-5 to FWD4-8) and 6 in. (FWD4-9, FWD5, and

FWD6) below the top of the base course. At each location, a set of FWD measurements were conducted along the north (N) and south (S) bound lanes in the outside (right) wheel path (W) and at the center of the lane (C). (For example, 1NW1 is a measurement at FWD1, north bound lane, wheel path and first set).

Table 3. Falling weight deflectometer (FWD) test locations.

Test Section		Northbound		Southbound		Pavement Profile			Centerline Elevation (ft)
		Wheel Path	Center	Center	Wheel Path	AC (in.)	Base (in.)	Subbase (in.)	
Geotextile at Subgrade	FWD1	1NW1	1NC1	1SC1	1SW1	0-5	5-20	20-38	146.824
	FWD2	2NW1	2NC1	2SC1	2SW1	0-5	5-12	12-41	165.218
	FWD3	3NW1	3NC1	3SC1	3SW1	0-5	5-12	12-34	162.172
	FWD4-1	4NW1	4NC1	4SC1	4SW1	0-6	6-24	24-44	162.266
	FWD4-2	4NW2	4NC2	4SC2	4SW2				162.270
	FWD4-3	4NW3	4NC3	4SC3	4SW3	0-5	5-24	24-36	162.439
	FWD4-4	4NW4	4NC4	4SC4	4SW4				162.489
Geogrid in Base Course and Geotextile at Subgrade	FWD4-5	4NW5	4NC5	4SC5	4SW5	0-5	5-19	19-34	167.088
	FWD4-6	4NW6	4NC6	4SC6	4SW6				167.758
	FWD4-7	4NW7	4NC7	4SC7	4SW7				170.106
	FWD4-8	4NW8	4NC8	4SC8	4SW8				169.795
	FWD4-9	4NW9	4NC9	4SC9	4SW9	0-5	6-20	20-34	167.732
Geogrid in Base Course	FWD5-1	5NW1	5NC1	5SC1	5SW1	0-6 ^a	6-19 ^a	19-34 ^a	160.331
	FWD5-1	5NW2	5NC2	5SC2	5SW2				160.995
	FWD6-1	6NW1	6NC1	6SC1	6SW1	0-6	6-18	18-42	171.523
	FWD6-2	6NW2	6NC2	6SC2	6SW2				171.413

NW = Northbound, wheel path

NC = Northbound, center lane

SW = Southbound, wheel path

SC = Southbound, center lane

^aEstimated

4.6.2 Falling weight deflectometer test schedule and conditions

Table 4 lists the seasonal FWD testing schedule. The conditions varied, as shown in Figure 17, with dry and wet pavement surfaces.

For testing during the spring thaw, the indication from the frost tubes of frost depth diminishing on 27 March 2014 showed that the pavement structure was completely thawed when the first FWD test was conducted

on 3 April 2014. During the 3 April 2014 test, the temperature at the base course was approximately at 37°F while the moisture in the base course was high at 2 ft depth and down to the subgrade. (Spring thaw can weaken conditions before moisture has time to redistribute). The asphalt temperature (near the surface) recorded by the FWD temperature sensor was between 45°F and 50°F.

Table 4. FWD test dates and conditions.

Seasonal Test	Date	Pavement Surface Temperature (°F)	Air Temperature (°F)	Description of Pavement Conditions
Spring	3 April 2014	44.6–55.4	44.6–48.2	Low temperature; snow in some spots in the banks; thawing conditions with high moisture in the base course and subgrade (25.6%, 35%, 32.7%, 32%, and 31% by volume at 1, 2, 3, 4, and 5 ft below the pavement surface); zero frost depth, and pavement was completely thawed; below asphalt, pavement temperature was 37 °F
	17 March 2015	35.6–42.8	33.8–37.4	Wet pavement surface from snow melt; thaw depth between 18 and 21 in. from the asphalt concrete along the wheel path and frozen layer below; snow in the banks
	1 April 2015	35.6–59	35.6–48.2	Low temperature; thawing; snow in spots in the banks
Summer	23 July 2014	75.2–120.2	— ^a	High temperature; several rain events with 7.6 in. of precipitation within one month prior to this test date; 0.3 in. of precipitation fell on this day; 30%–32.8% by volume at 3 to 5 ft below the pavement surface
Fall	27 October 2014	46.4–57.2 (a.m.)	46.2–55.4 (a.m.)	Mild temperature; 3.2 in. of precipitation within one month prior to this test date; 16% at 1 ft and 31% to 34% by volume at 2 to 5 ft below the pavement surface
		62.6–68 (p.m.)	55.4–59 (p.m.)	

^a Air temperature from the FWD sensor was not recorded.

The second FWD test was conducted on 23 July 2014 to characterize the pavement structure capacity during the summer season with a relatively dry condition. The temperatures below the asphalt pavement were 80°F and 70°F at 1 and 4 ft, respectively. The soil moisture content in the base course was lower than the previous spring (7.5% by volume at 1 ft depth below the pavement surface); however, the subbase and subgrade had high

soil moisture content (30%–32.8% by volume at 3 to 5 ft below the pavement surface). The asphalt temperature (near the surface) recorded by the FWD temperature sensor varied extremely throughout the day between 75.2°F and 120.2°F.

The conditions during the fall FWD (27 October 2014) test were almost identical to the summer conditions (23 July 2014), except that the fall temperatures below the asphalt pavement were 25°F cooler in the base course and 12°F in the subgrade (53°F at 1 ft, 57°F at 2 ft, and 3 ft, 58°F at 4 ft, and 60°F at 5 ft below the pavement surface). The soil moisture content in the base course was approximately 16% by volume at 1 ft depth below the pavement surface while the subbase and subgrade had high soil moisture content ranging from 31% to 34% by volume at 2 to 5 ft below the pavement surface.

The temperature sensors data during the 17 March 2015 test showed that the pavement temperatures were at 32.2°F, 32°F, 32.7°F, 34.2°F, and 36.9°F at 1, 2, 3, 4, and 5 ft, respectively. Soil can be frozen at temperature ranges of 29.7°F–32.2°F (Eaton 2015). In this case and based on the temperature sensors' location, a frozen layer in the pavement existed between approximately 1 ft and 2.1 ft. On the other hand, the frost tubes indicated a frost layer was present between approximately 18 and 42 in. at FT2 and between 22 and 44 in. at FT5. A partially thawed base course existed at varying depths with a frost layer at 12, 18, and 21 in. below the pavement surface and with varying thickness (of 12 to 24 in.) throughout the test section. Note that the temperature sensors and the frost tubes have spatial variability (FT2 is approximately 200 ft away south of the temperature sensors and FT5 is approximately 400 ft north of the temperature sensors (Figure 18) and is one of the causes for these inconsistencies.

The pavement conditions on 1 April 2015 showed that the temperatures were above freezing where the temperature sensors were installed (33.1°F, 33.4°F, 34.2°F, and 36.5°F at 1, 2, 4, and 5 ft, respectively). The frost tube at FT2 indicated no frost layer; at FT5, a frost layer of 16 in. was present between 18 and 44 in. below the pavement surface. Thus, it was likely that the test sections on 1 April 2015 had a varying layer of frost depth in the subbase and that in other places the pavement was totally thawed.

Figure 19. FWD along the test sections. *Top left*, 3 April 2014 at FWD4-4 southbound wheel path, 10:41 a.m.; *top right*, 17 March 2015 at FWD4-4 southbound wheel path, 10:32 a.m.; *bottom left*, 1 April 2015 at FWD4-3 southbound center lane, 12:23 p.m.; *bottom right*, 27 October 2014 at FWD4-1, southbound wheel path, 9:12 a.m.



4.6.3 Modulus estimation (back-calculation)

Back-calculation is an extremely extensive process and is primarily intended to estimate the in situ elastic modulus (E) of the different pavement layers. In this process, the deflection values are calculated for assumed elastic moduli values, then compared with the observed deflection values, and further adjusted for the next iteration. The iteration continues until the computer program obtains a minimal error between the measured and the computed deflection.

There are various models available to use for calculating the moduli from the FWD data. Each method of back-calculation has some advantages and limitations (Sharma and Das 2008). Any computer program will give a modulus value that may be obtained by minimizing the error between the measured and the computed deflection. Mehta and Roque (2003) had alerted users that, because the iterative process during back-calculation depends heavily on the initial (seed) value provided by the user, arriving at

a reasonable moduli value requires engineering judgment and thorough evaluation of all available data.

One of the programs used in our study was Pavement-Transportation Computer Assisted Structural Engineering (PCASE). The U.S. Army Corps of Engineers developed PCASE for use in the design and evaluation of roads and airfield pavements for the Army, Navy, and Air Force (current version PCASE 2.09, <https://transportation.erd.c.dren.mil/pcase/>). PCASE integrates the WESDEF program (based on the layered-elastic model) to calculate moduli for the individual pavement layers (Huang 1993). When given an initial estimate of the elastic modulus and a limiting range of moduli, the WESDEF back-calculation program uses an optimization routine to calculate the modulus of best fit between a measured deflection basin and the computed deflection basin.

The other program used in this study is the commercially available Evaluation of Layer Moduli and Overlay Design version 6 (ELMOD 6) from Dynatest, designed to calculate moduli for the individual pavement layers (Dynatest 2014). The ELMOD 6 program used the Odemark-Boussinesq method of equivalent thickness, in which the outer geophone readings are used to determine the non-linear characteristics of the subgrade and the inner geophones are used to determine the upper pavement layer moduli (Dynatest 2014). There are back-calculation methods in ELMOD 6 to select: the radius of curvature or the deflection basin fit method. The radius of curvature along with the actual or apparent non-linear subgrade properties is used to determine moduli within the pavement system. First, the subgrade material properties, stiffness and non-linearity, are calculated in ELMOD using the deflections from the outer geophones; then the radius of curvature from the central geophones can be used to assess the stiffness of the upper pavement layer. The stiffness of the remaining layers is then calculated based on the overall pavement response to the applied load. This ensures that the proposed pavement structure results in the correct central deflection under the measured load. On the other hand, the basin fit option methodology starts with a set of estimated moduli for the pavement structure and calculates the theoretical deflection bowl for the pavement structure. The error between the measured deflections and calculated deflections is then assessed. The moduli in the structure are then increased or decreased by a small amount (typically 10%), and if the error in either of these deflection bowls is less than the original deflection bowl,

this is taken to be a better solution. This process is iterated until error between the calculated and measured deflection bowls is minimal. If no seed moduli are entered using the deflection basin fit method, the program in ELMOD 6 will calculate seed values by using the radius of curvature method.

Knowing that there are a variety of back-calculation programs available to calculate the moduli values for the individual pavement layers, what is important in this analysis is to be consistent in using a specific method for the specific purpose. For a comparison, back-calculation analyses for the FWD data at Pickering Road was run using both PCASE 2.09 and ELMOD 6 and using the pavement profiles for each test section (Table 1). Appendix D shows a detailed comparison of back-calculation results between PCASE 2.09 and ELMOD 6. In this assessment, the pavement structure is composed of a three-layer system—surface course, base, and subbase—where the thickness values are entered for asphalt as a first layer, base course as a second layer, subbase as a third layer, and subgrade as the fourth layer.

In ELMOD 6, the estimated moduli values used the back-calculation approach based on the deflection basin fit method for the corresponding pavement profiles for each test section (Table 1). The back-calculations were run with seed moduli values (Table 5), and the results were comparable with the same root mean square. For consistency in our analysis, the back-calculation results are based on seed moduli values (Table 5) and with a root mean square less than or equal to 0.2. The back-calculation also uses the recorded asphalt temperature collected in the FWD infrared sensor. The average value for deflection basins from the second, third, and fourth drops is calculated for the various loadings: (approximately 6000; 10,000; 13,000; and 17,000 lb loads). The Results section describes the actual loads and the back-calculation results from ELMOD 6.

Table 5. Seed modulus used for back-calculation in the ELMOD6 program.

Material	Seed Modulus (ksi)
AC	150
Base Course	18
Subbase	12
Subgrade	6

5 Results

The results discussed in this section include the deflection measurements compared between test loads and the moduli values back-calculated between test loads and seasons using the ELMOD 6 program by Dynatest. The estimated moduli values used in the back-calculation approach are based on the deflection basin fit method. The back-calculated moduli* results reflected the pavement profile described in Table 1.

5.1 Loads and deflection

Table 6 summarizes the distribution of the actual impulse load for load settings and for all locations.

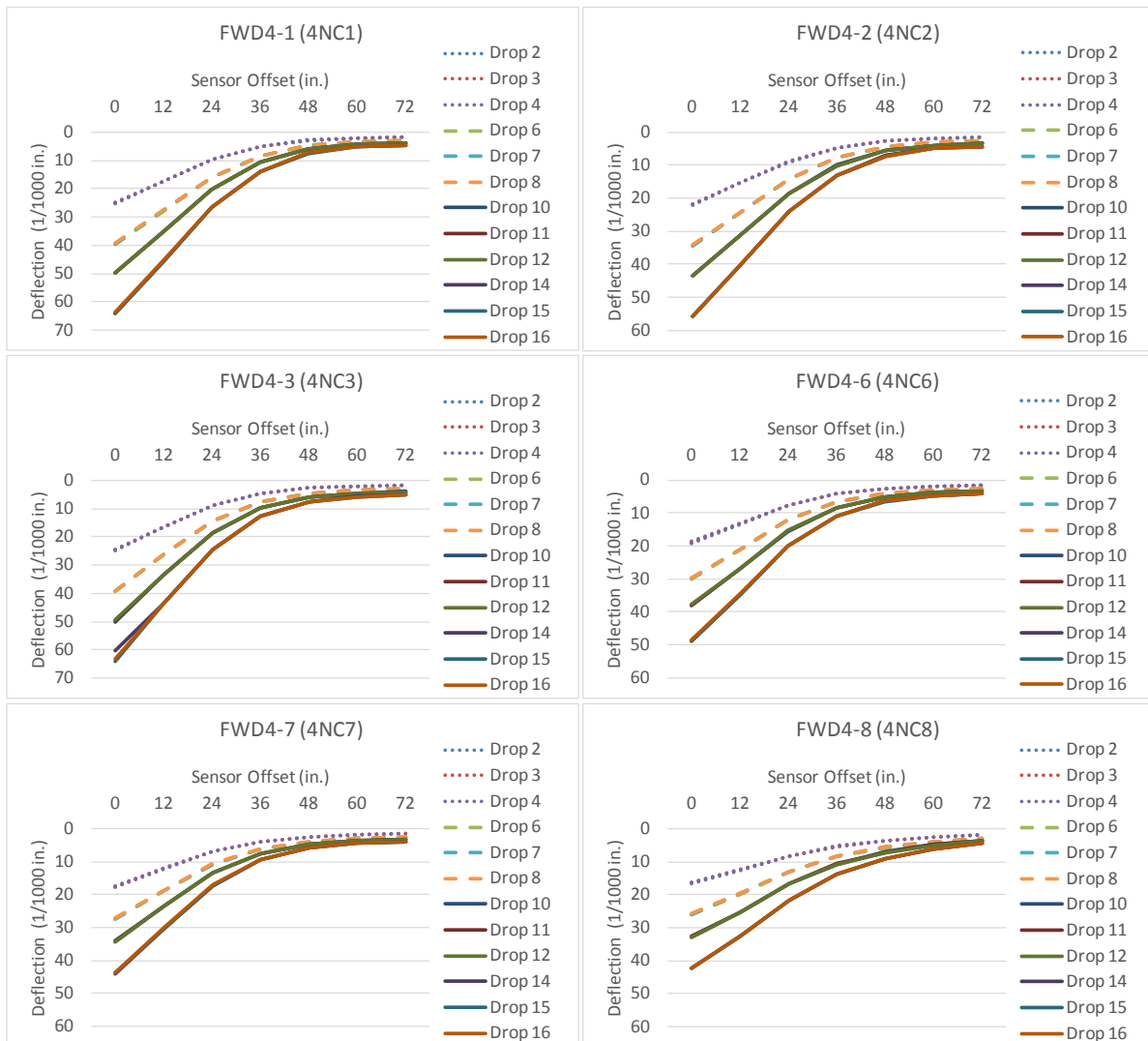
Table 6. Summary of the actual test loading distribution for four load settings and for all locations.

Loads (lb)	Drop #2-4	Drop #6-8	Drop #10-12	Drop #14-16
3 April 2014				
Average	6550	10,305	12,945	16,883
Maximum	6841	10,630	13,304	17,438
Minimum	6267	9941	12,451	16,388
23 July 2014				
Average	6290	9997	12,559	16,304
Maximum	6759	10,483	13,124	17,028
Minimum	6037	9597	12,025	15,568
27 October 2014				
Average	6158	10,004	13,066	17,191
Maximum	6595	10,450	13,764	18,193
Minimum	5840	9695	12,664	16,585
17 March 2015				
Average	6070	9209	12,593	17,199
Maximum	6431	9695	13,353	18,160
Minimum	5840	8875	12,057	16,503
1 April 2015				
Average	5956	8945	12,087	16,510
Maximum	6283	9433	13,025	17,832
Minimum	5627	8498	11,533	15,749

* The terms *back-calculated moduli* and *moduli* are used in this section interchangeably.

The average, maximum, and minimum values from the second, third and fourth drops are calculated for all four load settings. The actual loads can vary slightly, which is quite common in FWD tests. The typical deflection basins from the data collected along the test section showed lower deflection responses with lower loads and higher deflection responses with lower loads (Figure 20), and deflection responses are followed by a decreasing order at increasing distance from the center of loading plate. Figure 20 shows examples of typical deflection basin responses from the data collected along the test section. Within a set of loads, the deflection values showed very minimal variations; for example, the deflections from the second, third, and fourth drops are consistently the same. The responses are identical to other loads.

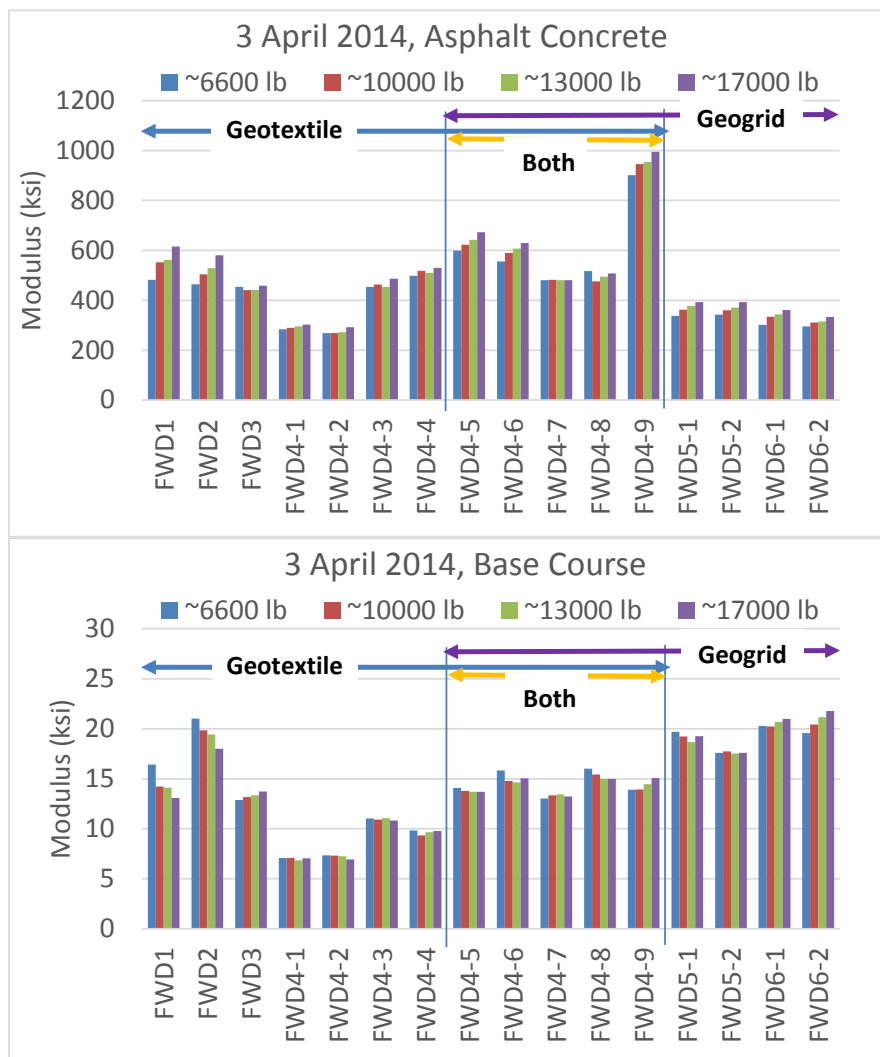
Figure 20. Deflection responses from the 3 April 2014 FWD test for selected test locations.



5.2 Moduli comparison between loads

The average values of the second, third, and fourth drops were calculated to compare the back-calculated moduli of the four load settings. For the asphalt concrete layer, the average back-calculated moduli values showed a degree of variability at each test location (Figure 21). These variations can be seen in all FWD tests for the asphalt concrete layer. However, in most cases, the average moduli values for the base-course layer at each location produced almost identical results for all four load settings. For example, at location FWD4-4 the average moduli values ranged from 498 to 530 for the asphalt concrete layer and ranged from 9 to 10 for the base-course layer. Appendix D shows the rest of the moduli comparisons between load settings.

Figure 21. Average values of back-calculated moduli for four loads.

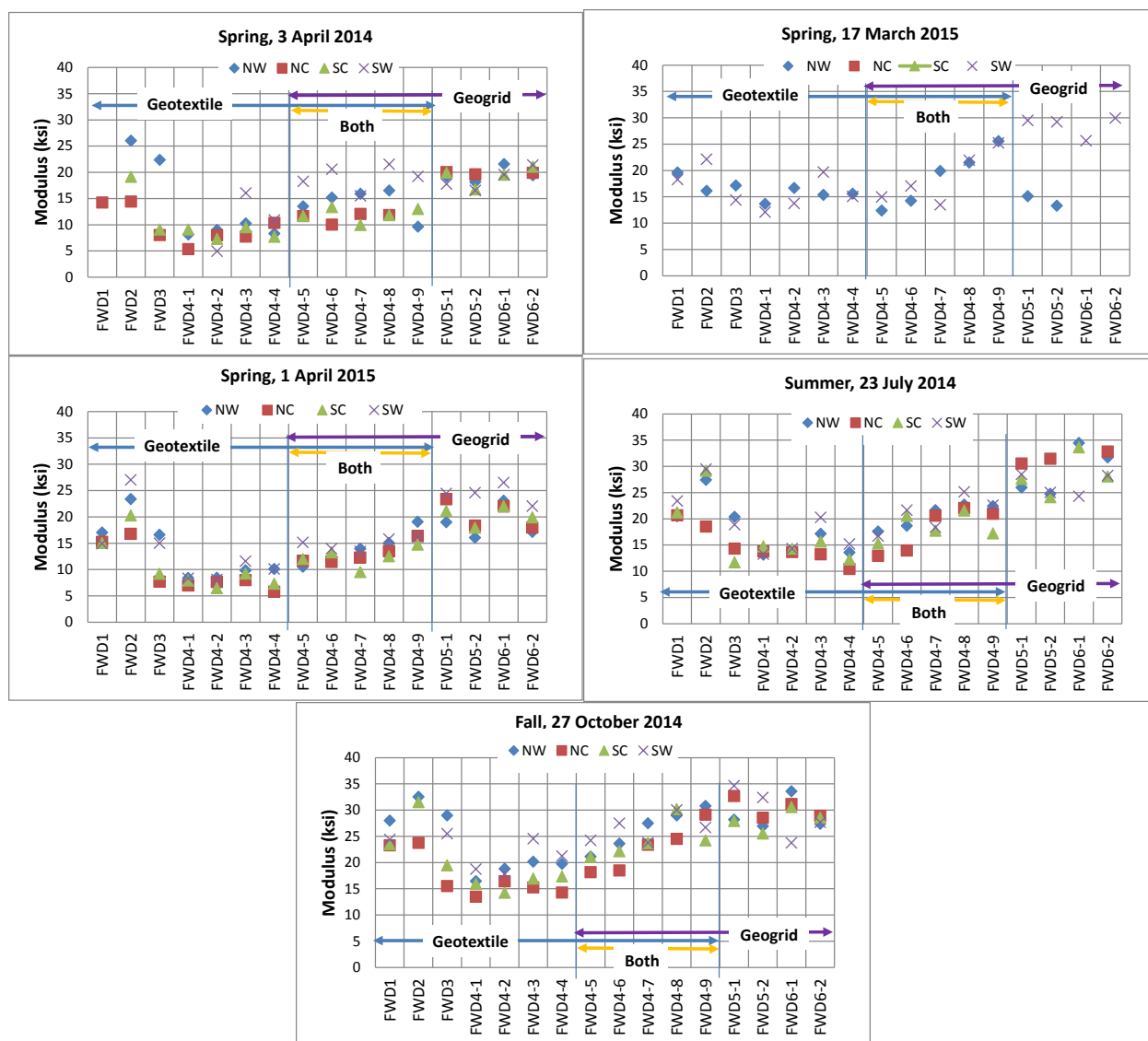


5.3 Seasonal moduli comparison

The seasonal moduli comparison used for this analysis is based on drops numbers 6, 7, and 8 in Table 6 (for the approximate 10,000 lb load). This load simulates a heavy loading condition such as that imposed by a typical FHWA Class 9 truck (18-wheeler tractor-trailer) that this road can encounter. Because the layer of interest in this study is the base course, the back-calculated modulus is compared between the wheel paths and center locations on both the north and south bound lanes. Figure 21 shows the performance between the non-reinforced and the geogrid-reinforced base course along the test sections. Within each test section (northbound, wheel paths, and southbound), the moduli showed variability (Figure 22) in most of the test locations. These variations are particularly consistent during the fall and summer moduli values. These variations in all test sections are likely to be a function of layer thickness, moisture content, drainage, topography, etc. Some of the moduli values along the wheel paths during spring tests, particularly on 3 April 2014 and 1 April 2015, were higher than in the center lanes (e.g., FWD2, FWD3, FWD4-5, etc.). Part of the factors in the moduli values' variability could be due to the presence of frost in the pavement and the trapped excess soil moisture.

The seasonal moduli values of the geogrid-reinforced and the non-reinforced base-course layer for the test locations correlated the performance with a consistent trend along the test sections from FWD1 to FWD6-2. This trend indicated that the weak sections remained relatively weak while the stronger sections maintained their relative strength from one test season to the next. The weak zones throughout the test sections were from FWD4-1 to FWD4-9 (Figure 22). The weak locations of the non-reinforced sections were along FWD4-1 through FWD4-4 and sections FWD4-5 to FWD4-9 for the reinforced sections. However, along these weak zones, the geogrid-reinforced base course provided slightly higher moduli than the non-reinforced base course (Figure 22).

Figure 22. Seasonal moduli values of reinforced and non-reinforced base-course layers for the test locations. NW means northbound wheel path; NC means northbound center lane; SW means southbound wheel path; SC means southbound center lane.



It is difficult to distinguish the influence of the geogrid location from the moduli values—the 3 in. (FWD4-5 and FWD4-8) versus the 6 in. (FWD4-9, FWD5, and FWD6) below the top of the base course. Boring information at FT3 was used to represent the profiles of geogrid being at 3 in. below the top of the base course from FWD4-5 to FWD4-8, which could likely have varying thickness along the test sections.

An average value is taken from the back-calculated modulus at the wheel paths and center locations along both the north- and southbound to compare the various FWD locations. Table 7 summarizes the back-calculated moduli for spring, summer, and fall 2014 and spring 2015 tests. In most of the test sections, the asphalt concrete layer was stiffer on 17 March 2015 than at the other times because of the temperature of the asphalt.

As shown in Figure 22, it is not unusual to discover that the moduli values in the base course are lower in the spring during thawed periods than in normal conditions (i.e., summer and fall). However, in some test locations during the 17 March 2015 test, the moduli were higher or stiffer than in the fall (27 October 2014) or comparable to summer (23 July 2014) values. This is likely because of the presence of a frozen layer between 18 and 44 in. below the pavement surface.

A modulus comparison to the ideal condition or a back-calculated ratio comparison, in this case using the fall (27 October 2014) test, is compared to other modulus to examine the difference in pavement structural responses (Table 8). The layer of interest in this study is the base course to examine the performance of the reinforced layer with geogrid and the non-reinforced section. It is difficult to discern the soil moisture conditions from the soil moisture sensors; however, based on the climate information, it can be inferred that that the pavement condition was relatively drier in the fall than in the summer as the area had relatively less precipitation in the fall than in the summer.

Examples of excessive moisture in pavement bases and subgrades are numerous and well known during springtime in New England. Conventional drainage is designed for saturated conditions, and most water movement near the surface occurs under unsaturated (and partially saturated) conditions. With excessive moisture in pavement bases and subgrades during the spring, drainage is problematic when the surface water level is high. This was a typical occurrence at Pickering Road with water ponding along the road shoulders. Positive drainage off of and away from the roadway is imperative to remove moisture from under the road which affects its load supporting capacity.

Table 7. Back-calculated layer moduli for spring, summer, and fall 2014 and spring 2015 tests.

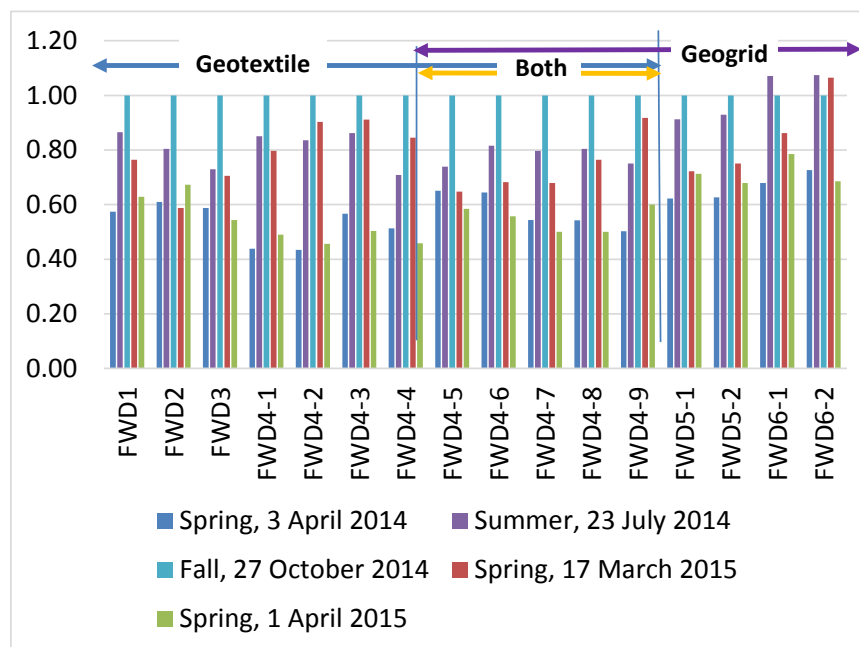
Test Section		Back-calculated Modulus (ksi)																			
		Asphalt Concrete					Base Course					Subbase					Subgrade				
Test Season		Spring, 3 April 2014	Spring, 17 March 2015	Spring, 1 April 2015	Summer, 23 July 2014	Fall, 27 October 2014	Spring, 3 April 2014	Spring, 17 March 2015	Spring, 1 April 2015	Summer, 23 July 2014	Fall, 27 October 2014	Spring, 3 April 2014	Spring, 17 March 2015	Spring, 1 April 2015	Summer, 23 July 2014	Fall, 27 October 2014	Spring, 3 April 2014	Spring, 17 March 2015	Spring, 1 April 2015	Summer, 23 July 2014	Fall, 27 October 2014
Geotextile at Subgrade	FWD1	552	1065	619	194	746	14	16	21	25	13	12	9	26	16	12	25	10	12	11	11
	FWD2	505	1192	499	241	676	20	22	22	26	33	15	10	10	23	16	12	19	13	11	17
	FWD3	441	784	437	189	537	13	12	12	16	22	9	14	7	20	15	10	17	10	9	12
	FWD4-1	290	515	324	127	398	7	8	8	14	16	8	14	9	15	11	12	23	8	9	10
	FWD4-2	268	463	306	133	412	7	8	8	14	17	8	16	7	15	10	11	18	9	10	12
Geogrid in Base Course & Geotextile	FWD4-3	463	662	455	187	601	11	10	10	17	19	9	11	7	18	12	9	21	9	10	11
	FWD4-4	519	796	442	195	581	9	8	8	13	18	6	13	5	13	9	9	20	12	8	9
	FWD4-5	622	995	636	217	744	14	12	12	16	21	8	10	6	17	11	10	24	10	9	11
	FWD4-6	590	954	563	220	717	15	13	13	19	23	10	9	7	21	14	9	22	11	9	11
	FWD4-7	482	724	521	214	652	13	12	12	20	25	10	12	8	25	18	9	18	10	11	12
Geogrid in Base Course	FWD4-8	476	629	498	260	673	15	14	14	23	28	11	12	10	32	18	11	18	11	12	14
	FWD4-9	946	622	435	295	885	14	17	17	21	28	5	13	9	18	9	12	25	13	9	14
	FWD5-1	362	875	630	157	648	19	22	22	28	31	14	14	12	21	13	10	21	12	9	14
	FWD5-2	360	946	669	164	637	18	19	19	26	28	14	13	10	21	14	10	23	13	9	13
	FWD6-1	335	487	424	190	490	20	23	23	33	30	18	16	17	26	19	13	25	13	11	13
FWD6-2	311	602	443	185	512	20	19	19	30	28	16	16	14	25	18	12	28	12	11	14	

Table 8. Back-calculated ratio comparison for spring, summer, and fall 2014 and spring 2015 tests.

Layers		Asphalt Concrete					Base Course					Subbase				
Test Season		Spring, 3 April 2014	Spring, 17 March 2015	Spring, 1 April 2015	Summer, 23 July 2014	Fall, 27 October 2014	Spring, 3 April 2014	Spring, 17 March 2015	Spring, 1 April 2015	Summer, 23 July 2014	Fall, 27 October 2014	Spring, 3 April 2014	Spring, 17 March 2015	Spring, 1 April 2015	Summer, 23 July 2014	Fall, 27 October 2014
Geotextile at Subgrade	FWD1	0.74	1.43	0.83	0.26	1	0.57	0.76	0.63	0.86	1	0.85	0.77	0.58	1.66	1
	FWD2	0.75	1.76	0.74	0.36	1	0.61	0.59	0.67	0.80	1	0.94	0.65	0.65	1.48	1
	FWD3	0.82	1.46	0.81	0.35	1	0.59	0.71	0.54	0.73	1	0.63	0.96	0.46	1.36	1
	FWD4-1	0.73	1.29	0.81	0.32	1	0.44	0.80	0.49	0.85	1	0.71	1.29	0.79	1.35	1
	FWD4-2	0.65	1.13	0.74	0.32	1	0.43	0.90	0.46	0.84	1	0.78	1.62	0.68	1.49	1
Geogrid in Base Course & Geotextile	FWD4-3	0.77	1.10	0.76	0.31	1	0.57	0.91	0.50	0.86	1	0.69	0.89	0.56	1.43	1
	FWD4-4	0.89	1.37	0.76	0.34	1	0.51	0.84	0.46	0.71	1	0.73	1.44	0.60	1.50	1
	FWD4-5	0.84	1.34	0.86	0.29	1	0.65	0.65	0.58	0.74	1	0.76	0.89	0.57	1.57	1
	FWD4-6	0.82	1.33	0.78	0.31	1	0.64	0.68	0.56	0.82	1	0.70	0.63	0.49	1.47	1
	FWD4-7	0.74	1.11	0.80	0.33	1	0.54	0.68	0.50	0.80	1	0.55	0.70	0.47	1.41	1
Geogrid in Base Course	FWD4-8	0.71	0.93	0.74	0.39	1	0.54	0.76	0.50	0.80	1	0.61	0.66	0.57	1.76	1
	FWD4-9	1.07	0.70	0.49	0.33	1	0.50	0.92	0.60	0.75	1	0.57	1.36	0.99	1.91	1
	FWD5-1	0.56	1.35	0.97	0.24	1	0.62	0.72	0.71	0.91	1	1.07	1.10	0.89	1.63	1
	FWD5-2	0.57	1.49	1.05	0.26	1	0.63	0.75	0.68	0.93	1	0.98	0.94	0.70	1.49	1
	FWD6-1	0.68	0.99	0.87	0.39	1	0.68	0.86	0.79	1.12	1	0.92	0.84	0.89	1.34	1
FWD6-2	0.61	1.17	0.86	0.36	1	0.73	1.06	0.69	1.07	1	0.89	0.89	0.80	1.42	1	

Although pavement practitioners expected that pavement structures would be the stronger in summer conditions than in other seasons, the back-calculated ratio comparison from the five FWD tests to assess the seasonal performance indicated that the moduli values during the fall FWD were the highest (Figure 23). The back-calculated ratio comparison between 27 October 2014 and 17 March 2015 shows that higher moduli values exist because of the frozen layer 18 and 44 in. below the pavement surface. The moduli values for the other spring FWD test were indicative of spring thaw responses on performance.

Figure 23. Seasonal moduli values of the base-course layer for the test locations.



5.4 Base-course equivalent thickness

To relate the non-reinforced base-course sections (the sections without geogrid) to the reinforced base course with a TriAx TX 160 geogrid, we conducted a back-calculation analysis by reducing the thickness of the reinforced base course. This is an iterative analysis to estimate the equivalent thickness so that the modulus value of the non-reinforced base course is similar to the modulus value of the reinforced base course by using the basin fit option and using the same seed modulus value in Table 5 in ELMOD6. The adjacent test sections, which are FWD4-1 to FWD 4-9, were analyzed and compared because these test sections were relatively

close to each other. An 18 to 19 in. range of non-reinforced base course is equivalent to a range of 8 to 11 in. of reinforced base course with a TriAx TX 160 geogrid (Table 9). The estimated equivalent thicknesses are based on the road conditions observed on Pickering Road and may not be the same in other locations. In this case, a reinforced base course with a TriAx TX 160 geogrid in this location and under these conditions indicated a significant performance increase. In these test sections, the reinforced base-course sections with a TriAx TX 160 geogrid provided a reduction of thickness between 1.5–1.7 times that of the non-reinforced ones due to the (added) stiffness of the grid mesh. Or, the aggregate layer thickness can be reduced 33%–42% with reinforcement in the base course. However, these numbers are based just on the moduli values by backing out what the thickness would be and do not account for other factors affecting the performance, such as moisture content, drainage, topography, frost penetration, etc. In addition, the reduction in thickness is evaluated based only on the stiffness performance. The results for the pavement structure do not account for other performance factors, such as deformation, fatigue, and thermal cracking

Table 9. Non-reinforced and reinforced base-course equivalent thickness and moduli values.

Test Section		Base-Course Layer Thickness, in.		3 April 2014 Moduli (ksi)	1 April 2015 Moduli (ksi)	27 October 2014 Moduli (ksi)
Non-reinforced Base Course (Geotextile at subgrade)	FWD4-1	18	Actual thickness	7	8	16
	FWD4-2			7	8	17
	FWD4-3	19		11	10	19
	FWD4-4			9	8	18
Reinforced Base Course (Geogrid in base course & geotextile at subgrade)	FWD4-5	12	Equivalent or modified thickness	6	4	17
	FWD4-6			8	4	17
	FWD4-7			8	6	15
	FWD4-8			11	5	18
	FWD4-9	11		9	8	20

It is important to note that the results provided in this study reflected only the seasonal conditions and environmental factors at Pickering Road and for the type of geogrid used. Reduction in thickness due to a reinforced base-course layer may differ from one region to another with varying seasonal and environmental conditions.

6 Summary and Conclusions

For many years, pavement researchers have studied reinforced base course with geogrid. These studies claimed that the use of geogrid at the unbound aggregate have helped to improve pavement performance and to extend service life. To date, the effectiveness of geogrid continues to be a controversy with regard to the degree of aggregate–grid interlock, the quality of the base-course materials, and the installation locations or position of the grid in the pavement structure.

This study encompassed the seasonal assessment by using a non-destructive method (i.e., FWD tests on selected dates) at Pickering Road, in Rochester, NH, to provide a comparative assessment between the reinforced and non-reinforced base course.

For the Rochester, NH, area, frost penetration was measured as between 33 and 38 in. in the 2014 winter and spring. The maximum depth of frost in 2015 was 42 to 45 in. The 2013–14 winter had 1031.6°C freezing degree-days (higher than the average of 708.3°C) and the 2014–15 winter was at 1162.4°C freezing degree-days—the highest of the last 15 measured years. Both years were much colder and longer than average.

The modulus (strength) of the asphalt concrete was nine times that of the base and subbase courses and 25 times that of the subgrade (Table 5) during most of the year. However, the summer modulus of the asphalt (when the pavement surface temperature was greater than 120°F) was approximately one-third of the spring or fall values when the pavement temperature is below 90°F (Table 7).

The seasonal modulus (strength) for the geogrid (reinforced) and non-reinforced base-course layer can be summarized as follows:

- The fall modulus values had a higher stiffness than other seasons, with lower stiffness during the spring thawing period than the normal conditions (i.e., summer and fall).
- The performance along the test sections showed a consistent trend or similar pattern from one FWD test to another. This trend indicated

that the weak sections remained relatively weak while the stronger sections maintained their relative strength from one test season to the next.

- The weak zones throughout the test sections were from FWD4-1 to FWD4-9.
- The weak locations of the non-reinforced base-course (a geotextile separator between only the subgrade soil and the subbase course) sections were along FWD4-1 through FWD4-4.
- The weak sections FWD4-5 to FWD4-9 were along the reinforced sections with a geogrid reinforcement within the base course and a geotextile separator between the subgrade and the base course.
- Overall, the geogrid-reinforced base course provided higher moduli than the non-reinforced base-course (a geotextile separator between only the subgrade soil and the subbase course) sections.

Because of the added stiffness effect of the grid mesh, the 11 to 12 in. geogrid-reinforced base course with a TriAx TX 160 in this study was equivalent to 18–19 in. of base course without geogrid. In other words, the aggregate layer thickness can be reduced to 33%–42% with reinforcement in the base course. However, these numbers are based on just the moduli values by backing out what the thickness would be and do not account for other attributable factors affecting the performance, such as moisture content, drainage, topography, etc. In addition, we assessed the reduction in thickness based only on the stiffness performance. The results do not account for other performance factors, such as deformation, fatigue, and thermal cracking.

7 Recommendations

For better and more definitive answers, we recommend constructing a more representative test by using 200–300 ft long test sections with fewer variables. The study should have uniform subgrades with the same water table, identical pavement thicknesses, similar drainage conditions, the same topography, and similar traffic conditions to compare geogrid (at the top of the base, in the middle of the base course, and at the base-course and subgrade interface), geotextile, and no reinforcement. The study should assess the overlaps at transverse and longitudinal connections of joints. In addition, the test should include a better instrumentation scheme and increased monitoring of subsurface conditions for better characterization of the non-reinforced and reinforced base-course performance.

A thorough geogrid cost-benefit analysis should be evaluated for further study. The assessment should examine not only the purchase price of the geogrid and the savings from reduced base and subbase-course materials but also the added installation cost during the construction, the long-term maintenance, and the performance costs and savings (with potentially less resultant cracking, etc.).

To reduce the construction, maintenance, and operations resources and to increase pavement life, we recommend that new products be evaluated under the New Hampshire environmental, traffic, and soil conditions to optimize the transportation system.

References

- AASHTO (American Association of State Highway and Transportation Officials). 1993. *Guide for Design of Pavement Structures*. Washington, DC: American Association of State Highway and Transportation Officials.
- . 2010. Calibrating the Load Cell and Deflection Sensors for a Falling Weight Deflectometer. R32-09. In *Standard Specifications for Transportation Materials and Methods of Sampling and Testing, Part 1B: Specifications*. Washington, DC: Association of State Highway and Transportation Officials.
- Al-Qadi, I. L., S. H. Dessouky, K. Jayhyun, and E. Tutumluer. 2008. Geogrid in Flexible Pavements: Validated Mechanism. *Transportation Research Record: Journal of the Transportation Research Board* 2045:102–109.
- Al-Qadi, I. L., S. H. Dessouky, J. Kwon, and E. Tutumluer. 2012. Geogrid-Reinforced Low-Volume Flexible Pavements: Pavement Response and Geogrid Optimal Location. *Journal of Transportation Engineering* 138:1083–1090.
- ASTM International. 2015a. *Standard Guide for Calculating In Situ Equivalent Elastic Moduli of Pavement Materials Using Layered Elastic Theory*. ASTM D5858-96. Philadelphia, PA: ASTM International.
- . 2015b. *Standard Test Method for Deflections with a Falling-Weight-Type Impulse Load Device*. ASTM D4696-09. Philadelphia, PA: ASTM International.
- . 2015c. *Standard Guide for General Pavement Deflection Measurements*. ASTM D4695-03. Philadelphia, PA: ASTM International.
- Austin, R. A., and A. J. T. Gilchrist. 1996. Enhanced Performance of Asphalt Pavements Using Geocomposites. *Geotextile and Geomembranes* 14:175–86.
- Bocci, M., A. Grilli, F. A. Santagata, and A. Virgili. 2007. Influence of Reinforcement Geosynthetics on Flexion Behaviour of Double-Layer Bituminous Systems. In *International Conference on Advanced Characterisation of Pavement and Soil Engineering Materials*, 1415–1424.
- Brown, S. F., N. H. Thom, and P. J. Sanders. 2001. A Study of Grid Reinforced Asphalt to Combat Reflection Cracking. *Association Asphalt Paving Technologists* 70:543–569.
- Bush, A. J., III, and D. R. Alexander. 1985. Pavement Evaluation Using Deflection Basin Measurements and Layered Theory. *Transportation Research Record* 1022:16–28.
- Cancelli, A., and F. Montanelli. 1999. In-Ground Test for Geosynthetic Reinforced Flexible Paved Roads. In *Proceedings of Geosynthetics '99, April, Boston, MA*, 2:863–878.
- Doré, G., and H. Zubeck. 2009. *Cold Regions Pavement Engineering*. Reston, VA: American Society of Civil Engineers Press.

- Dynatest. 2014. "ELMOD 6" Dynatest International A/S, Denmark
<http://dynatest.com/pavement-engineering/downloads/software/program-trials/the-elmod%C2%AE-ver-6-program.aspx> (accessed May 2014).
- Eaton, R. 2015. Personal communication on temperature frozen soils. CRREL and NHDOT pavement researcher, retired.
- Goel, A., and A. Das. 2008. Non-destructive Testing of Asphalt pavements For Structural Condition Evaluation: a State of the Art. *Nondestructive Testing and Evaluation* 23 (2): 121–140
- Hass, R., J. Walls, and R. G. Carroll. 1988. Geogrid Reinforcement of Granular Bases in Flexible Pavements. *Transportation Research Record* 1188:19–27.
- Henry, K. S., E. R. Cortez, L. S. Danyluk, G. Brentrup, N. Lamie, and T. W. Arnold. 2008. Construction and Instrumentation of Full-Scale Geogrid Reinforced Pavement Test Sections. ERDC/CRREL TR-08-6. Hanover, NH: U.S. Army Engineer Research and Development Center.
<http://www.crrel.usace.army.mil/library/technicalreports/ERDC-CRREL-TR-08-6.pdf>.
- Henry, K. S., J. Clapp, W. Davids, D. Humphrey, and L. Barna. 2009. *Structural Improvements of Flexible Pavements Using Geosynthetics for Base Course Reinforcement*. ERDC/CRREL TR-09-11. Hanover, NH: U.S. Army Engineer Research and Development Center.
- Huang, Y. H. 1993. *Pavement Analysis and Design*. Englewood Cliffs, NJ: Prentice Hall.
- ICT International. n.d. Decagon 5TM VWC + Temp. Armidale, Australia: ICT International. http://www.ictinternational.com/pdf/?product_id=255 (accessed 9 October 2014).
- Janoo, V. C., and R. L. Berg. 1992. Layer Moduli Determination During Freeze-Thaw Periods. *Transportation Research Record* 1377:26–35.
- Kinney, T., J. Abbott, and J. Schuler. 1998a. Benefits of Using Geogrids for Base Reinforcement with Regard to Rutting. *Transportation Research Record* 1611:86–96.
- . 1998b. Using Geogrids for Base Reinforcement as Measured by Falling Weight Deflectometer in Full-Scale Laboratory Study. *Transportation Research Record* 1611:70–77.
- Kwon, J., E. Tutumluer, I. Al-Qadi, and S. Dessouky. 2008. Effectiveness of Geogrid Base-Reinforcement in Low-Volume Flexible Pavements. In *Proceedings of GeoCongress 2008: Geosustainability and Geohazard Mitigation, 9–12 March, New Orleans, LA*, GSP 178:1057–1064. Reston, VA: American Society of Civil Engineers.
- Mehta, Y., and R. Roque. 2003. Evaluation of FWD Data for Determination of Layer Moduli of Pavements. *Journal of Materials in Civil Engineering* 15:25–31.

- Raymond, G., and I. Ismail. 2003. The Effect of Geogrid Reinforcement on Unbound Aggregates. *Geotextile and Geomembranes* 21 (6): 355–380.
- Ricard, A., W. Tobiasson, and A. Greatorex. 1976. *The Field Assembled Frost Gage*. Technical Note. Hanover, NH: U.S. Army Cold Regions Research and Engineering Laboratory.
- Sanders, R. 2014. Personal communication on road construction and as-built information. Durham, NH: NHDOT District 6.
- Sebaaly, P. E., N. Tabatane, and T. Scullion. 1991. Comparison of Backcalculated Moduli from Falling Weight Deflectometer and Truck Loading. *Transportation Research Record* 1377:17–25.
- Sharma, J., and R. N. Stubstad. 1980. Evaluation of Pavement in Florida by Using Falling Weight Deflectometer. *Transportation Research Record* 755:42–48.
- Sharma, S., and A. Das. 2008. Backcalculation of Pavement Layer Moduli from Falling Weight Deflectometer Data using an Artificial Neural Network. *Canadian Journal of Civil Engineering* 35:57–66.
- Shu, X., H. Wu, S. Zhao, and B. Huang. 2014. Evaluating Geogrid Performance with Loaded Wheel Tester. *Ground Improvement and Geosynthetics* GSP 238:363–369.
- Zornberg, J. G. 2015. Geosynthetic Reinforcements For Paved Roads. <http://gr2015.net.br/trabalhos-arquivos/arquivos/5384.pdf> (accessed 12 September 2015).
- Zornberg, J. G., and R. Gupta. 2009. Reinforcement of Pavements over Expansive Clay Subgrades. In *Proceedings of the Seventeenth International Conference of Soil Mechanics and Geotechnical Engineering, 5–9 October, Alexandria, Egypt*, 765–768.
- . 2010. Geosynthetics in Pavements: North American Contributions. Theme Speaker Lecture. In *Proceedings of the 9th International Conference on Geosynthetics, Guarujá, Brazil*, 1:379–400.

Appendix A: Pickering Road Construction Background, Geogrid Specification, and Cross Sections

ROCHESTER 15863

Roadway: Pickering Road; Rochester, NH

SRI: N3890505

Project Length: 2.0 miles

Project Limits: From pavement joint just south of Brickyard Drive (Urban Compact) southerly to pavement joint south of England Road (end of State Maintenance).

Construction Timeline:

- 2010: 5 asphalt cores were taken in support of the project design phase. Base course sampling was performed at all 5 locations to a depth of 5 feet below the pavement. Grain Size analyses were performed on all recovered samples. See attached core report. See LIMS for gradation results.
- 2011: Full box reconstruction with 3 inches of new HBP (3" binder). Work was performed under contract: Rochester 15863. Contractor was Pike Industries with bid of \$993,460.
- 2012: 1-inch wearing course overlay to increase total pavement thickness to 4 inches. Work was performed as part of the Resurfacing District 6 16166A contract. Contractor was Continental Paving.

Soil Reinforcement:

- Tensar Triax TX160 Geogrid
 - Product was donated by Tensar. Approx. 20,000 SYs
 - Special Provision for Item 415.9, Triax Geogrid Installation, was created for this project. Pike bid \$0.30/SY for a total of \$15,394/SYs



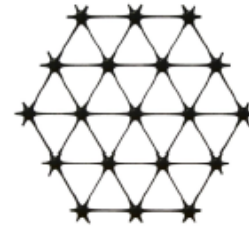
Product Specification - TriAx® TX160 Geogrid

Tensor International Corporation reserves the right to change its product specifications at any time. It is the responsibility of the person specifying the use of this product and of the purchaser to ensure that product specifications relied upon for design or procurement purposes are current and that the product is suitable for its intended use in each instance.

Tensor TriAx® Geogrid

General

1. The geogrid is manufactured from a punched polypropylene sheet, which is then oriented in three substantially equilateral directions so that the resulting ribs shall have a high degree of molecular orientation, which continues at least in part through the mass of the integral node.
2. The properties contributing to the performance of a mechanically stabilized layer include the following:



Index Properties	Longitudinal	Diagonal	Transverse	General
<ul style="list-style-type: none"> ▪ Rib pitch⁽²⁾, mm (in) ▪ Mid-rib depth⁽²⁾, mm (in) ▪ Mid-rib width⁽²⁾, mm (in) ▪ Rib shape ▪ Aperture shape 	40 (1.60)	40 (1.60)	-	Rectangular Triangular
	-	1.6 (0.06)	1.4 (0.06)	
	-	1.0 (0.04)	1.2 (0.05)	
Structural Integrity				
<ul style="list-style-type: none"> ▪ Junction efficiency⁽³⁾, % ▪ Radial stiffness at low strain⁽⁴⁾, kN/m @ 0.5% strain (lb/ft @ 0.5% strain) 				93 300 (20,580)
Durability				
<ul style="list-style-type: none"> ▪ Resistance to chemical degradation⁽⁵⁾ ▪ Resistance to ultra-violet light and weathering⁽⁶⁾ 				100% 70%

Dimensions and Delivery

The TX geogrid shall be delivered to the jobsite in roll form with each roll individually identified and nominally measuring 3.0 meters (9.8 feet) and/or 4.0 meters (13.1feet) in width and 75 meters (246 feet) in length.

Notes

1. Unless indicated otherwise, values shown are minimum average roll values determined in accordance with ASTM D4759-02. Brief descriptions of test procedures are given in the following notes.
2. Nominal dimensions.
3. Load transfer capability determined in accordance with ASTM D6637-10 and ASTM D7737-11 and expressed as a percentage of ultimate tensile strength.
4. Radial stiffness is determined from tensile stiffness measured in any in-plane axis from testing in accordance with ASTM D6637-10.
5. Resistance to loss of load capacity or structural integrity when subjected to chemically aggressive environments in accordance with EPA 9090 immersion testing.
6. Resistance to loss of load capacity or structural integrity when subjected to 500 hours of ultraviolet light and aggressive weathering in accordance with ASTM D4355-05.

Tensor International Corporation
 2500 Northwinds Pkwy.
 Atlanta, Georgia 30009
 Phone: 800-TENSAR-1
www.tensorcorp.com

This specification supersedes any and all prior specifications for the product designated above and is not applicable to any product shipped prior to January 31, 2014. Tensor and TriAx are trademarks of Tensor International Corporation or its affiliates in the US and many other countries. TriAx® geogrid and the use thereof are protected by U.S. Patent No. 7,001,112. Patents or patent applications also exist in other countries. Final determination of the suitability of the above-mentioned information or product for the use contemplated, and its manner of use are the sole responsibility of the user. Tensor International Corporation disclaims any and all express, implied or statutory warranties, including but not limited to, any warranty of merchantability or fitness for a particular purpose regarding this product or the Company's other products, technologies or services. The information contained herein does not constitute engineering advice.
 TX_SPEC_TX160_2.14

**State of New Hampshire Department of Transportation
Bureau of Materials and Research**

Cr. Stone Fine (304.4)

Sample ID:	AA65506	Federal No:	
Project:	ROCHESTER	Source:	Brox Ind
Proj No:	15863	Report to:	Ralph Sanders
NH Lab No:		Submittal	10/5/2011
Material:	Cr Stone Fine	Sample	10/3/2011
Sampled from:	Stockpile Rochester	Sampled by:	R. SANDERS
Lot #:			
Purpose:	304.4 Cr. Stone Fine		
Analysis Validated by:	JA	Date:	10/10/2011
		Sample Validated	JA
		Date:	10/10/2011

Remarks:

METHOD	ANALYSIS	RESULT	UNIT	MIN	MAX	VIOLATIONS
	Tested By:	RD				
T27	2 in (50 mm) Sieve	100.0	% Passing	100		
T27	1 1/2 in (37.5 mm) Sieve	94.5	% Passing	85	100	
T27	1 in (25 mm) Sieve	60.3	% Passing			
T27	3/4 in (19 mm) Sieve	42.2	% Passing	45	75	Failed
T27	1/2 in (12.5 mm) Sieve	30.5	% Passing			
T27	#4 (4.75 mm) Sieve	19.54	% Passing	10	45	
T27	#10 (2.00 mm) Sieve	78.1	% Passing			
T27	#20 (0.850 mm) Sieve	56.7	% Passing			
T27	#40 (0.425 mm) Sieve	41.5	% Passing			
T27	#100 (0.150 mm) Sieve	27.89	% Passing			
T27	#200 (0.075 mm) Sieve	17.26	% Passing			
T27	% Passing #200 in Total Sample	3.37	% Passing	0	5	

Comments: There will not be a proctor test performed on this material to establish a maximum dry density. The material retained on the #4 sieve exceeds the maximum allowable of 40% per AASHTO T99. A test strip should be performed in the field per 304.3.8 of the standard specifications, which is also described in the construction manual section 704.7.4.

Monday, October 10, 2011

**State of New Hampshire Department of Transportation
Bureau of Materials and Research**

Nuclear Density

<p>Sample ID: AA65824 Project: ROCHESTER Proj No: 15863 NH Lab No: Material: Pickering Rd. CSB Sampled from: Sta. 28+50, 6' Lt. Lot #: Purpose: 304.4 - Crs.Stone Base</p>	<p>Federal No: Source: Brox Inds. Report to: Ralph Sanders Submittal 10/13/2011 Sample 10/6/2011 Sampled by: K. COGSWELL</p>
---	---

Analysis Validated by: JA **Date:** 10/17/2011 **Sample Validated** JA **Date:** 10/17/2011

Remarks:

METHOD	ANALYSIS	RESULT	UNIT	MIN	MAX	VIOLATIONS
	Gauge ID	20730				
	Calibration/Verification Date	4/2011				
	Standardization Data	2196/648				
T310	Test Depth	6	inches			
T310	Height of Fill	1	Feet			
T310	Wet Density of soil	152.2	lbs/ft3			
T27	No 4 (4.75mm) Sieve	-	% Retained			
T310	Weight of H2O in Sample	5.8	lbs/ft3			
T310	% Moisture	4.8	%			
T310	Dry Density	146.4	lbs/ft3			
T99	Maximum Dry Density	145	lbs/ft3			
T224	Corr. Max. Dry Den.	145	lbs/ft3			
	% Compaction	100 +	%	95		
	Tested By:	K.C.				

Comments: Informational/Acceptance in-place density test, based on assumed MDD = 145 pcf

Monday, October 17, 2011

**State of New Hampshire Department of Transportation
Bureau of Materials and Research**

Nuclear Density

Sample ID: AA65823
Project: ROCHESTER
Proj No: 15863
NH Lab No:
Material: Pickering Rd. CSB
Sampled from: Sta. 17+60, 5' Rt.
Lot #:
Purpose: 304.4 - Crs.Stone Base

Federal No:
Source: Brox Inds.
Report to: Ralph Sanders
Submittal: 10/13/2011
Sample: 10/6/2011
Sampled by: K. COGSWELL

Analysis Validated by: JA **Date:** 10/17/2011 **Sample Validated** JA **Date:** 10/17/2011

Remarks:

METHOD	ANALYSIS	RESULT	UNIT	MIN	MAX	VIOLATIONS
	Gauge ID	20730				
	Calibration/Verification Date	4/2011				
	Standardization Data	2196/648				
T310	Test Depth	6	inches			
T310	Height of Fill	1	Feet			
T310	Wet Density of soil	150.4	lbs/ft3			
T27	No 4 (4.75mm) Sieve	-	% Retained			
T310	Weight of H2O in Sample	6.0	lbs/ft3			
T310	% Moisture	4.2	%			
T310	Dry Density	144.5	lbs/ft3			
T99	Maximum Dry Density	145	lbs/ft3			
T224	Corr. Max. Dry Den.	145	lbs/ft3			
	% Compaction	99.7	%	95		
	Tested By:	K.C.				

Comments: Informational/Acceptance in-place density test, based on assumed MDD = 145 pcf

Monday, October 17, 2011

**State of New Hampshire Department of Transportation
Bureau of Materials and Research**

Nuclear Density

Sample ID: AA65821
Project: ROCHESTER
Proj No: 15863
NH Lab No:
Material: Pickering Rd. CSB
Sampled from: Sta. 6+00, 2' Rt.
Lot #:
Purpose: 304.4 - Crs.Stone Base
Federal No:
Source: Brox Inds.
Report to: Ralph Sanders
Submittal: 10/13/2011
Sample: 10/6/2011
Sampled by: K. COGSWELL
Analysis Validated by: JA **Date:** 10/17/2011 **Sample Validated** JA **Date:** 10/17/2011
Remarks:

METHOD	ANALYSIS	RESULT	UNIT	MIN	MAX	VIOLATIONS
	Gauge ID	20730				
	Calibration/Verification Date	4/2011				
	Standardization Data	2196/648				
T310	Test Depth	8	inches			
T310	Height of Fill	1	Feet			
T310	Wet Density of soil	144.3	lbs/ft3			
T27	No 4 (4.75mm) Sieve	-	% Retained			
T310	Weight of H2O in Sample	5.0	lbs/ft3			
T310	% Moisture	3.6	%			
T310	Dry Density	139.3	lbs/ft3			
T99	Maximum Dry Density	145	lbs/ft3			
T224	Corr. Max. Dry Den.	145	lbs/ft3			
	% Compaction	96.1	%		95	
	Tested By:	K.C.				

Comments: Informational/Acceptance in-place density test, based on assumed MDD of 145 pcf

Monday, October 17, 2011

State of New Hampshire Department of Transportation
Bureau of Materials and Research
Cr. Stone Coarse (304.5)

Sample ID:	AA65507	Federal No:	
Project:	ROCHESTER	Source:	Brox Ind
Proj No:	15863	Report to:	Ralph Sanders
NH Lab No:		Submittal	10/5/2011
Material:	Crushed Stone Coarse	Sample	10/3/2011
Sampled from:	Stockpile Rochester	Sampled by:	R. SANDERS
Lot #:			
Purpose:	304.5 Crushed Stone Coarse		
Analysis Validated by:	JA	Date:	10/17/2011
Sample Validated	JA	Date:	10/17/2011

Remarks:

METHOD	ANALYSIS	RESULT	UNIT	MIN	MAX	VIOLATIONS
	Tested By:	RD				
T27	3 1/2 in (90 mm) Sieve	100.0	% Passing	100		
T27	3 in (75 mm) Sieve	96.5	% Passing	85	100	
T27	2 in (50 mm) Sieve	71.8	% Passing			
T27	1 1/2 in (37.5 mm) Sieve	49.2	% Passing	60	90	Failed
T27	1 in (25 mm) Sieve	29.6	% Passing			
T27	3/4 in (19 mm) Sieve	25.2	% Passing	40	70	Failed
T27	1/2 in (12.5 mm) Sieve	21.7	% Passing			
T27	#4 (4.75 mm) Sieve	18.09	% Passing	15	40	
T27	#10 (2.00 mm) Sieve	79.9	% Passing			
T27	#20 (0.850 mm) Sieve	60.9	% Passing			
T27	#40 (0.425 mm) Sieve	45.1	% Passing			
T27	#100 (0.150 mm) Sieve	24.49	% Passing			
T27	#200 (0.075 mm) Sieve	16.77	% Passing			
T27	% Passing #200 in Total Sample	2.70	% Passing	0	5	

Comments: Although aggregate retained on the 1 1/2 " and 3/4 " sieves is too coarse for DOT 304.5 gradation requirements, the extra stone should still make the material suitable for this roadway's application. Please Note - There will not be a proctor test performed on this material to establish a maximum dry density. The material retained on the #4 sieve exceeds the maximum allowable of 40% per AASHTO T99. Previous Test Strip data on this Crushed Stone Base product can be applied in the field per 304.3.6 of the standard specifications, which is also described in the construction manual section 704.7.4.

Monday, October 17, 2011

**State of New Hampshire Department of Transportation
Bureau of Materials and Research**

Cr. Stone Fine (304.4)

Sample ID:	AA65506	Federal No:	
Project:	ROCHESTER	Source:	Brox Ind
Proj No:	15863	Report to:	Ralph Sanders
NH Lab No:		Submittal	10/5/2011
Material:	Cr Stone Fine	Sample	10/3/2011
Sampled from:	Stockpile Rochester	Sampled by:	R. SANDERS
Lot #:			
Purpose:	304.4 Cr. Stone Fine		

Analysis Validated by: **Date:** 12/30/1899 **Sample Validated** **Date:** 12/30/1899

Remarks:

METHOD	ANALYSIS	RESULT	UNIT	MIN	MAX	VIOLATIONS
	Tested By:	RD				
T27	2 in (50 mm) Sieve	100.0	% Passing	100		
T27	1 1/2 in (37.5 mm) Sieve	94.5	% Passing	85	100	
T27	1 in (25 mm) Sieve	60.3	% Passing			
T27	3/4 in (19 mm) Sieve	42.2	% Passing	45	75	Failed
T27	1/2 in (12.5 mm) Sieve	30.5	% Passing			
T27	#4 (4.75 mm) Sieve	19.54	% Passing	10	45	
T27	#10 (2.00 mm) Sieve	78.1	% Passing			
T27	#20 (0.850 mm) Sieve	56.7	% Passing			
T27	#40 (0.425 mm) Sieve	41.5	% Passing			
T27	#100 (0.150 mm) Sieve	27.89	% Passing			
T27	#200 (0.075 mm) Sieve	17.26	% Passing			
T27	% Passing #200 in Total Sample	3.37	% Passing	0	5	

Comments: There will not be a proctor test performed on this material to establish a maximum dry density. The material retained on the #4 sieve exceeds the maximum allowable of 40% per AASHTO T99. A test strip should be performed in the field per 304.3.8 of the standard specifications, which is also described in the construction manual section 704.7.4.

Wednesday, October 05, 2011

State of New Hampshire Department of Transportation
Bureau of Materials and Research
Sand Fine & Coarse (304.1)

Sample ID: AA64715

Project: ROCHESTER

Proj No: 15863

NH Lab No:

Material: sand

Sampled from: Roadway

Lot #:

Purpose: 304.1 Sand

Federal No:

Source: Pike Ind.

Report to: Ralph Sanders

Submittal 9/15/2011

Sample 9/12/2011

Sampled by: R. SANDERS

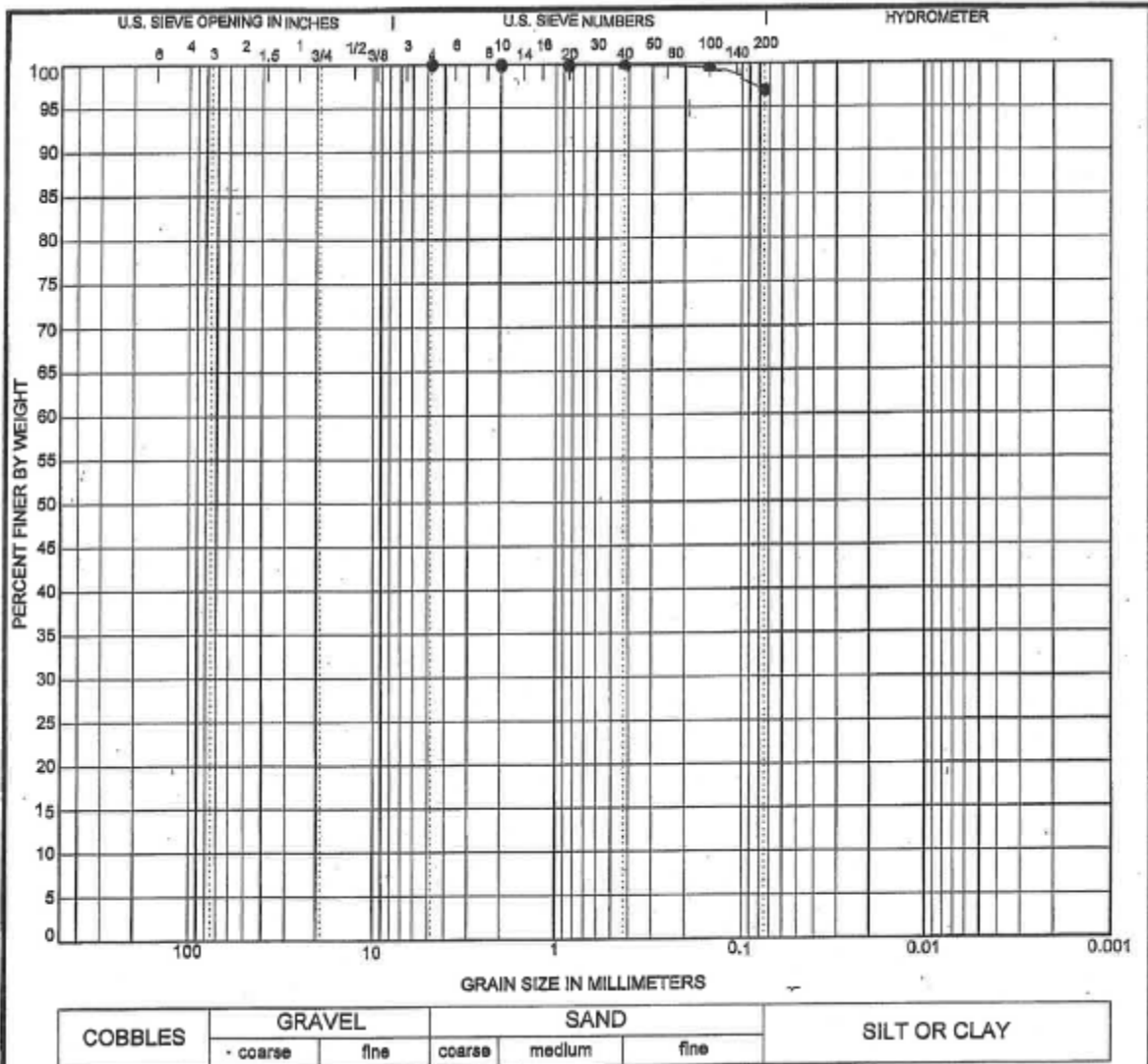
Analysis Validated by: **Date:** 12/30/1899 **Sample Validated** **Date:** 12/30/1899

Remarks:

METHOD	ANALYSIS	RESULT	UNIT	MIN	MAX	VIOLATIONS
T27	6 in (150 mm) Sieve	100.0	% Passing	100		
T27	2 in (50 mm) Sieve	96.4	% Passing			
T27	1 1/2 in (37.5 mm) Sieve	91.5	% Passing			
T27	1 in (25 mm) Sieve	86.0	% Passing			
T27	3/4 in (19 mm) Sieve	82.8	% Passing			
T27	1/2 in (12.5 mm) Sieve	78.3	% Passing			
T27	#4 (4.75 mm) Sieve	65.53	% Passing	70	100	Failed
T27	#10 (2.00 mm) Sieve	87.6	% Passing			
T27	#20 (0.850 mm) Sieve	66.7	% Passing			
T27	#40 (0.425 mm) Sieve	44.8	% Passing			
T27	#100 (0.150 mm) Sieve	16.00	% Passing			
T27	#200 (0.075 mm) Sieve	7.52	% Passing	0	12	
	Tested By:	RD				

Comments: Meets specifications for 304.2 Gravel


Thursday, September 15, 2011



COBBLES	GRAVEL		SAND			SILT OR CLAY
	coarse	fine	coarse	medium	fine	

Specimen Identification	USCS Classification	LL	PL	PI	Cc	Cu
● Pickering Rd., 1 0.0	SILT (ML)	33	27	6		

Specimen Identification	D100	D60	D30	D10	%Gravel	%Sand	%Silt	%Clay
● Pickering Rd., 1 0.0	4.75				0.0	3.1	96.9	


 State of New Hampshire
 Department of Transportation
 Bureau of Materials & Research
 Project: Rochester
 Location: Pickering Road
 Number: 15863

GRAIN SIZE DISTRIBUTION

AASHTO T27/T11 - Sieve Analysis of Fine and Coarse Aggregates/Materials Finer Than No. 200 Sieve in Mineral Aggregates by Washing

U.S. GRAIN SIZE ANALYSIS REPORT 12/25/2011 1:45:45 PM U.S. GRAIN SIZE



PAVEMENT CORE / BASE SOIL SAMPLE REPORT

Bureau of Materials and Research, 5 Hazen Drive, Concord, New Hampshire 03301
 Phone (603) 271-3151 Fax (603) 271-8700

Project: Rochester
Project Number: Special (10892-934)
Roadway: Pickering Rd
Sample Date: 1/11/2010
Sampled By: Craig Cleveland
Base Soil VC By:
Pavement VC By: Brian Kulacz / Matt Courser

1/26/2010

CORE	LOCATION	PAVEMENT		BASE SOIL(S)				NOTES		
		Thickness (in)	Visual Classification	Sample	Depth (ft)	Visual Classification	% Pass #4		% Pass #200	
C01	MM	5"	3/8"	3/8 Mix	S-1	0.0'-1.5'	GRAVEL, Med sand, trace silt	64.47	5.21	S-1 B/C 170/150/45/25 Frost estimated at 1 foot S-2 B/C 20/23/25/25 Asphalt Approx 5 1/4 inches *GPS coordinates collected at each core location was for DigSafe information. Close to exact core but not right on it
	STA									
	NORTH 282299.078		1/2"	PMST	S-2	1.5'-4.0'	SILT	95.37	71.78	
	EAST 1168660.254									
	LANE Northbound		1 1/2"	3/8 Mix						
	OFFSET									
	LEFT		2 5/8"	1/2 Mix						
	RIGHT 6' from center line									
OTHER										
C02	MM	3 1/2"	3/4"	3/8 Mix	S-1	0.0'-2.0'	SAND, Med, trace silt	72.55	7.76	S-1 B/C 90/130/85/30 Frost estimated at 1 foot S-2 B/C 20/21/15/16 Asphalt Approx 3 1/2 inches *GPS coordinates collected at each core location was for DigSafe information. Close to exact core but not right on it
	STA									
	NORTH 280434.921		2 3/4"	PMST	S-2	2.0'-4.0'	SAND, Med/fine, silty - various colors	79.35	25.95	
	EAST 1171214.588									
	LANE southbound									
	OFFSET									
	LEFT 6' from center line									
	RIGHT									
OTHER										
C03	MM	7 1/2"	5"	Various lifts of 3/8 Mix	S-1	0.0'-2.0'	SAND, Med, some silt	92.21	16.37	S-1 B/C 32/22/12/8 Frost estimated at 1 foot S-2 B/C 7/8/14/17 Asphalt Approx 7 1/2 inches *GPS coordinates collected at each core location was for DigSafe information. Close to exact core but not right on it
	STA									
	NORTH 278366.185		2 1/2"	Cutback	S-2	2.0'-4.0'	SILT	94.32	70.08	
	EAST 1172194.488									
	LANE Northbound									
	OFFSET									
	LEFT									
	RIGHT 6' from center line									
OTHER										

CORE	LOCATION	PAVEMENT		BASE SOIL(S)					NOTES	
		Thickness (In)	Visual Classification	Sample	Depth (ft)	Visual Classification	% Pass #4	% Pass #200		
C04	MM	6"	2 1/2"	Various lifts of 3/8 Mix	S-1	0.0'-2.0'	SAND Med/fine, some silt	85.05	12.67	S-1 B/C 30/34/19/12 Frost estimated at 1 foot S-2 B/C 8/8/11/14 Asphalt Approx 6 inches *GPS coordinates collected at each core location was for DigSafe information. Close to exact core but not right on it
	STA									
	NORTH 276171.226		2"	Various lifts of PMST	S-2	2.0'-4.0'	SILT	98.78	63.7	
	EAST 1173230.434									
	LANE southbound		1 1/2"	Cutback						
	OFFSET									
	LEFT 6' from center line									
	RIGHT									
OTHER										
C05	MM	?	2"	Various lifts of 3/8 Mix	S-1	0.0'-2.0'	GRAVELY Sand, Med	64.52	3.3	S-1 B/C 125/100/73/28 Frost estimated at 1 foot S-2 B/C 15/14/12/10 Asphalt Approx 6 7/8 inches *GPS coordinates collected at each core location was for DigSafe information. Close to exact core but not right on it
	STA									
	NORTH 274473.271		2"	Various lifts of PMST	S-2	2.0'-4.0'	SAND, some silt	78	17.05	
	EAST 1175060.877									
	LANE Northbound		?	Cutback						
	OFFSET			Can't measure Cutback lifts (Broken up)						
	LEFT									
	RIGHT 6' from center line									
OTHER										

Figure A-1. The as-built cross section of the test section FWD1. Horizontal scale is equal to vertical scale.

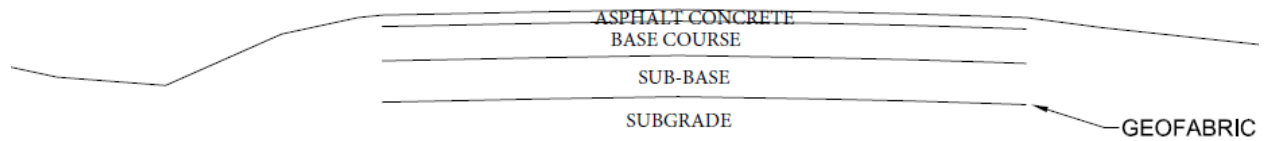


Figure A-2. The as-built cross section of the test section FWD2. Horizontal scale is equal to vertical scale.

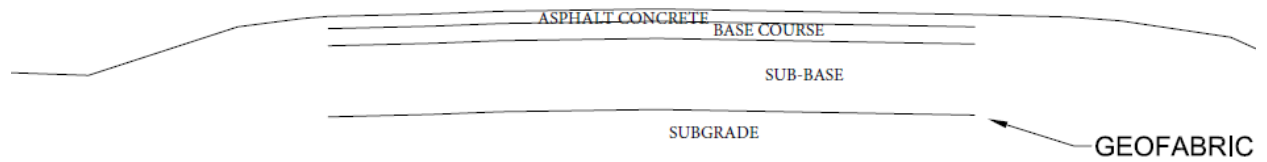


Figure A-3. The as-built cross section of the test section FWD3. Horizontal scale is equal to vertical scale.

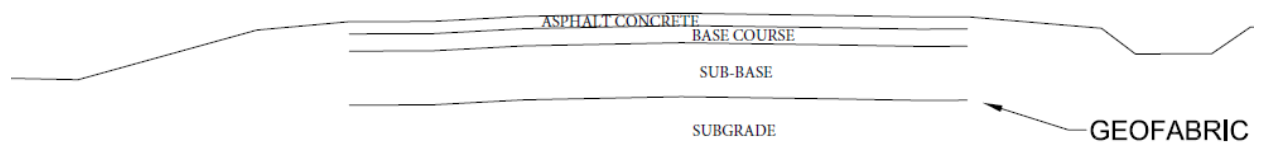


Figure A-4. The as-built cross section of the test section FWD4-1. Horizontal scale is equal to vertical scale.

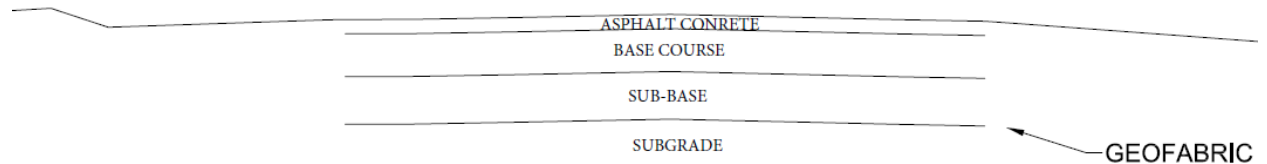


Figure A-5. The as-built cross section of the test section FWD4-2. Horizontal scale is equal to vertical scale.

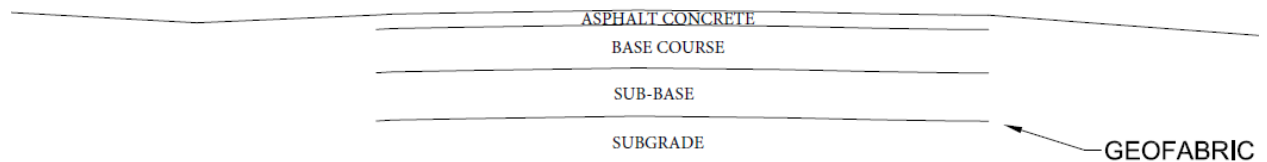


Figure A-6. The as-built cross section of the test section FWD4-3. Horizontal scale is equal to vertical scale.

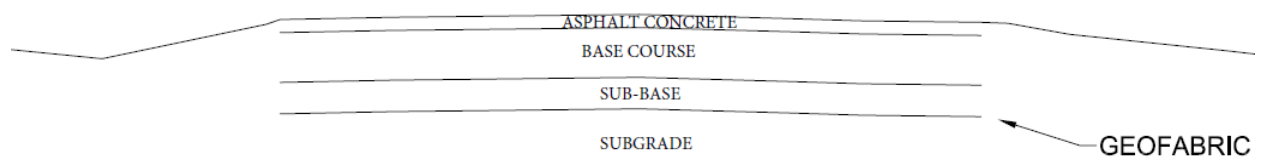


Figure A-7. The as-built cross section of the test section FWD4-4. Horizontal scale is equal to vertical scale.

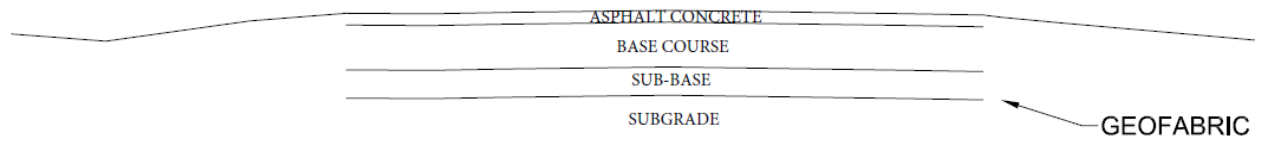


Figure A-8. The as-built cross section of the test section FWD4-5. Horizontal scale is equal to vertical scale.

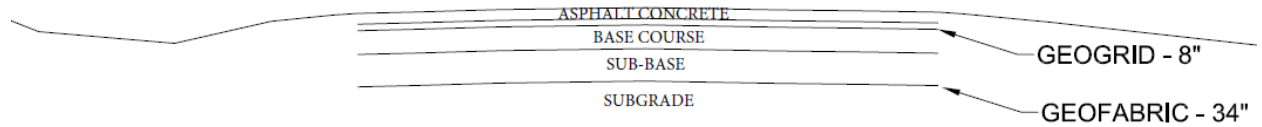


Figure A-9. The as-built cross section of the test section FWD4-6. Horizontal scale is equal to vertical scale.

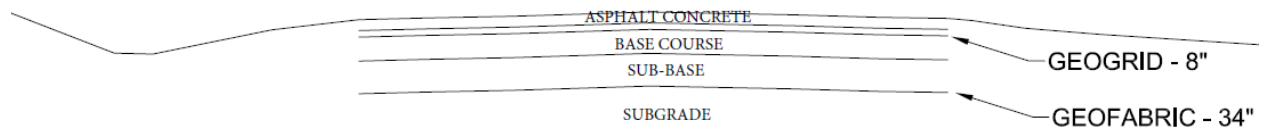


Figure A-10. The as-built cross section of the test section FWD4-7. Horizontal scale is equal to vertical scale.

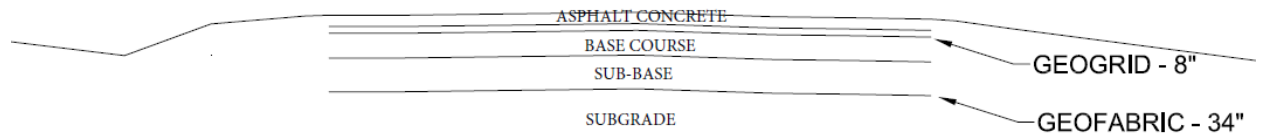


Figure A-11. The as-built cross section of the test section FWD4-8. Horizontal scale is equal to vertical scale.

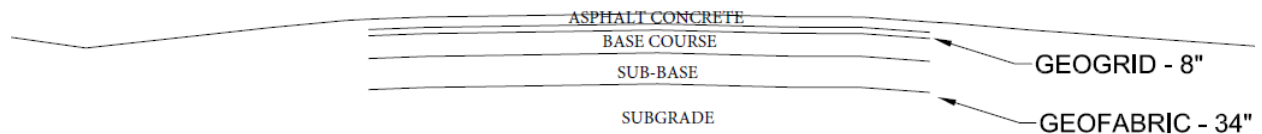


Figure A-12. The as-built cross section of the test section FWD4-9. Horizontal scale is equal to vertical scale.

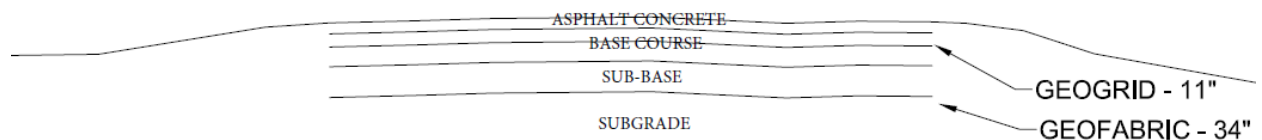


Figure A-13. The as-built cross section of the test section FWD5-1. Horizontal scale is equal to vertical scale.

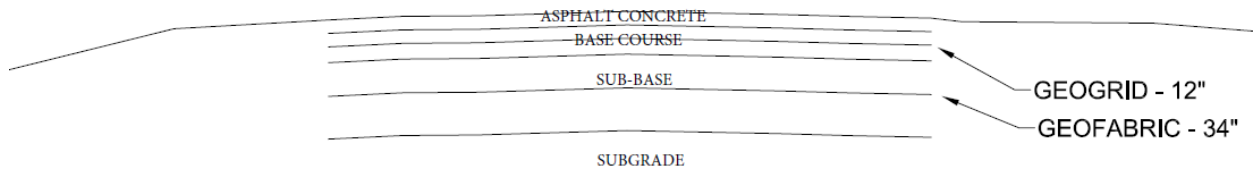


Figure A-14. The as-built cross section of the test section FWD5-2. Horizontal scale is equal to vertical scale.

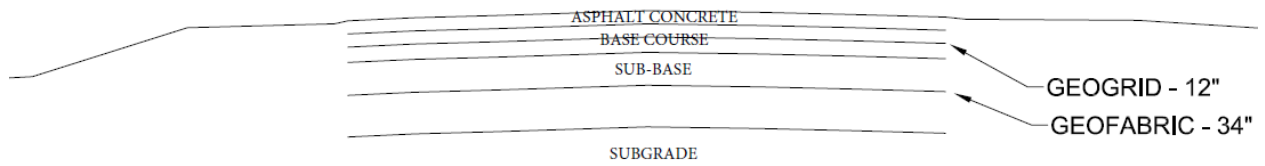


Figure A-15. The as-built cross section of the test section FWD6-1. Horizontal scale is equal to vertical scale.

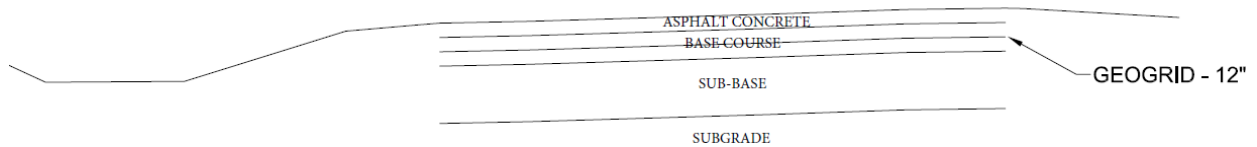
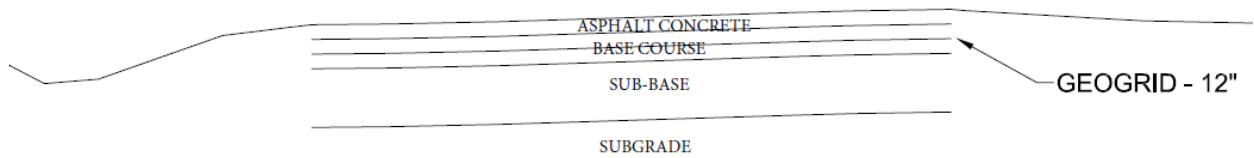



Figure A-16. The as-built cross section of the test section FWD6-2. Horizontal scale is equal to vertical scale.



Appendix B: Pickering Road Test-Boring Report and AASHTO Soil Classifications

TEST BORING REPORT										
STATE OF NEW HAMPSHIRE DEPARTMENT OF TRANSPORTATION MATERIALS & RESEARCH BUREAU - GEOTECHNICAL SECTION										
PROJECT NAME ROCHESTER 15680S						BRIDGE NO. <u>N/A</u>				
DESCRIPTION <u>Pickering Road Reinforced Base Course Materials</u>										
GROUNDWATER					EQUIPMENT		SAMPLER	CASING	CORE	
DATE	TIME	DEPTH (ft)	ELEV. (ft)	BOTTOM OF CASING	BOTTOM OF HOLE	TYPE:	SL	HW	Pavement	
1/30/14				0	6	SIZE LD. (in):	3	4	6.0	
						HAMMER WT. (lb):	140		DRILL RIG	
						HAMMER FALL (in):	30		CME 45-C Trlr	
						HAMMER TYPE:	Automatic		EAST/NORTH (ft) <u>1172288/278182</u>	
BORING NO. FT1										
SHEET NO. <u>1</u> OF <u>1</u>										
STA. <u>51+80</u> OFF. <u>RT 08</u>										
BASELINE <u>CL</u>										
ELEVATION (ft) <u>162.3</u>										
START/END <u>1/30/14 / 1/30/14</u>										
DRILLER <u>C. Cleveland (NHDOT)</u>										
INSPECTOR <u>Aaron Smart</u>										
CLASSIFIER <u>ALS</u>										
DEPTH (ft)	STRATUM CHANGE (ft)	BLOWS PER 0.5 ft	SAMPLE NUMBER	SAMPLER RECOVERY (ft) (%)	DEPTH RANGE (ft)	FIELD CLASSIFICATION AND REMARKS				STRATUM SYMBOL
0	0.5	161.8	PC1	0.5 [100]	0.0 - 0.5	PC1: 0"-6" ASPHALT PAVEMENT (7/8" 3/8 inch mix, 2" 5/8 inch mix, 3-1/8" 5/8 inch mix), core remained intact upon retrieval.				[Symbol]
			SL1	0.5 [100]	0.5 - 1.0	SL1: Mostly light brown to brown, medium to coarse SAND, some medium to coarse subrounded to angular gravel.				
	3.7	158.6	SL2	2.0 [100]	2.0 - 4.0	SL2 (upper): 0"-20" Similar to lower SL1. Single layer of GEOFABRIC at 20".				[Symbol]
5			SL3	2.0 [100]	4.0 - 6.0	SL2 (lower): 20"-24" Mostly olive gray sandy SILT, some orange and dark maroon mottling. SL3: Similar to lower SL2.				
Bottom of Exploration @ 6.0 ft (El. 156.3)										
NOTES:										
1) SPT N-values not obtained with use of non-standard SL-sized sampler.										
2) 60" deep frost tube installed in 1" ID PVC pipe (capped at bottom). Top of pipe 3" below surface. Top of road box (standard pentagonal road box wrench) mounted										
Sampler Identification		COHESIVE SOILS			NON-COHESIVE SOILS			Soil Descriptions		Proportion
S	Standard Split Spoon	Blows/foot (N)	Consistency	Blows/foot (N)	Apparent Density	Capitalized Soil Name	Major Component			
SL	Large Spoon (O.D.= 3 in)	0 - 1	Very Soft	0 - 4	Very Loose	Lower Case Adjective	35% - 50%			
T	Thin Wall Tube	2 - 4	Soft	5 - 10	Loose	Some	20% - 35%			
U	Undisturbed Piston	5 - 8	Medium Stiff	11 - 30	Medium Dense	Little	10% - 20%			
O	Open End Rod	9 - 15	Stiff	31 - 50	Dense	Trace	1% - 10%			
A	Auger Flight	16 - 30	Very Stiff	> 50	Very Dense					
C	Core Barrel	> 30	Hard	WOR - Weight of Rod WOH - Weight of Hammer		ENGLISH				
NR	Not Recorded									

TB-12: S:\MATERIALS-RESEARCH\RESARCH\PROJECTS\SPR PROJECTS\SPR PROJECTS\STRUCTURAL CONDITION ASSESSMENT OF BASE COURSE\PICKERING\LOGS\15680S\PICKERING FT GP 1 2010\2015 1 18:41 PM TB-12

TEST BORING REPORT										BORING NO. FT3	
STATE OF NEW HAMPSHIRE DEPARTMENT OF TRANSPORTATION MATERIALS & RESEARCH BUREAU - GEOTECHNICAL SECTION											
PROJECT NAME ROCHESTER 15680S BRIDGE NO. N/A										SHEET NO. 1 OF 1	
DESCRIPTION Pickering Road Reinforced Base Course Materials										STA. 55+67 OFF. RT 07	
GROUNDWATER										BASELINE CL	
EQUIPMENT										ELEVATION (ft) 164.9	
SAMPLER										START/END 1/30/14 / 1/30/14	
CASING										DRILLER C. Cleveland (NHDOT)	
CORE										INSPECTOR Aaron Smart	
DATE										CLASSIFIER ALS	
TIME										EAST/NORTH (ft) 1172142/278553	
DEPTH (ft)										TYPE:	
ELEV. (ft)										SL	
BOTTOM OF CASING										HW	
BOTTOM OF HOLE										Pavement	
1/30/14										SIZE I.D. (in): 3	
										HAMMER WT. (lb): 140	
										HAMMER FALL (in): 30	
										HAMMER TYPE: Automatic	
										DRILL RIG	
										CME 45-C Trlr	
DEPTH (ft)	STRATUM CHANGE (ft)		BLOWS PER 0.5 ft	SAMPLE NUMBER	SAMPLER RECOVERY (ft) [%]	DEPTH RANGE (ft)	FIELD CLASSIFICATION AND REMARKS				STRATUM SYMBOL
	DEPTH	ELEVATION									
0	0.4	164.5		PC1	0.4 [100]	0.0 - 0.4	PC1: 0-5" ASPHALT PAVEMENT (5/8" 3/8 inch mix, 2-1/8" 5/8 inch mix, 2-1/4" 5/8 inch mix), core separated between lower and middle layers upon retrieval. SL1 (upper): 0"-3" Mostly light brown to brown, medium to coarse SAND, some medium to coarse subrounded to angular gravel, single layer of GEOGRID at 3" SL1 (lower): 3"-14" Similar to upper SL1. 14"-24" Mostly brown medium SAND, little coarse rounded gravel. SL2 (upper): 0"-5" Similar to lower SL1. Single layer of GEOFABRIC at 5" SL2 (lower): 5"-24" Mostly olive gray sandy SILT, some orange and dark maroon mottling. Advanced without sampling.				
	0.7	164.2		SL1	2.0 [100]	0.4 - 2.4					
	2.8	162.1		SL2	2.0 [100]	2.4 - 4.4					
5							Bottom of Exploration @ 6.4 ft (El. 158.5)				
NOTES: 1) SPT N-values not obtained with use of non-standard SL-sized sampler. 2) 60" deep frost tube installed in 1" ID PVC pipe (capped at bottom). Top of pipe 3" below surface. Top of road box (standard pentagonal road box wrench) mounted 1" below surface.											
10											
15											
20											
25											

Sampler Identification		COHESIVE SOILS		NON-COHESIVE SOILS		Soil Descriptions		Proportion	
S	Standard Split Spoon	Blows/foot (N)	Consistency	Blows/foot (N)	Apparent Density	Capitalized Soil Name	Major Component		
SL	Large Spoon (O.D.= 3 in)	0 - 1	Very Soft	0 - 4	Very Loose	Lower Case Adjective	35% - 50%		
T	Thin Wall Tube	2 - 4	Soft	5 - 10	Loose	Some	20% - 35%		
U	Undisturbed Piston	5 - 8	Medium Stiff	11 - 30	Medium Dense	Little	10% - 20%		
O	Open End Rod	9 - 15	Stiff	31 - 50	Dense	Trace	1% - 10%		
A	Auger Flight	16 - 30	Very Stiff	> 50	Very Dense				
C	Core Barrel	> 30	Hard						
NR	Not Recorded								

ENGLISH

TB-12, S:\MATERIALS-RESEARCH\RESEARCH\PROJECTS\SPR PROJECTS\15680S - STRUCTURAL CONDITION ASSESSMENT OF BASE COURSE\PICKERING\LOG\SI15680H PICKERING FT.GPJ, 2/10/2015, 1:16:44 PM, TB-12

TEST BORING REPORT										BORING NO. FT5	
STATE OF NEW HAMPSHIRE DEPARTMENT OF TRANSPORTATION MATERIALS & RESEARCH BUREAU - GEOTECHNICAL SECTION										SHEET NO. <u>1</u> OF <u>1</u>	
PROJECT NAME ROCHESTER 15680S BRIDGE NO. <u>N/A</u>										STA. <u>59+94</u> OFF. <u>RT 08</u>	
DESCRIPTION <u>Pickering Road Reinforced Base Course Materials</u>										BASELINE <u>CL</u>	
GROUNDWATER										ELEVATION (ft) <u>167.9</u>	
EQUIPMENT										START/END <u>1/31/14 / 1/31/14</u>	
SAMPLER										DRILLER <u>C. Cleveland (NHDOT)</u>	
CASING										INSPECTOR <u>Drill Crew</u>	
CORE										CLASSIFIER <u>ALS</u>	
DATE										EAST/NORTH (ft) <u>1171990/278944</u>	
TIME											
DEPTH (ft)											
ELEV. (ft)											
BOTTOM OF CASING											
BOTTOM OF HOLE											
TYPE:											
SIZE I.D. (in):										3	
HAMMER WT. (lb):										140	
HAMMER FALL (in):										30	
HAMMER TYPE:										Automatic	
										DRILL RIG	
										CME 45-C Trlr	
DEPTH (ft)	STRATUM CHANGE (ft)		BLOWS PER 0.5 ft	SAMPLE NUMBER	SAMPLER RECOVERY (ft) (%)	DEPTH RANGE (ft)	FIELD CLASSIFICATION AND REMARKS				STRATUM SYMBOL
	DEPTH	ELEVATION									
0	0.5	167.4		PC1	0.5 [100]	0.0 - 0.5	PC1: 0-5-1/2" ASPHALT PAVEMENT (3/4" 3/8 inch mix, 2-1/4" 5/8 inch mix, 2-1/2" 5/8 inch mix), core remained intact upon retrieval. SL1 (upper): 0"-5" Mostly light brown to brown, medium to coarse SAND, (some medium to coarse subrounded gravel, single layer of GEOGRID at 5" SL1 (lower): 5"-12" Similar to upper SL1. 15"-24" Mostly brown medium SAND, some coarse subrounded gravel. SL2 (upper): 0"-4" Similar to lower SL1. Single layer of GEOFABRIC at 4". SL2 (lower): 4"-24" Mostly brown fine to medium SAND.				
	1.0	166.9		SL1	2.0 [100]	0.5 - 2.5					
	2.8	165.2		SL2	1.3 [65]	2.5 - 4.5	SL3: Mostly olive gray sandy SILT, some orange and dark maroon mottling.				
	4.4	163.5		SL3	2.0 [100]	4.5 - 6.5					
Bottom of Exploration @ 6.5 ft (El. 161.4)											
NOTES:											
1) SPT N-values not obtained with use of non-standard SL-sized sampler.											
2) 60" deep frost tube installed in 1" ID PVC pipe (capped at bottom). Top of pipe 4" below surface. Top of road box (standard pentagonal road box wrench) mounted 1" below surface.											
Sampler	Identification	COHESIVE SOILS				NON-COHESIVE SOILS				Soil Descriptions	Proportion
S	Standard Split Spoon	Blows/foot (N)	Consistency	Blows/foot (N)	Apparent Density	Capitalized Soil Name	Major Component				
SL	Large Spoon (O.D.= 3 in)	0 - 1	Very Soft	0 - 4	Very Loose	Lower Case Adjective	35% - 50%				
T	Thin Wall Tube	2 - 4	Soft	5 - 10	Loose	Some	20% - 35%				
U	Undisturbed Piston	5 - 8	Medium Stiff	11 - 30	Medium Dense	Little	10% - 20%				
O	Open End Rod	9 - 15	Stiff	31 - 50	Dense	Trace	1% - 10%				
A	Auger Flight	16 - 30	Very Stiff	> 50	Very Dense						
C	Core Barrel	> 30	Hard	WOR - Weight of Rod		ENGLISH					
NR	Not Recorded			WOH - Weight of Hammer							

TB-12 S:\MATERIALS-RESEARCH\RESEARCH\PROJECTS\SPR PROJECTS\15680S - STRUCTURAL CONDITION ASSESSMENT OF BASE COURSE\PICKERING\LOG\5115980H PICKERING FT.GPJ 2/10/2015 1:16:45 PM TB-12

TEST BORING REPORT										BORING NO. PC1			
STATE OF NEW HAMPSHIRE DEPARTMENT OF TRANSPORTATION MATERIALS & RESEARCH BUREAU - GEOTECHNICAL SECTION													
PROJECT NAME ROCHESTER 15680S BRIDGE NO. <u>N/A</u>										SHEET NO. <u>1</u> OF <u>1</u>			
DESCRIPTION <u>Pickering Road Reinforced Base Course Materials</u>										STA. <u>15+53</u> OFF. <u>RT 06</u>			
										BASELINE <u>CL</u>			
										ELEVATION (ft) <u>146.7</u>			
										START/END <u>12/29/14 / 12/29/14</u>			
										DRILLER <u>C. Cleveland (NHDOT)</u>			
										INSPECTOR <u>Drill Crew</u>			
										CLASSIFIER <u>ALS</u>			
										EAST/NORTH (ft) <u>1174174/275172</u>			
GROUNDWATER					EQUIPMENT	SAMPLER	CASING	CORE					
DATE	TIME	DEPTH (ft)	ELEV. (ft)	BOTTOM OF CASING	BOTTOM OF HOLE	TYPE:	S	NW					
						SIZE I.D. (in):	1.375	3					
						HAMMER WT. (lb):	140	DRILL RIG					
						HAMMER FALL (in):	30						
						HAMMER TYPE:							
DEPTH (ft)	STRATUM CHANGE (ft)		BLOWS PER 0.5 ft	SAMPLE NUMBER	SAMPLER RECOVERY (ft) [%]	DEPTH RANGE (ft)	FIELD CLASSIFICATION AND REMARKS				STRATUM SYMBOL		
	DEPTH	ELEVATION											
0	0.4	146.3				0.4	PC1: 0"-5" ASPHALT PAVEMENT (X" 3/8 inch mix, X" 5/8 inch mix, X" 5/8 inch mix), core remained intact upon retrieval. SL1: 0"-17" Mostly light brown to brown, medium to coarse gravelly SAND. 17"-18" Mostly brown medium SAND. SL2 (upper): 0"-8" Similar to lower SL1. Single layer of GEOFABRIC at 8". SL2 (lower): 8"-24" Mostly olive gray sandy SILT, some orange and dark maroon mottling.						
	3.2	143.5			2.4								
	4.4	142.3			4.4								
5	Bottom of Exploration @ 4.4 ft												
10	NOTES: 1) SPT N-values not obtained with use of non-standard SL-sized sampler.												
15													
20													
25													
Sampler Identification				COHESIVE SOILS			NON-COHESIVE SOILS			Soil Descriptions		Proportion	
S	Standard Split Spoon			Blows/foot (N)	Consistency	Blows/foot (N)	Apparent Density	Capitalized Soil Name		Major Component			
SL	Large Spoon (O.D.= 3 in)			0 - 1	Very Soft	0 - 4	Very Loose	Lower Case Adjective		35% - 50%			
T	Thin Wall Tube			2 - 4	Soft	5 - 10	Loose	Some		20% - 35%			
U	Undisturbed Piston			5 - 8	Medium Stiff	11 - 30	Medium Dense	Little		10% - 20%			
O	Open End Rod			9 - 15	Stiff	31 - 50	Dense	Trace		1% - 10%			
A	Auger Flight			16 - 30	Very Stiff	> 50	Very Dense						
C	Core Barrel			> 30	Hard	WOR - Weight of Rod WOH - Weight of Hammer		ENGLISH					
NR	Not Recorded												


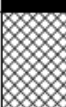
125 S:\MATERIALS-RESEARCH\RESEARCH\PROJECTS\SPR PROJECTS\15680S - STRUCTURAL CONDITION ASSESSMENT OF BASE COURSE\PICKERING\LOG\515680H PICKERING FT.GPJ 2/10/2015 1:20:41 PM TB-12

TEST BORING REPORT										BORING NO. PC2	
STATE OF NEW HAMPSHIRE DEPARTMENT OF TRANSPORTATION MATERIALS & RESEARCH BUREAU - GEOTECHNICAL SECTION											
PROJECT NAME ROCHESTER 15680S BRIDGE NO. <u>N/A</u>										SHEET NO. <u>1</u> OF <u>1</u>	
DESCRIPTION <u>Pickering Road Reinforced Base Course Materials</u>										STA. <u>29+65</u> OFF. <u>RT 06</u>	
GROUNDWATER										BASELINE <u>CL</u>	
EQUIPMENT										ELEVATION (ft) <u>165.1</u>	
SAMPLER										START/END <u>12/29/14 / 12/29/14</u>	
CASING										DRILLER <u>C. Cleveland (NHDOT)</u>	
CORE										INSPECTOR <u>Drill Crew</u>	
DATE										CLASSIFIER <u>ALS</u>	
TIME										EAST/NORTH (ft) <u>1173207/276178</u>	
DEPTH (ft)										TYPE: S NW	
ELEV. (ft)										SIZE ID. (in): 1.375	
BOTTOM OF CASING										HAMMER WT. (lb): 140	
BOTTOM OF HOLE										HAMMER FALL (in): 30	
										HAMMER TYPE:	
										DRILL RIG	
DEPTH (ft)	STRATUM CHANGE (ft)		BLOWS PER 0.5 ft	SAMPLE NUMBER	SAMPLER RECOVERY (ft) [%]	DEPTH RANGE (ft)	FIELD CLASSIFICATION AND REMARKS			STRATUM SYMBOL	
	DEPTH	ELEVATION									
0	0.4	164.7				0.4	PC2: 0"-5" ASPHALT PAVEMENT (X" 3/8 inch mix, X" 5/8 inch mix, X" 5/8 inch mix), core remained intact upon retrieval. SL1: 0"-8" Mostly light brown to brown, medium to coarse gravelly SAND. 8"-20" Mostly brown medium SAND. SL2 (upper): 0"-12" Similar to lower SL1. SL2 (lower): 12"-24" Mostly olive gray sandy SILT, some orange and dark maroon mottling.				
	3.4	161.7			2.4						
	4.4	160.7			4.4	Bottom of Exploration @ 4.4 ft					
NOTES:											
1) SPT N-values not obtained with use of non-standard SL-sized sampler.											

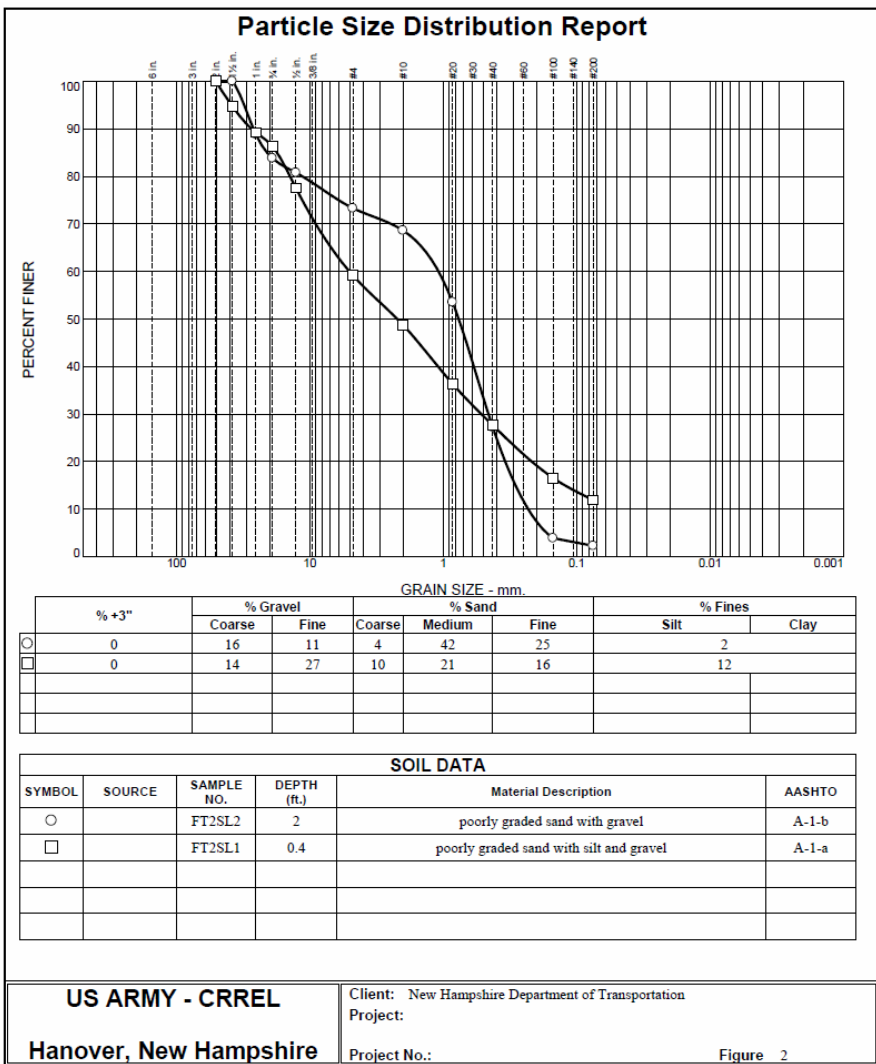
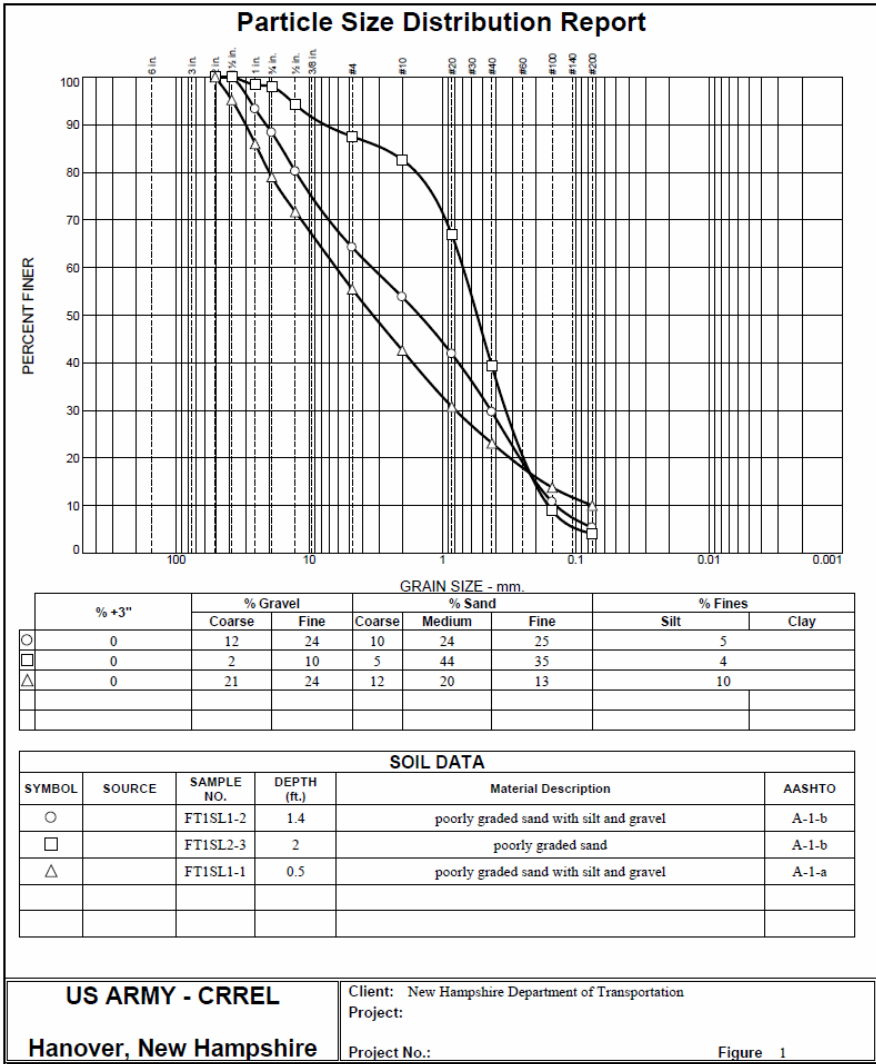
Sampler Identification		COHESIVE SOILS		NON-COHESIVE SOILS		Soil Descriptions		Proportion	
Code	Description	Blows/foot (N)	Consistency	Blows/foot (N)	Apparent Density	Capitalized Soil Name	Major Component	Lower Case Adjective	Percentage
S	Standard Split Spoon	0 - 1	Very Soft	0 - 4	Very Loose			35% - 50%	
SL	Large Spoon (O.D.= 3 in)	2 - 4	Soft	5 - 10	Loose			20% - 35%	
T	Thin Wall Tube	5 - 8	Medium Stiff	11 - 30	Medium Dense			10% - 20%	
U	Undisturbed Piston	9 - 15	Stiff	31 - 50	Dense			Trace	1% - 10%
O	Open End Rod	16 - 30	Very Stiff	> 50	Very Dense				
A	Auger Flight								
C	Core Barrel								
NR	Not Recorded								

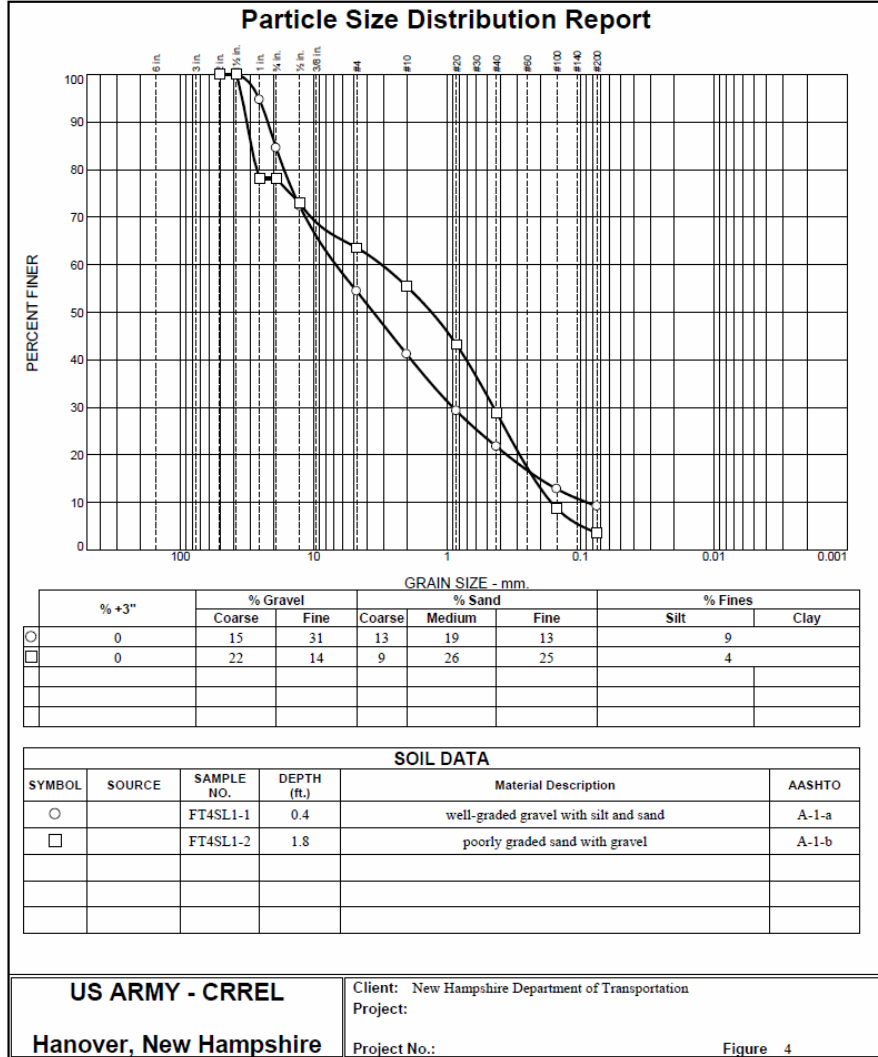
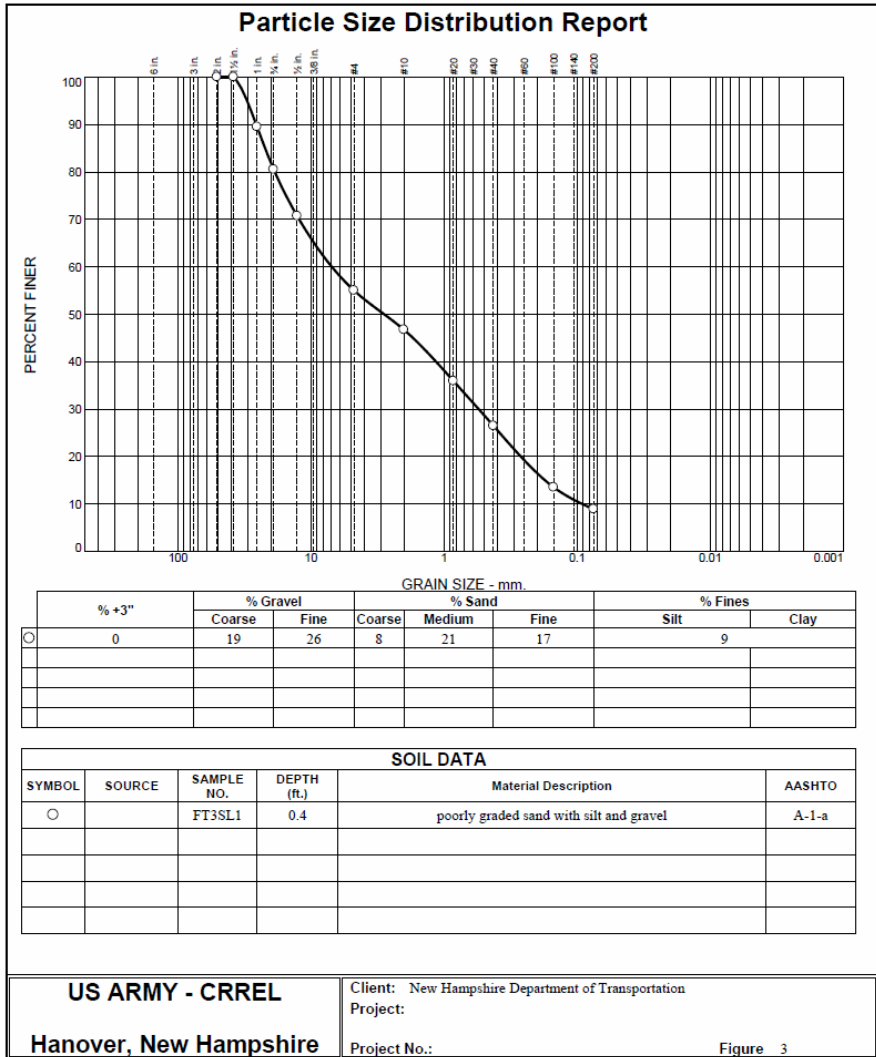
WOR - Weight of Rod	ENGLISH
WOH - Weight of Hammer	

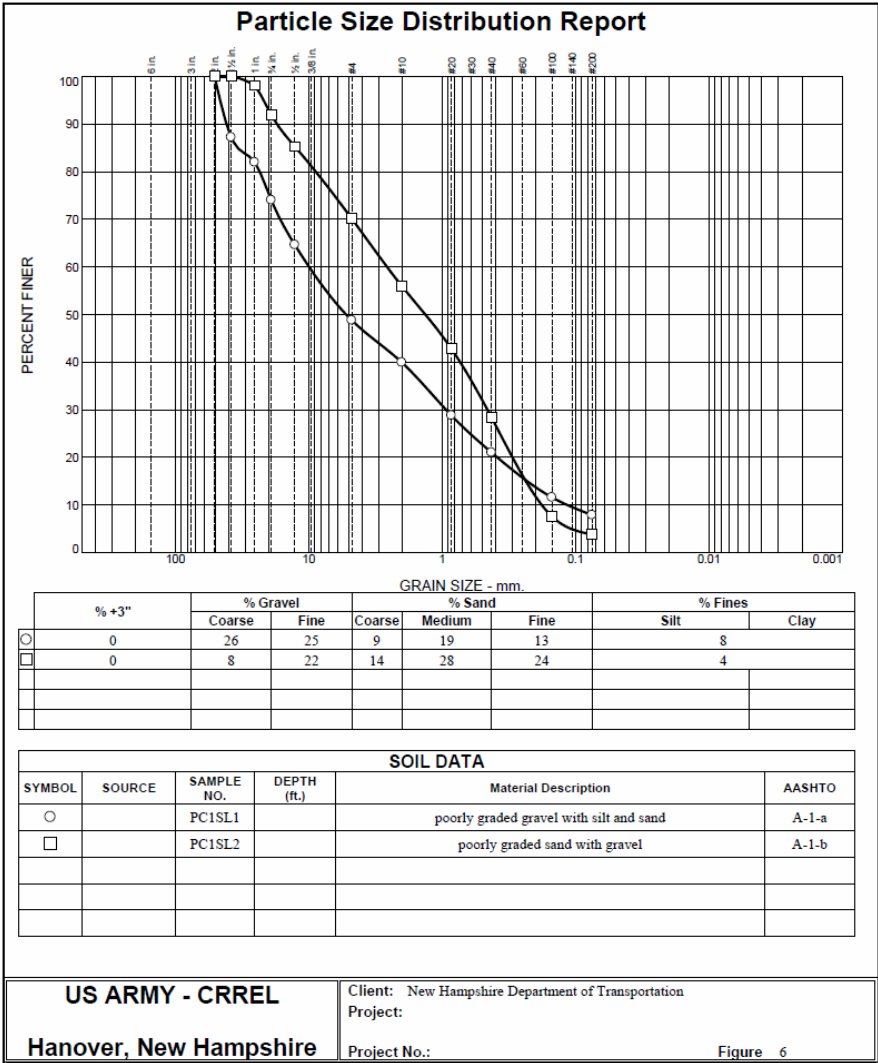
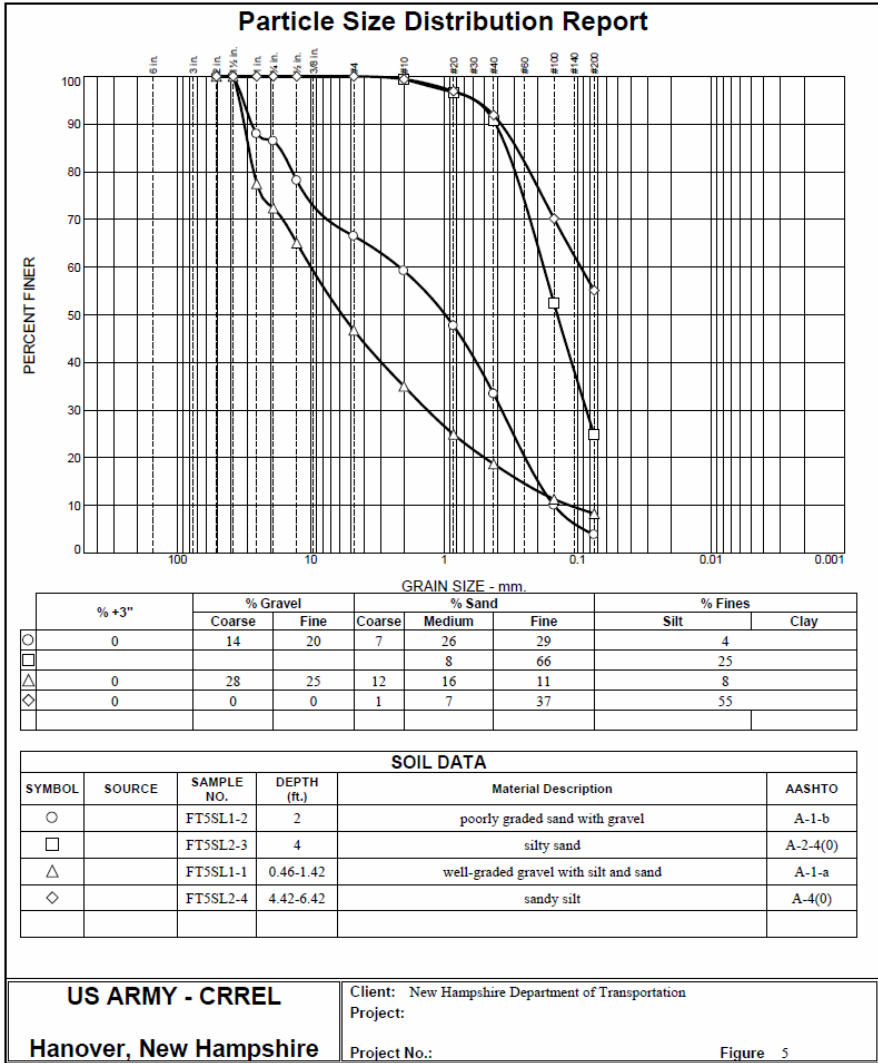
12-29-14 1:20:43 PM TB-12 S:\WATERIALS-RESEARCH\RESEARCH\PROJECTS\SPR\PROJECTS\15680S - STRUCTURAL CONDITION ASSESSMENT OF BASE COURSE\PICKERING\LOGS\15680H\PICKERING_FT.GPJ

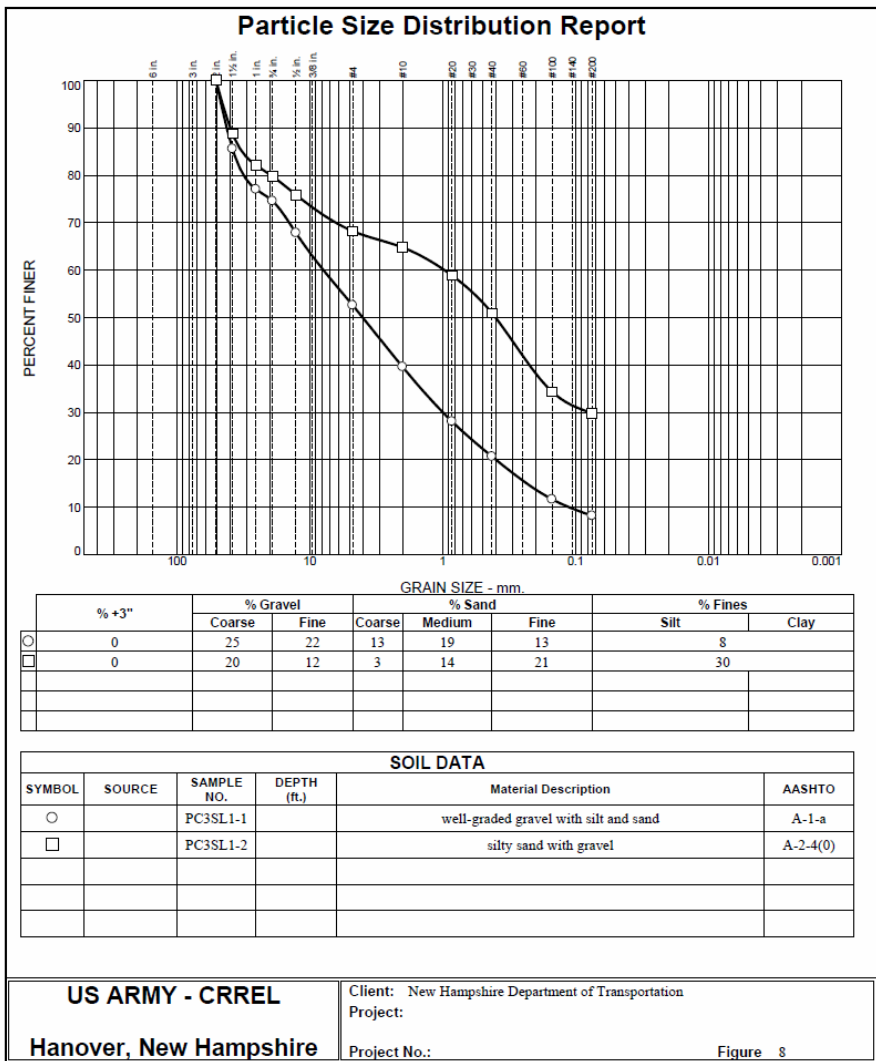
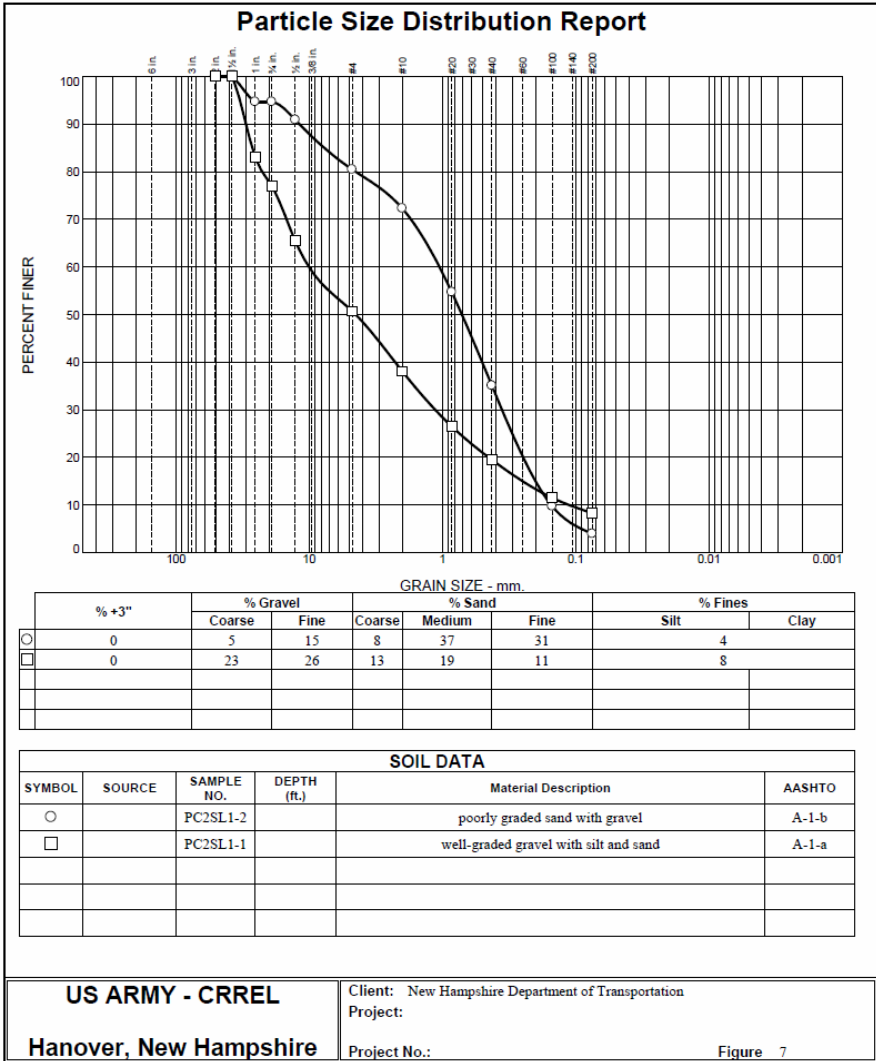
TEST BORING REPORT										
STATE OF NEW HAMPSHIRE DEPARTMENT OF TRANSPORTATION MATERIALS & RESEARCH BUREAU - GEOTECHNICAL SECTION									BORING NO. PC3	
PROJECT NAME ROCHESTER 15680S							BRIDGE NO. N/A			
DESCRIPTION Pickering Road Reinforced Base Course Materials										
GROUNDWATER					EQUIPMENT	SAMPLER	CASING	CORE		
DATE	TIME	DEPTH (ft)	ELEV. (ft)	BOTTOM OF CASING	BOTTOM OF HOLE	TYPE:	S	NW		
						SIZE I.D. (in):	1.375	3		
						HAMMER WT. (lb):	140	DRILL RIG		
						HAMMER FALL (in):	30			
						HAMMER TYPE:				
		ELEVATION (ft)		START/END		DRILLER		INSPECTOR		
		162.1		12/29/14 / 12/29/14		C. Cleveland (NHDOT)		Drill Crew		
								CLASSIFIER		
								ALS		
								EAST/NORTH (ft)		
								1172620/277302		
DEPTH (ft)	STRATUM CHANGE (ft)		BLOWS PER 0.5 ft	SAMPLE NUMBER	SAMPLER RECOVERY (ft) [%]	DEPTH RANGE (ft)	FIELD CLASSIFICATION AND REMARKS			STRATUM SYMBOL
0	DEPTH	ELEVATION					PC3: 0"-5" ASPHALT PAVEMENT (X" 3/8 inch mix, X" 5/8 inch mix, X" 5/8 inch mix), core remained intact upon retrieval. SL1: 0"-8" Mostly light brown to brown, medium to coarse gravelly SAND. 8"-16". Mostly brown medium SAND.			
	0.4	161.7		SL1	1.3 [65]	0.4				
	2.8	159.3		SL2	2.0 [100]	2.4				
	4.4	157.7				4.4				
5	Bottom of Exploration @ 4.4 ft									
10	NOTES: 1) SPT N-values not obtained with use of non-standard SL-sized sampler.									
15										
20										
25										
Sampler Identification		COHESIVE SOILS			NON-COHESIVE SOILS			Soil Descriptions		Proportion
S	Standard Split Spoon	Blows/foot (N)	Consistency	Blows/foot (N)	Apparent Density	Capitalized Soil Name		Major Component		
SL	Large Spoon (O.D.= 3 in)	0 - 1	Very Soft	0 - 4	Very Loose	Lower Case Adjective		35% - 50%		
T	Thin Wall Tube	2 - 4	Soft	5 - 10	Loose	Some		20% - 35%		
U	Undisturbed Piston	5 - 8	Medium Stiff	11 - 30	Medium Dense	Little		10% - 20%		
O	Open End Rod	9 - 15	Stiff	31 - 50	Dense	Trace		1% - 10%		
A	Auger Flight	16 - 30	Very Stiff	> 50	Very Dense					
C	Core Barrel	> 30	Hard	WOR - Weight of Rod		ENGLISH				
NR	Not Recorded			WOH - Weight of Hammer						

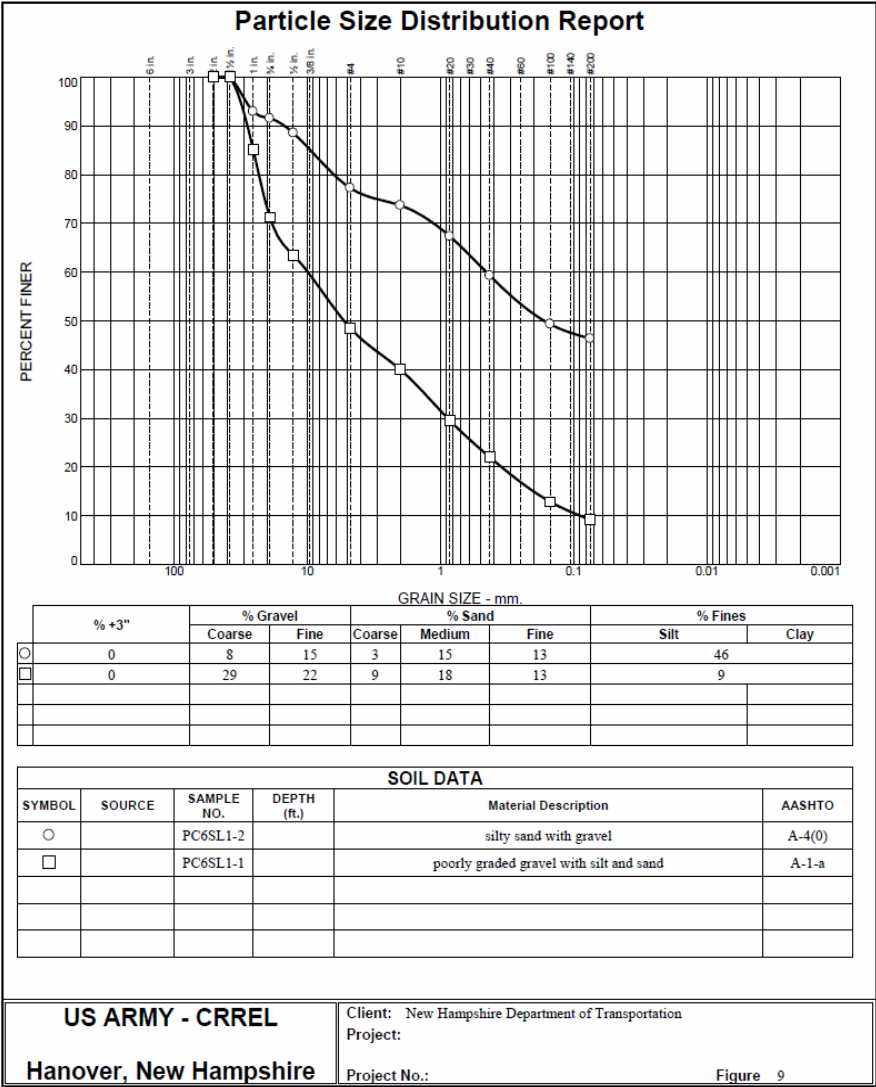
TS-12. S:\MATERIALS-RESEARCH\RESEARCH\PROJECTS\PROJECTS\15680S - STRUCTURAL CONDITION ASSESSMENT OF BASE COURSE\PICKERING\LOGS\15680H PICKERING FT.GPJ 2/10/2015 1:20:44 PM TB-12











Appendix C: Climate

The following precipitation data was collected at the Skyhaven Airport in Rochester, NH. Because this location is only 3 miles from Pickering Road, the climate data is acceptable to use for our Pickering Road analysis. Figures C-1 to C-4 show Rochester’s daily precipitation in millimeters over a 1-year span. It is important to look at 2014 and 2015 as that is when the FWD testing took place. As seen in Table C-1, the average yearly precipitation from 2000 to 2014 was 1080.2 mm while the total precipitation in 2014 was 943.8 mm, implying that this might have been a relatively dry year. Data was collected for only half of 2015, so it is impossible to compare precipitation totals for that year; but it is still useful to look at the first six months. Table C-2 also shows total precipitation per year but only through 30 June. The average 1 January to 30 July precipitation from 2000 to 2014 was 505 mm, much higher than the 311.1 mm recorded in the first six months of 2015. Such a low value implies that 2015 is also a relatively dry year.

Figure C-1. Precipitation data from Skyhaven Airport in Rochester, NH, for 2000 to 2003.

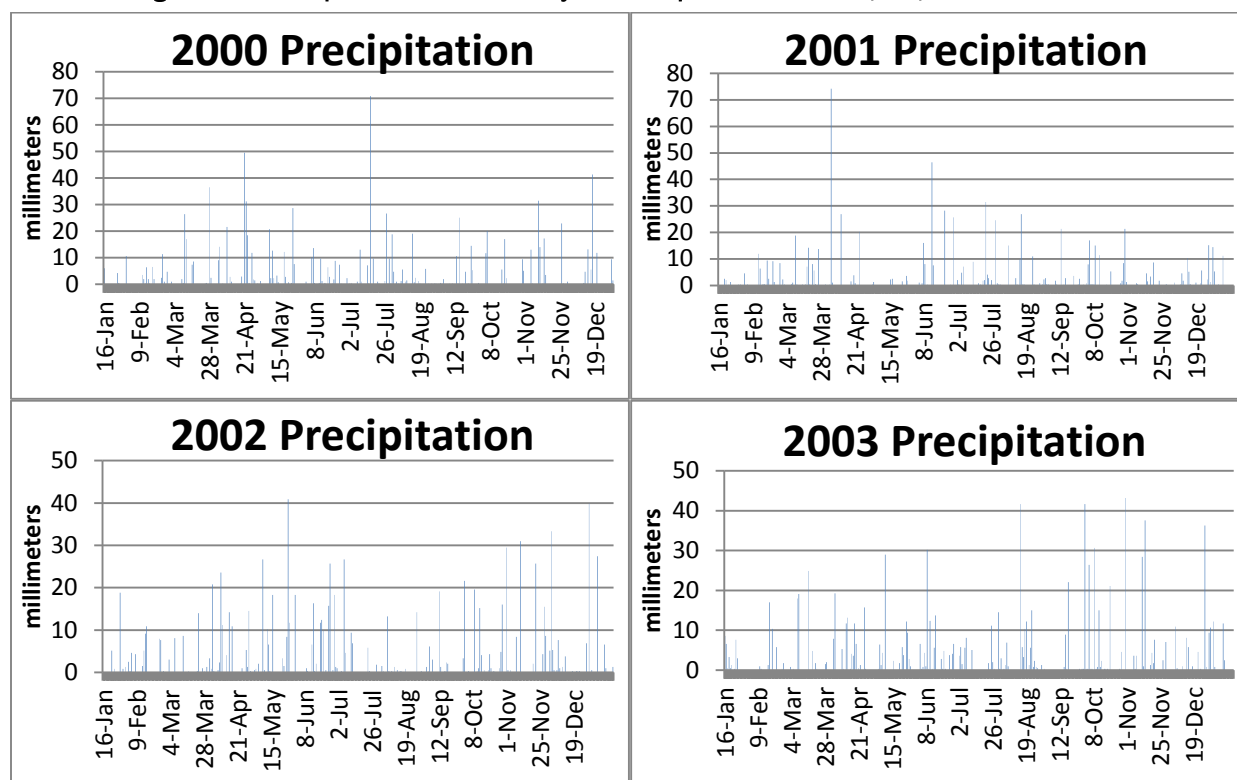


Figure C-2. Precipitation data from Skyhaven Airport in Rochester, NH, for 2004 to 2007.

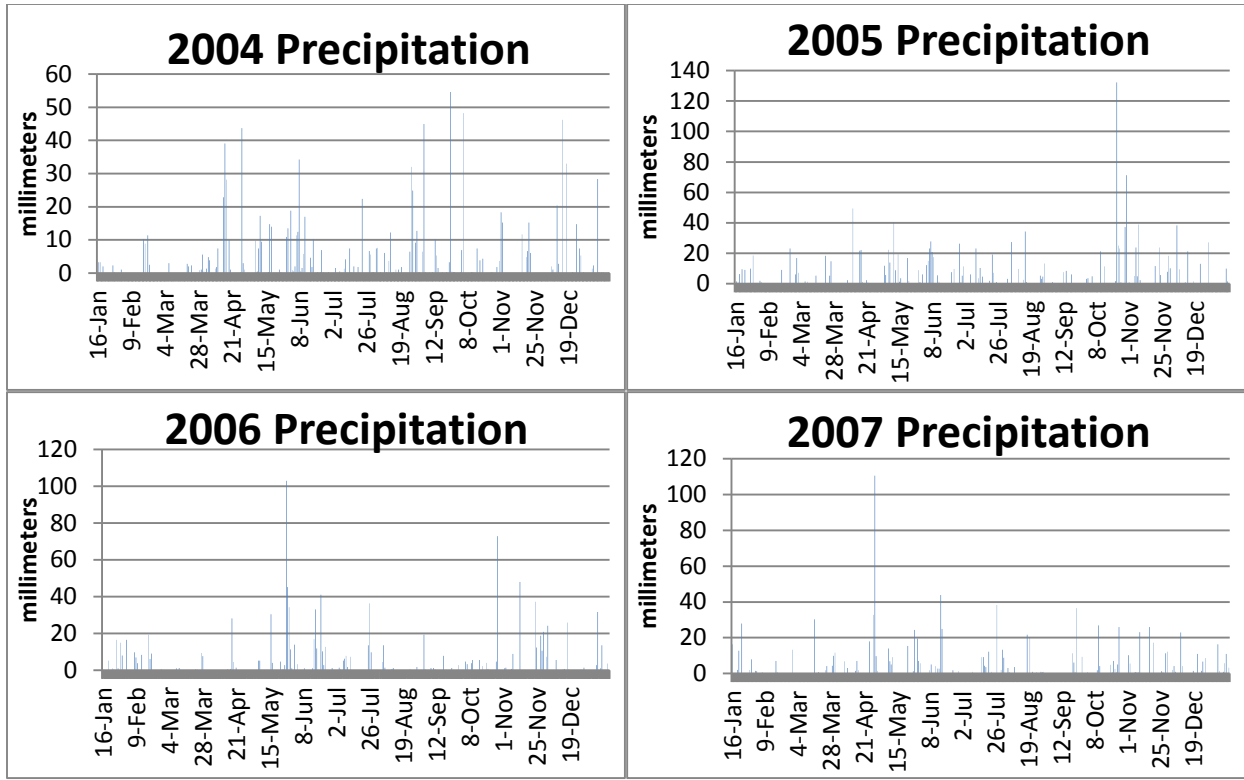


Figure C-3. Precipitation data from Skyhaven Airport in Rochester, NH, for 2008 to 2011.

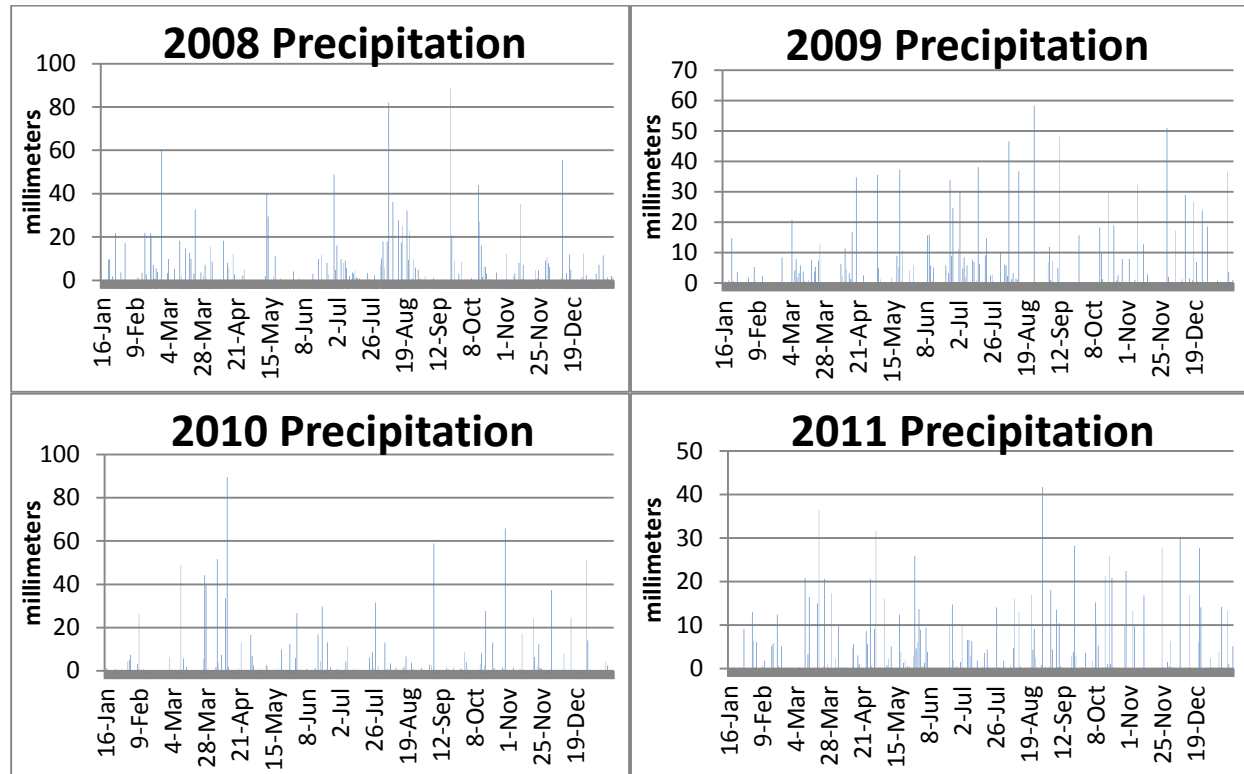


Figure C-4. Precipitation data from Skyhaven Airport in Rochester, NH, for 2012 to 2015.

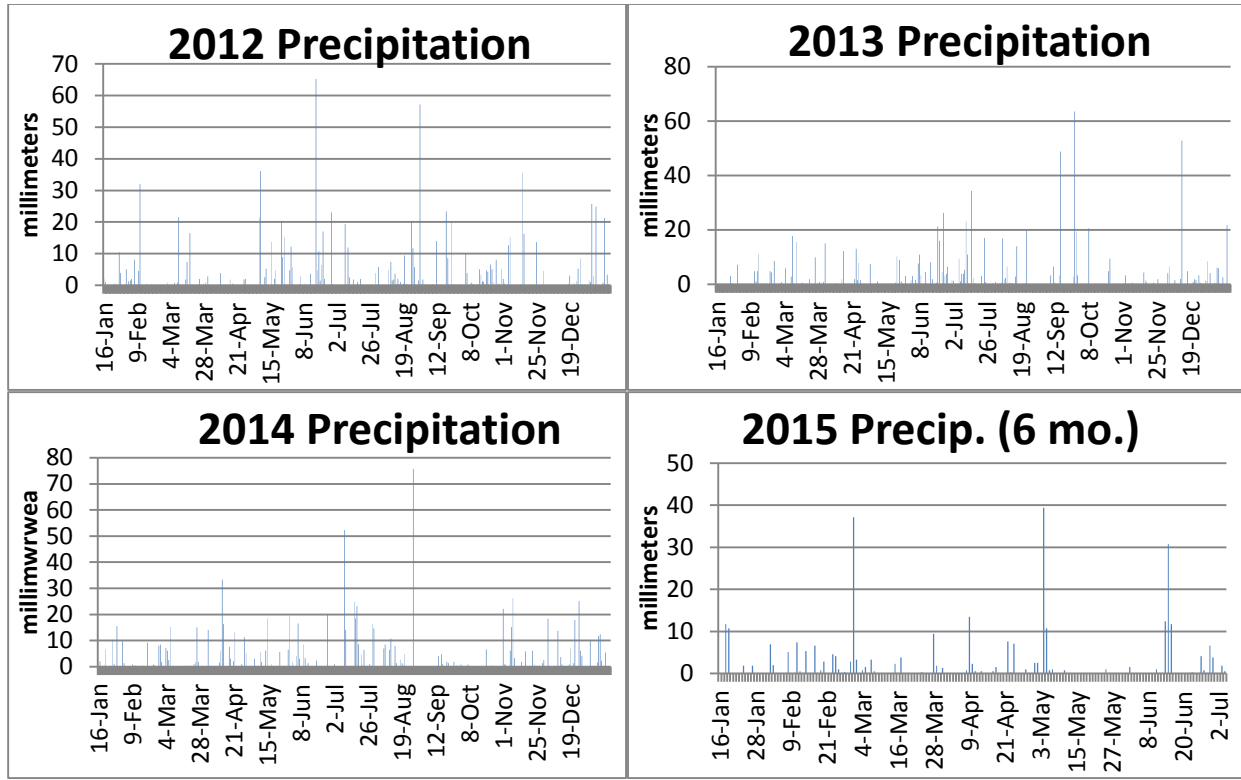


Table C-1. Total yearly precipitation for Skyhaven Airport in Rochester, NH.

Year	Precipitation (mm)
2000	1037
2001	808.7
2002	993.5
2003	1035.7
2004	1094
2005	1448
2006	1118.1
2007	1070
2008	1487.9
2009	1243.1
2010	1082.4
2011	1062.1
2012	944.6
2013	834.8
2014	943.8
Average	1080.2

Table C-2. Total yearly precipitation for Skyhaven Airport (through June 30).

Year	Precipitation (mm)
2000	492.4
2001	426.6
2002	553.6
2003	453.2
2004	476.8
2005	662.9
2006	612.3
2007	551.3
2008	662.1
2009	524
2010	578.9
2011	489
2012	467.3
2013	379.7
2014	439.3
2015	311.1
Average	505

Figures C-5 to C-9 show the maximum daily temperatures at Skyhaven Airport from 2000 to the first half of 2015. In each chart, the curves consistently peak around 26°C and have very similar slopes before and after peaking. Maximum temperatures in 2014 and 2015 also peak around the 26°C mark, implying that the maximum temperatures in these years were not abnormal. The 2014 and 2015 curves also have the same shape and slope as the other years' curves, further showing 2014 and 2015's routine temperature behavior.

Figure C-5. Maximum daily temperatures for 2000 to 2002.

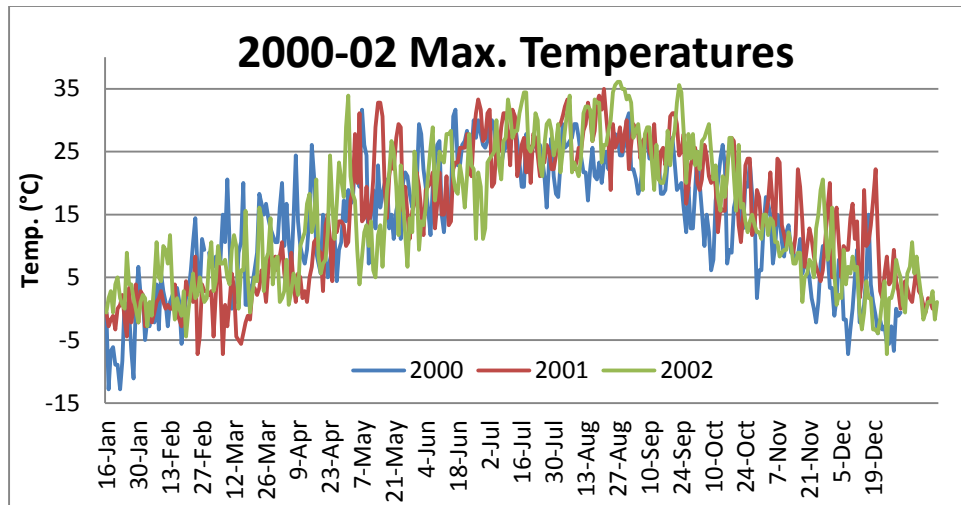


Figure C-6. Maximum daily temperatures for 2003 to 2005.

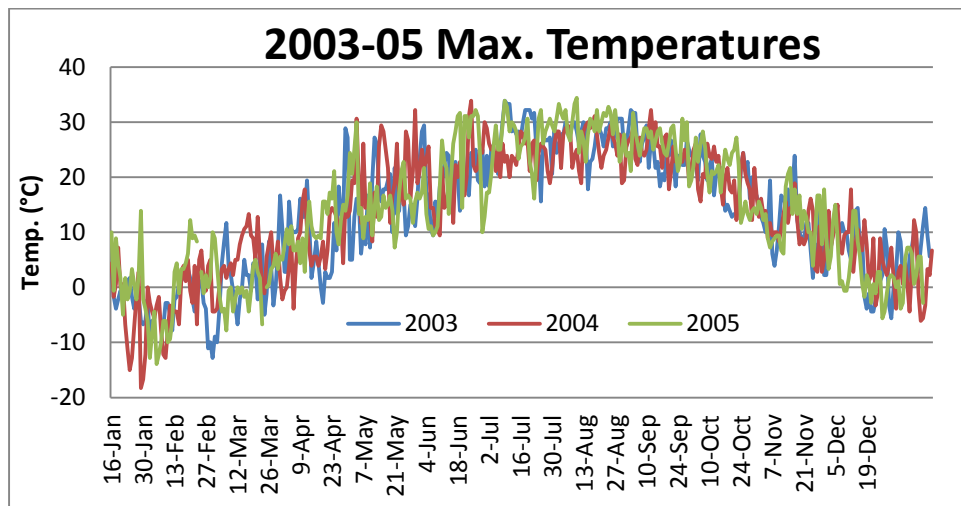


Figure C-7. Maximum daily temperatures for 2006 to 2008.

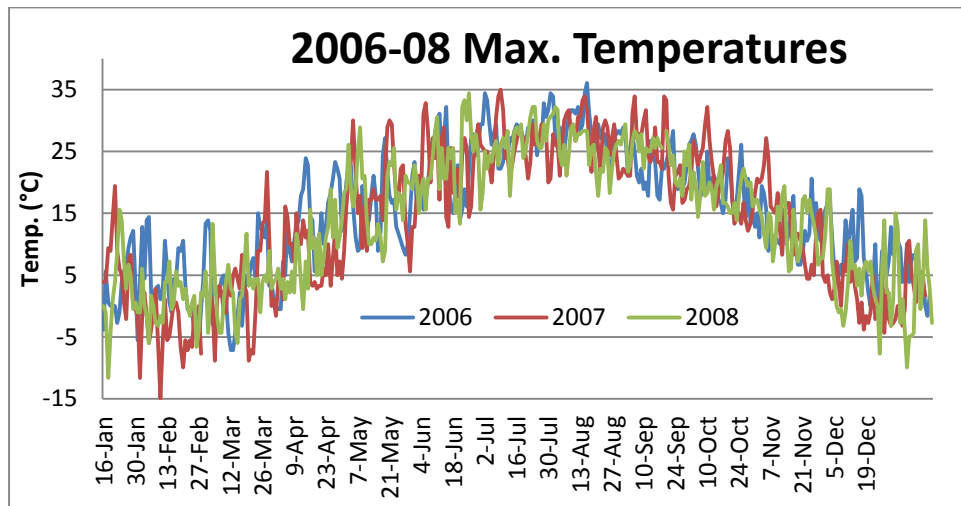


Figure C-8. Maximum daily temperatures for 2009 to 2011.

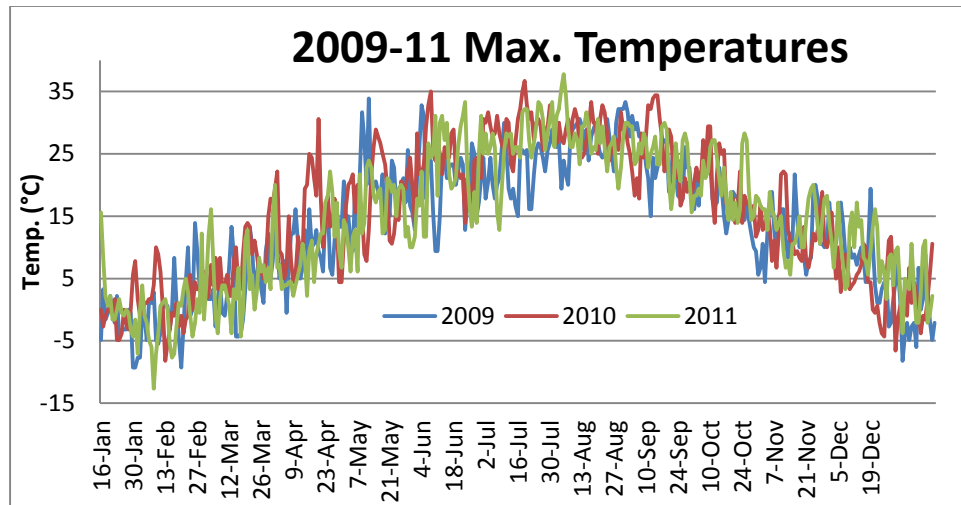
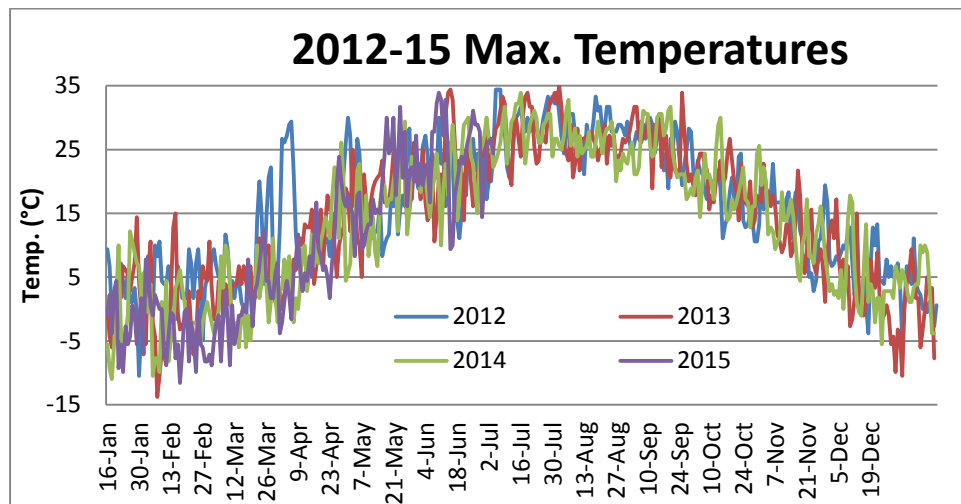


Figure C-9. Maximum daily temperatures for 2012 to 2015.



Figures C-10 to C-14 show the minimum daily temperatures at Skyhaven Airport from 2000 to the first half of 2015. In each chart, the curves consistently peak around 17°C and have very similar slopes before and after peaking. Minimum temperatures in 2014 and 2015 also peak around the 17°C mark, implying that the minimum temperatures in these years were not abnormal. The 2014 and 2015 curves also have the same shape and slope as the other years' curves, further showing 2014 and 2015's routine temperature behavior.

Figure C-10. Minimum daily temperatures for 2000 to 2002.

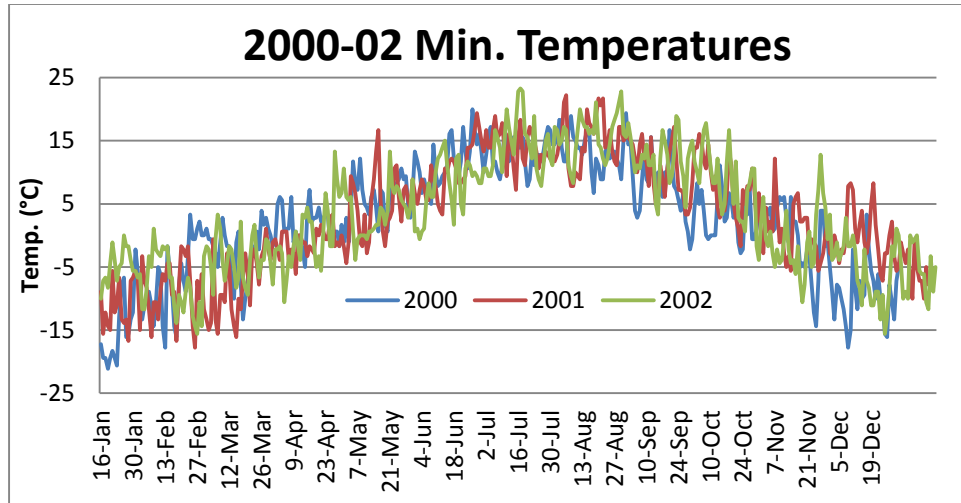


Figure C-11. Minimum daily temperatures for 2003 to 2005.

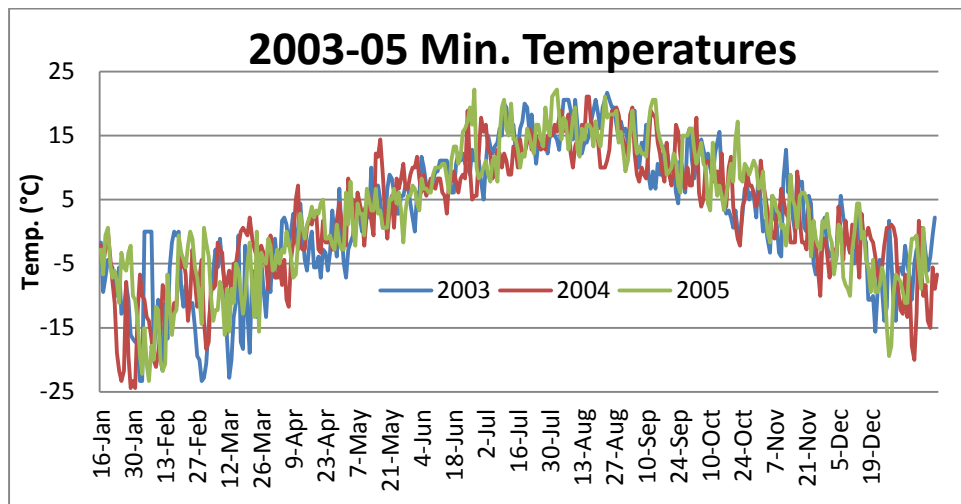


Figure C-12. Minimum daily temperatures for 2006 to 2008.

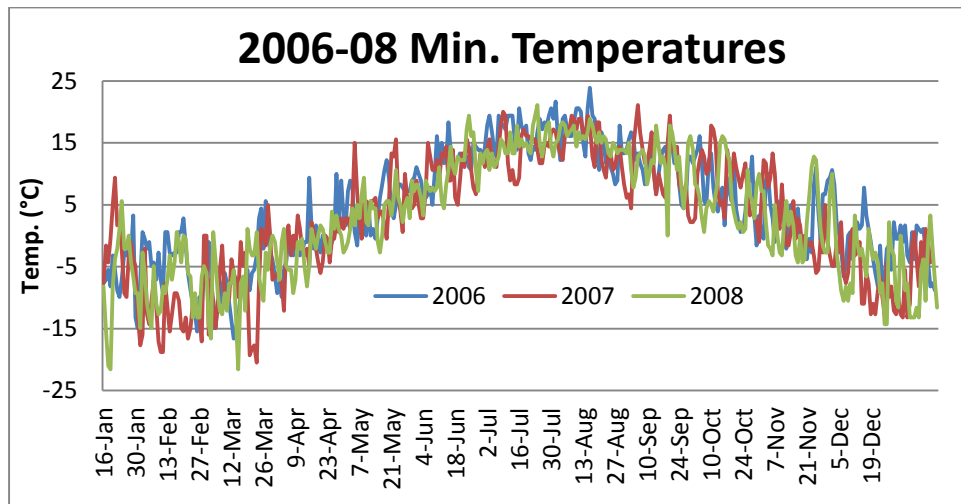


Figure C-13. Minimum daily temperatures for 2009 to 2011.

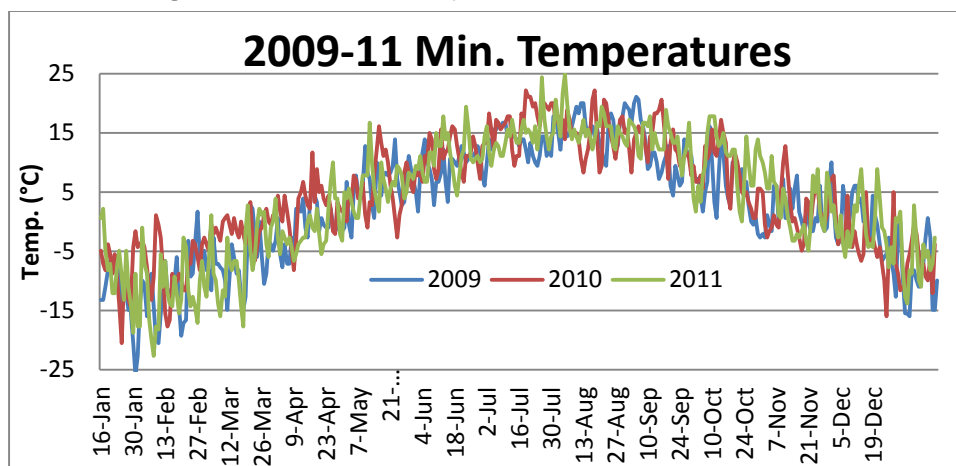
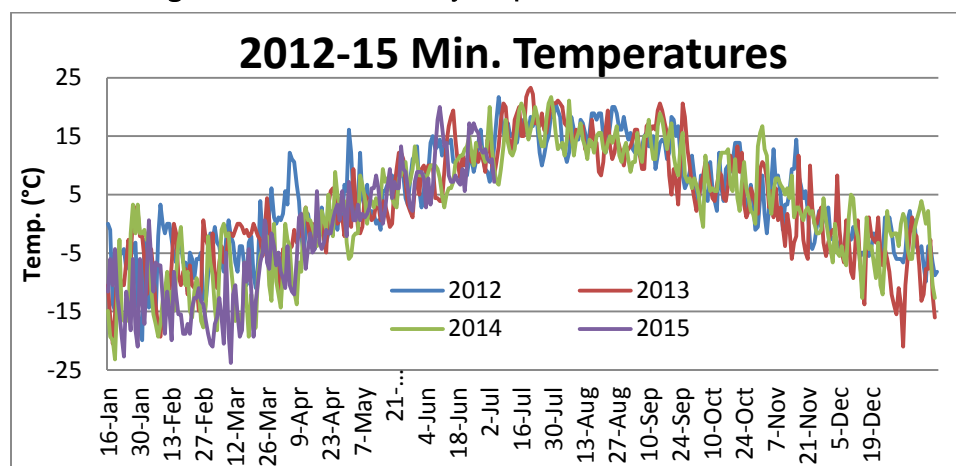


Figure C-14. Minimum daily temperatures for 2012 to 2015.



We determined which days of a given year had an average temperature below 0°C and considered the freeze season over if there were four consecutive days with an above freezing average temperature. Table C-3 shows the length of each year's freezing season at Skyhaven Airport and an average length from all the years. This table shows that the 2013–14 season was 24 days longer than the 87 day average season length while the 2014–15 freeze season was only 4 days longer. Both seasons ended at nearly the same time (27 and 29 March, respectively), which is perhaps more significant than the length of the seasons given that data was collected in the spring, summer, and fall. When compared to the other years' freeze seasons, it is apparent that the 2013–14 and 2014–15 seasons end at least two weeks later than all other seasons besides that of 2002–03. Based on this analysis, the 2013–14 and 2014–15 freeze seasons ended unusually late, perhaps delaying ground thaw and therefore skewing FWD data.

Table C-3. Length of freeze season by year.

Year	Freeze Season Length (days)
2000-01	102
2001-02	81
2002-03	109
2003-04	88
2004-05	91
2005-06	93
2006-07	57
2007-08	96
2008-09	91
2009-10	74
2010-11	95
2011-12	81
2012-13	51
2013-14	111
2014-15	91
Average	87

Figures C-15 and C-16 and Table C-4 below show the cumulative freezing degree-days (FDD) for each freezing season from 2000 to 2015. We gathered this data by summing the average daily temperatures from when the freeze season began (sum of daily temperatures is zero) to when the sum of the daily temperatures reached zero again. In other words, negative-temperature days cause the cumulative FDD to decrease while positive-temperature days do the opposite. As seen in Table C-4, the average number of FDD from 2000 to 2015 was 141 days; and the average cumulative temperature was $-708.26^{\circ}\text{C-days}$. Both the 2013–14 and 2014–15 FDD seasons were longer than the average at 164 and 145 days respectively. These seasons also reached colder cumulative temperatures than the average at $-1031.6^{\circ}\text{C-days}$ and $-1162.4^{\circ}\text{C-days}$, respectively. Based on this data, the 2013–14 and 2014–15 winter seasons were colder and longer than usual.

Figure C-15. Cumulative freezing degree-days (FDD) for winter 2000–01 to winter 2007–08.

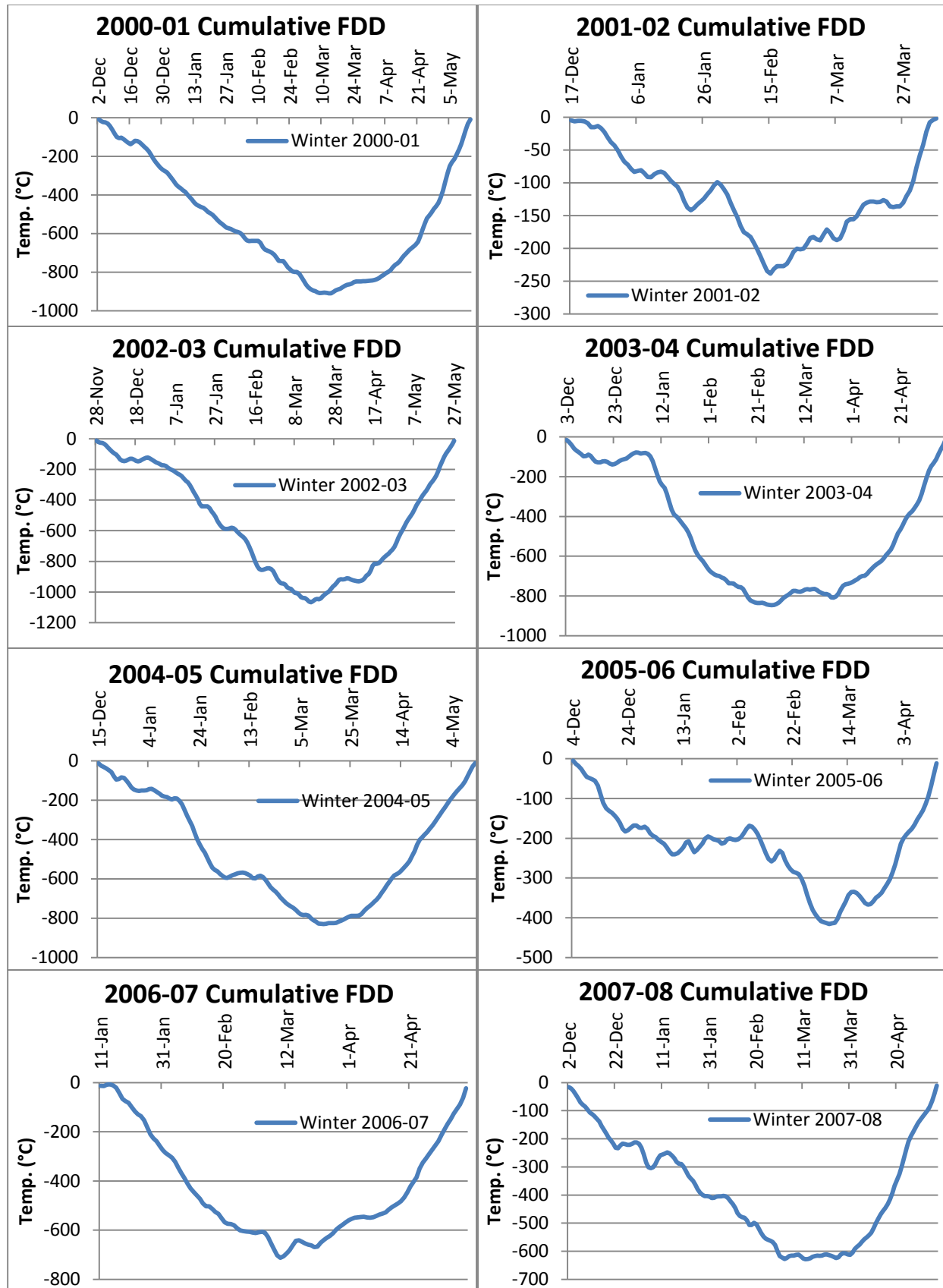


Figure C-16. Cumulative freezing degree-days (FDD) for winter 2008–09 to winter 2014–15.

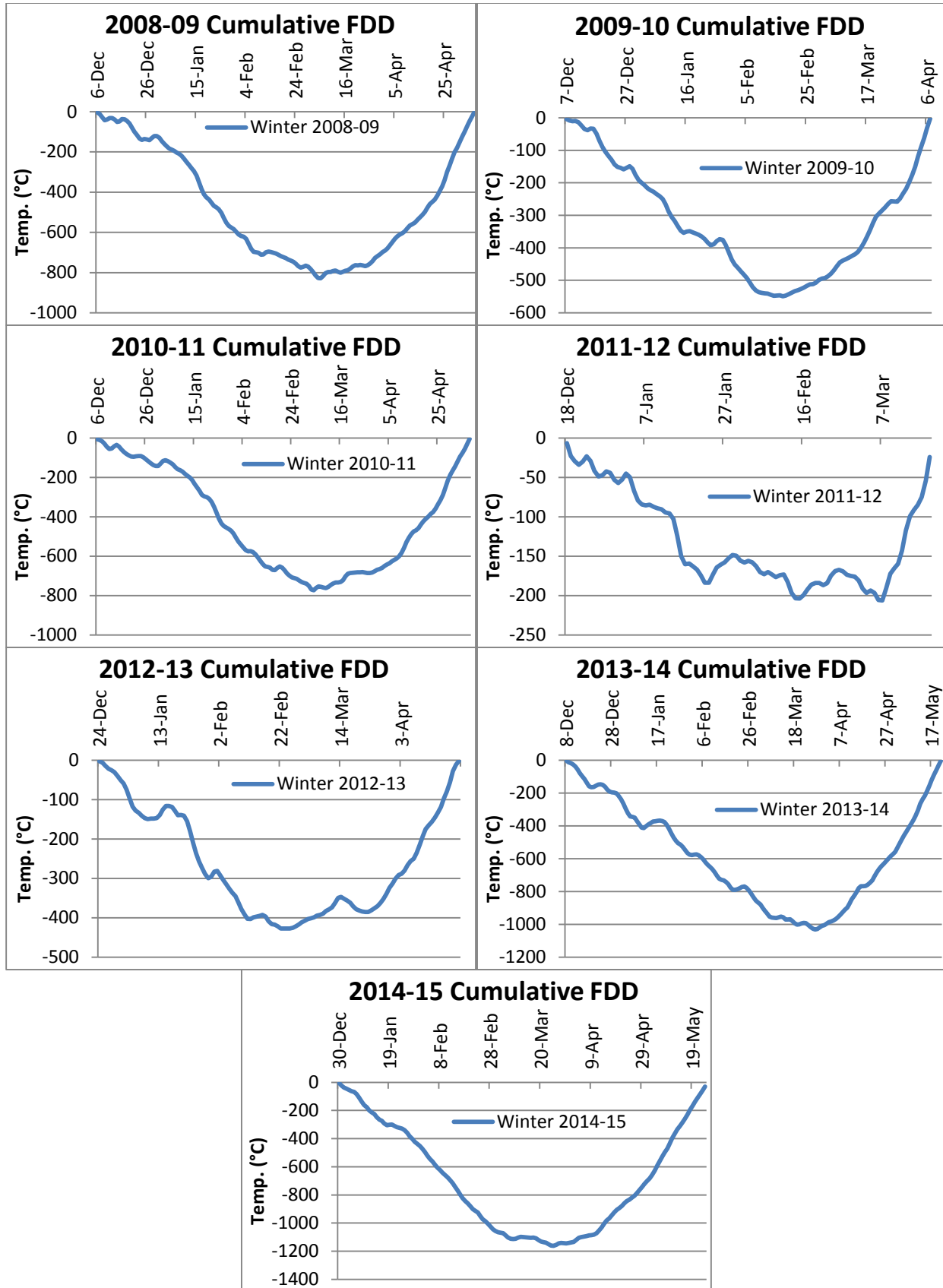


Table C-4. Cumulative freezing degree-days (FDD) from 2000 to 2015.

Year	Length (days)	Cumulative FDD (°C-days)
2000-01	162	-909.25
2001-02	111	-238.55
2002-03	181	-1066.75
2003-04	160	-846.05
2004-05	150	-830.15
2005-06	132	-415.45
2006-07	117	-711.75
2007-08	158	-628
2008-09	152	-828.5
2009-10	121	-548.8
2010-11	153	-772.9
2011-12	92	-206.3
2012-13	119	-427.45
2013-14	164	-1031.6
2014-15	145	-1162.4
Average	141	-708.26

Appendix D: Moduli Comparison Between Loads, and PCASE vs. ELMOD FWD Analysis

Figures D-1 to D-5 give comparisons between loads for asphalt concrete and Figures D-6 to D-10 compare the loads for the base-course layer.

Figure D-1. Load comparisons for asphalt concrete for 3 April 2014.

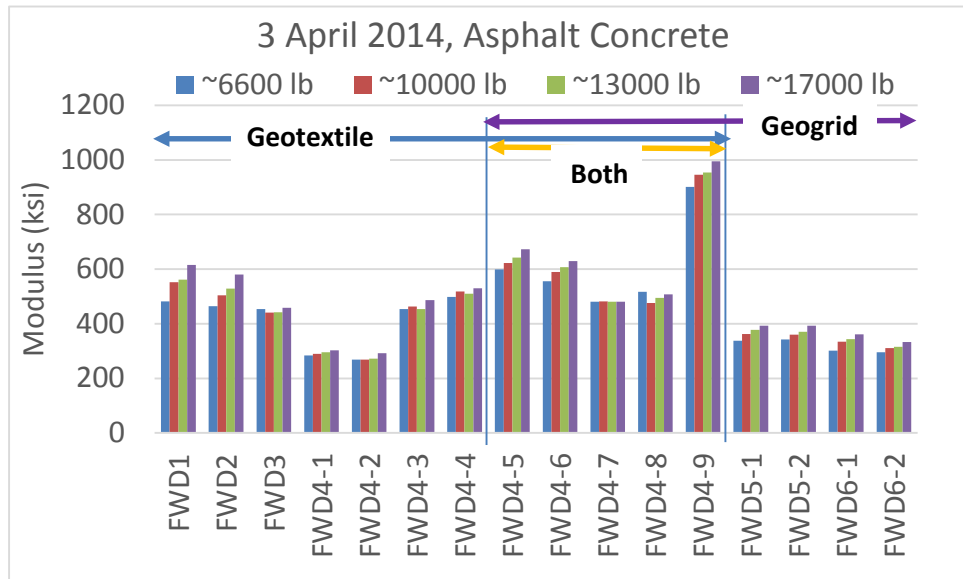


Figure D-2. Load comparisons for asphalt concrete for 17 March 2015.

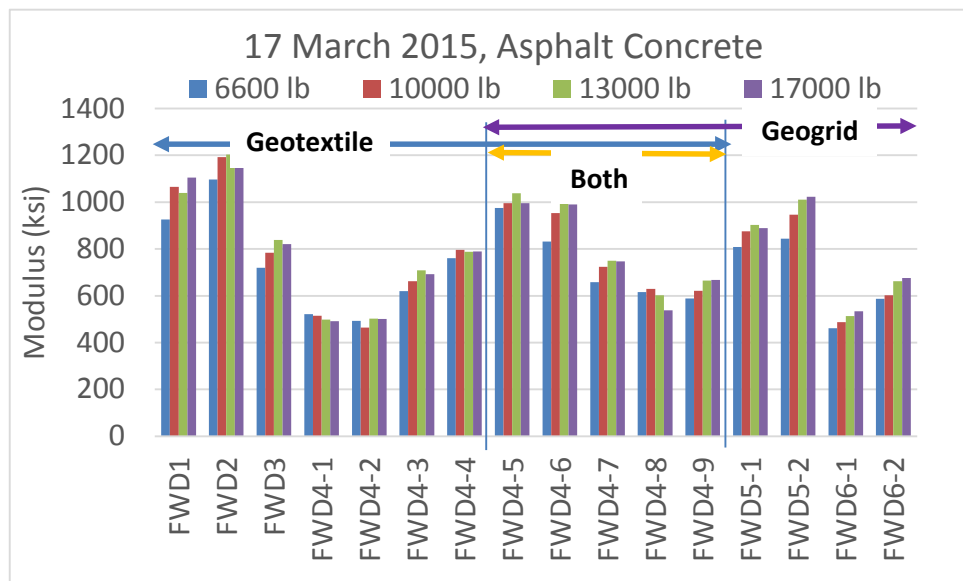


Figure D-3. Load comparisons for asphalt concrete for 1 April 2015.

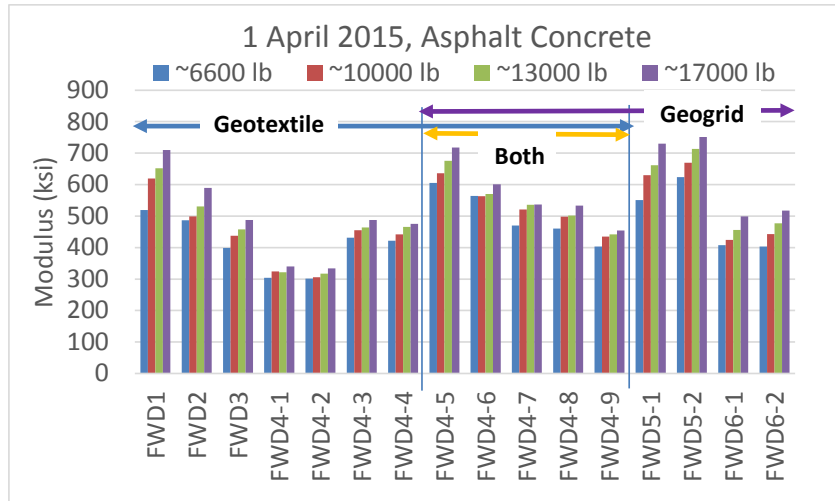


Figure D-4. Load comparisons for asphalt concrete for 23 July 2014.

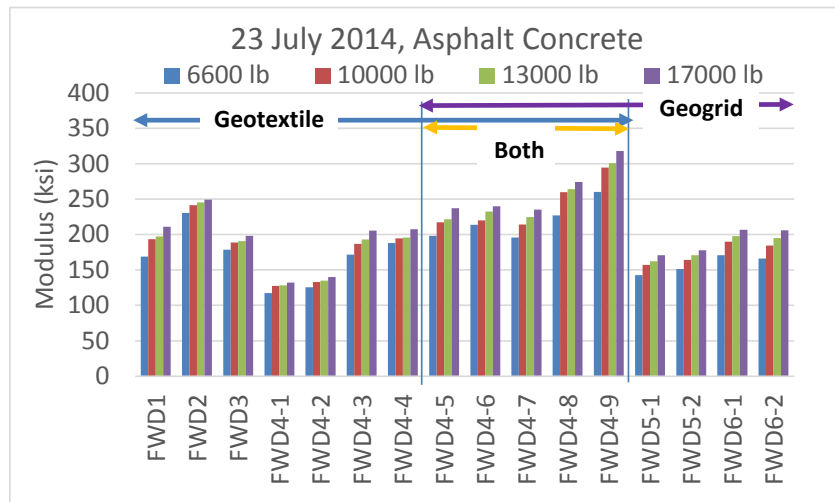


Figure D-5. Load comparisons for asphalt concrete for 27 October 2014.

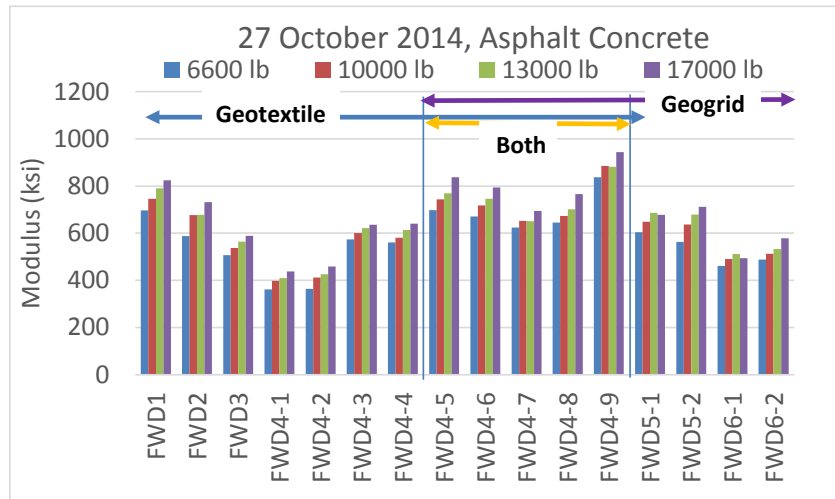


Figure D-6. Load comparisons for the base course for 3 April 2014.

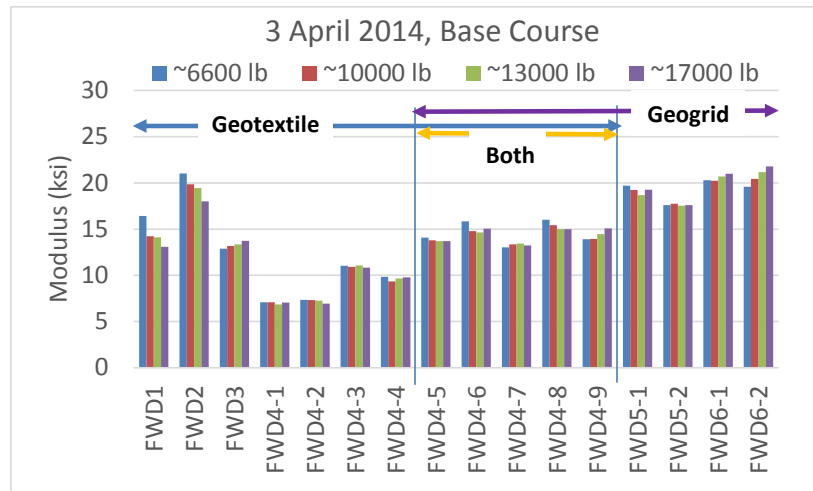


Figure D-7. Load comparisons for the base course for 17 March 2015.

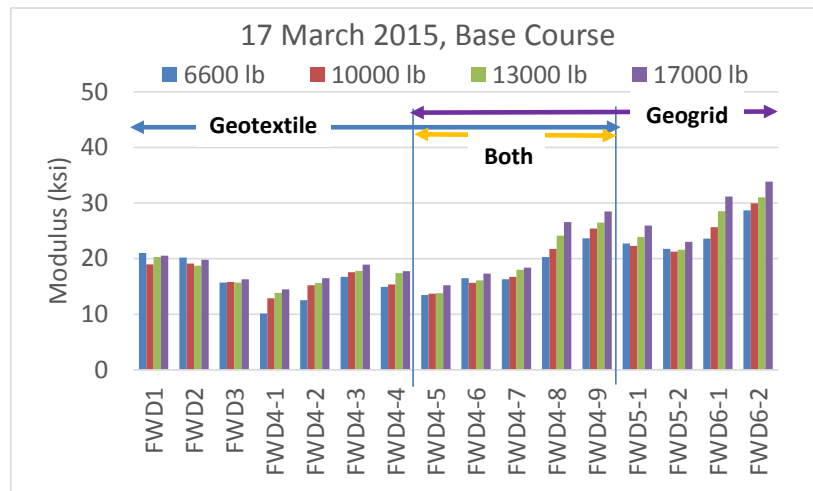


Figure D-8. Load comparisons for the base course for 1 April 2015.

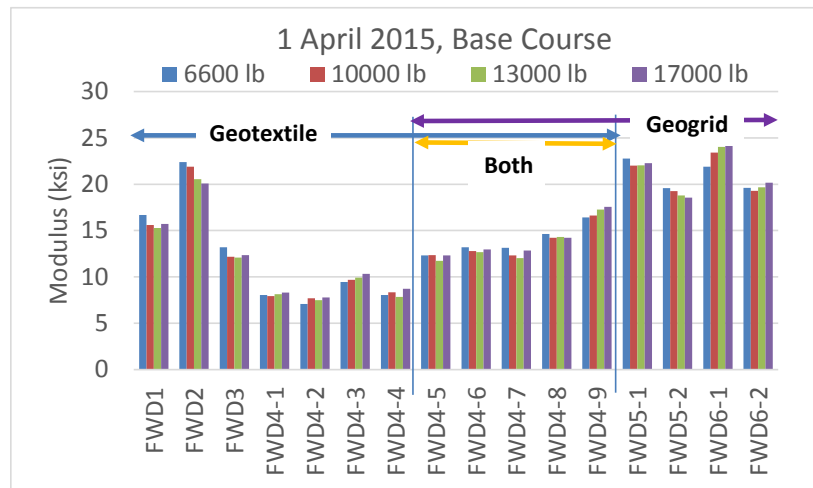


Figure D-9. Load comparisons for the base course for 23 July 2014.

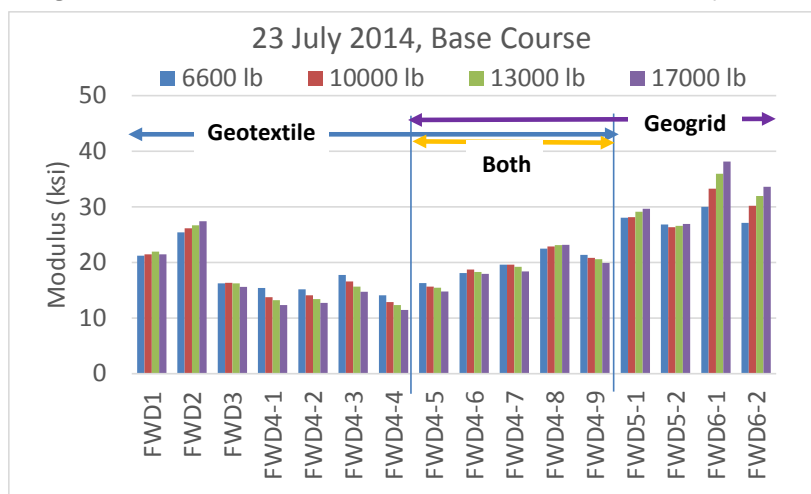
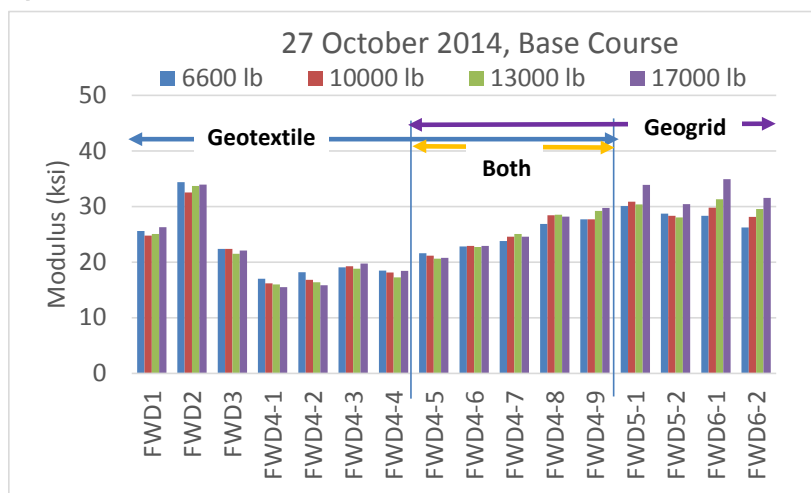


Figure D-10. Load comparisons for the base course for 27 October 2014.



The following data compared ELMOD6 versus PCASE FWD analyses. We used PCASE 2.09, a software used for designing and evaluating airfield and roadway pavements. Though primarily used for the design of future roads and runways, PCASE is also able to back-calculate moduli of existing surfaces using FWD data. To determine the base layer moduli at Pickering Road, the FWD data and pavement profiles for the various test sections were imported; and PCASE used the WESDEF program (developed by the former U.S. Army Engineer Waterways Experiment Station [WES]) to calculate moduli for the individual pavement layers. When given an initial estimate of the elastic modulus values and a limiting range of moduli, WESDEF will use a computer optimization routine to calculate the modulus values of best fit between a measured deflection basin and the computed deflection basin. After back-calculation in PCASE, the moduli for

the base layers were grouped by test section and plotted, as seen in Figures D-11 to D-16.

Figure D-11. Moduli for the base layers from the 27 October 2014 tests from ELMOD6.

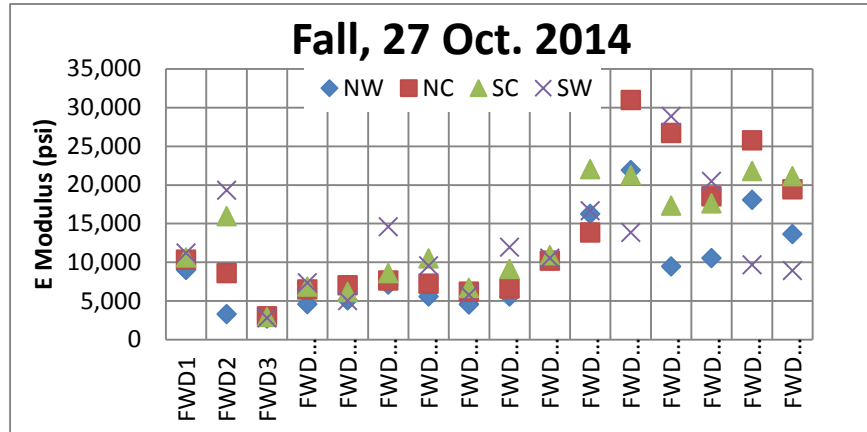


Figure D-12. Averages of the moduli for the base layers from the 27 October 2014 tests from ELMOD6.

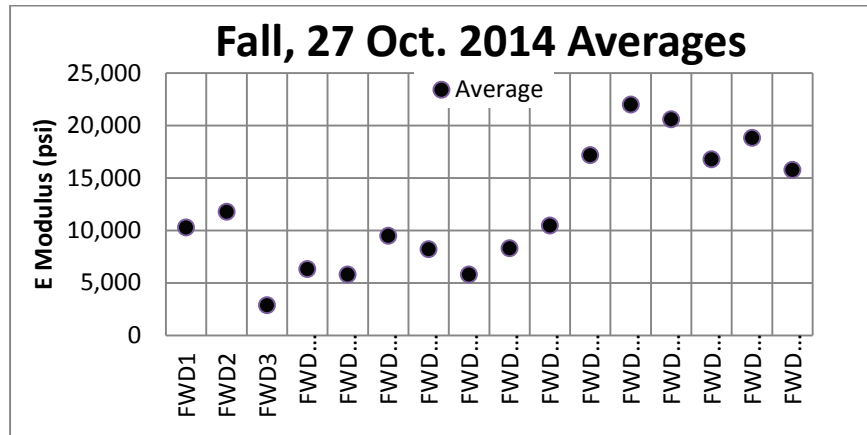


Figure D-13. Moduli for the base layers from the 23 July 2014 tests from ELMOD6.

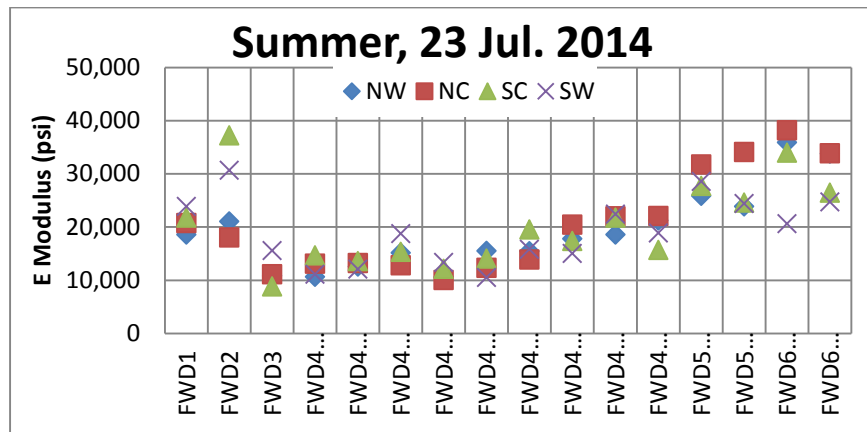


Figure D-14. Averages of the moduli for the base layers from the 23 July 2014 tests from ELMOD6.

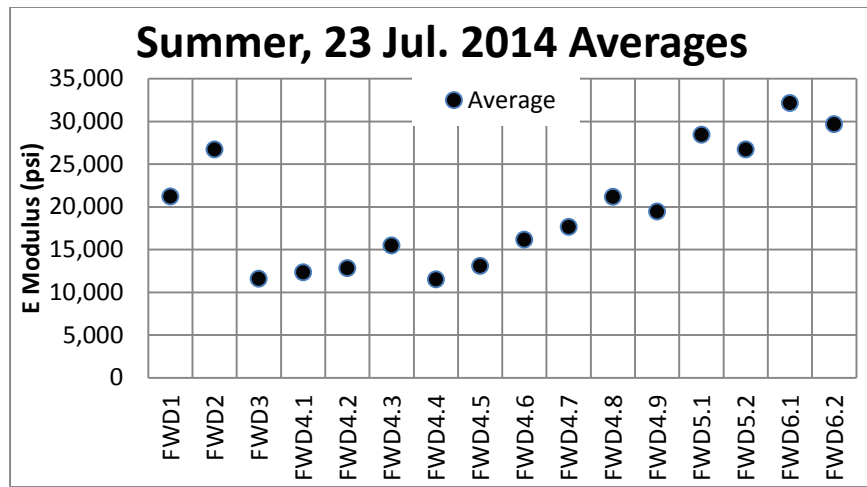


Figure D-15. Moduli for the base layers from the 1 April 2015 tests from ELMOD6.

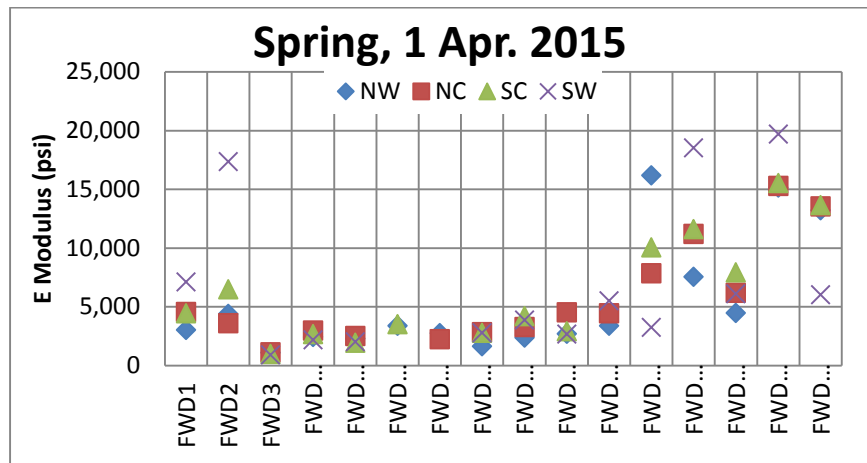
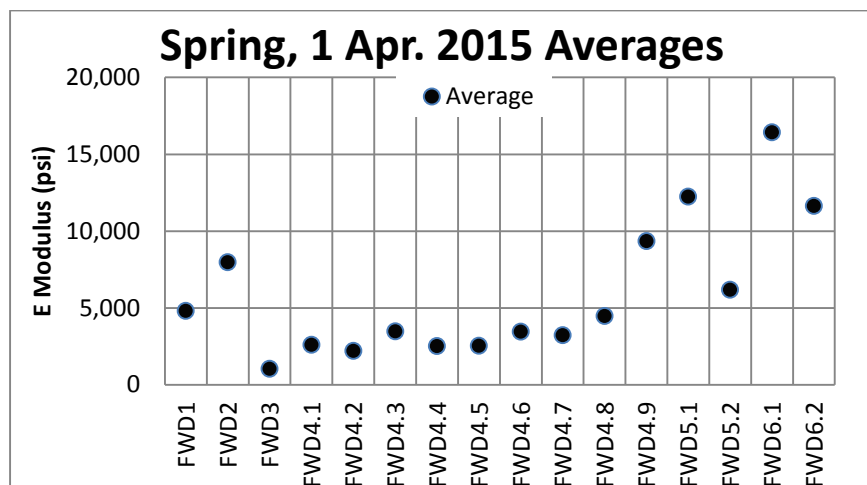


Figure D-16. Averages of the moduli for the base layers from the 1 April 2015 tests from ELMOD6.



Figures D-17 to D-19 compare the PCASE FWD analysis with the ELMOD6 FWD analysis.

Figure D-17. A comparison of the PCASE and ELMOD6 FWD analyses.

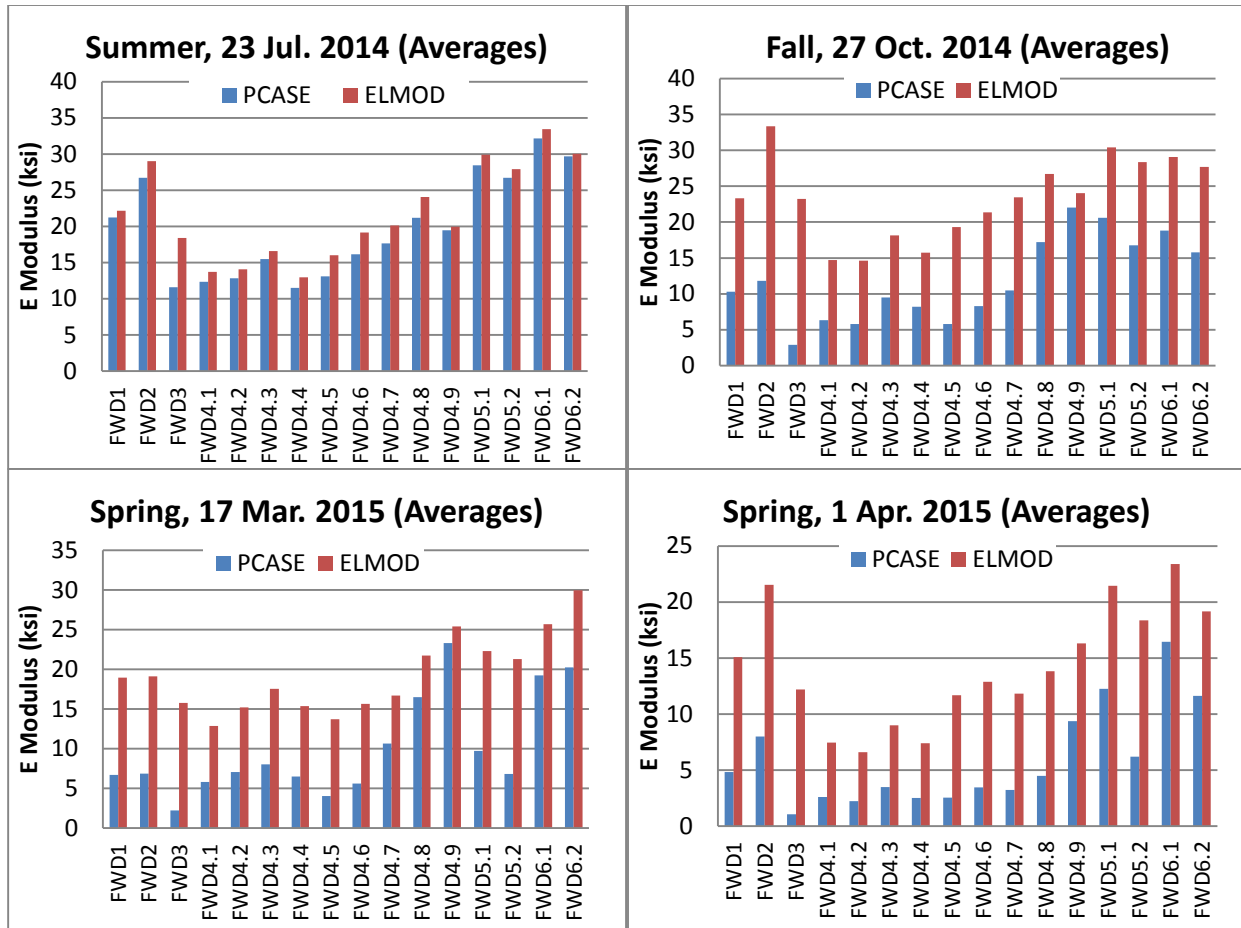


Figure D-18. Averages of the moduli for the base layers from PCASE.

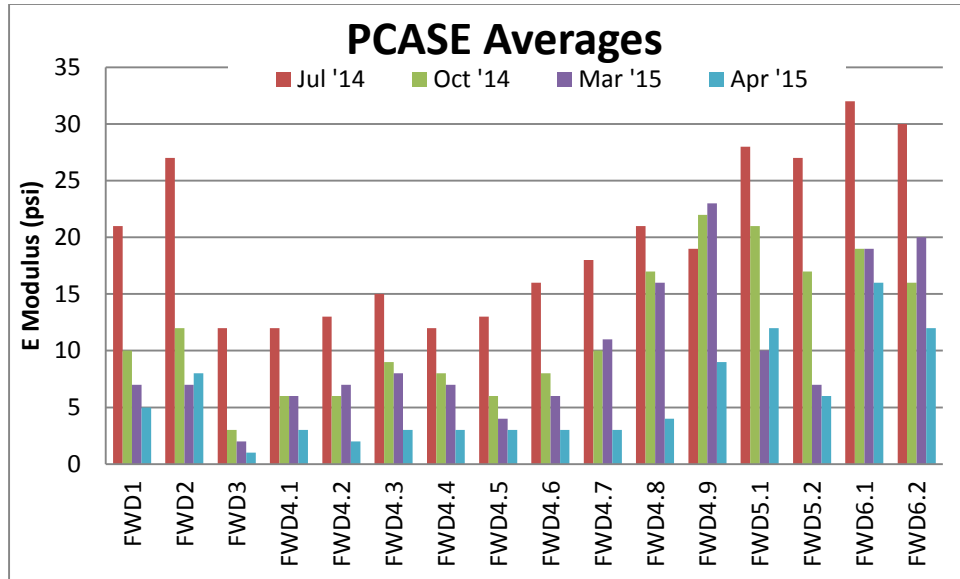


Figure D-19. Averages of the moduli for the base layers from ELMOD6.

